Microwave Journal®

INTELLIGENT POWER AMPLIFIERS

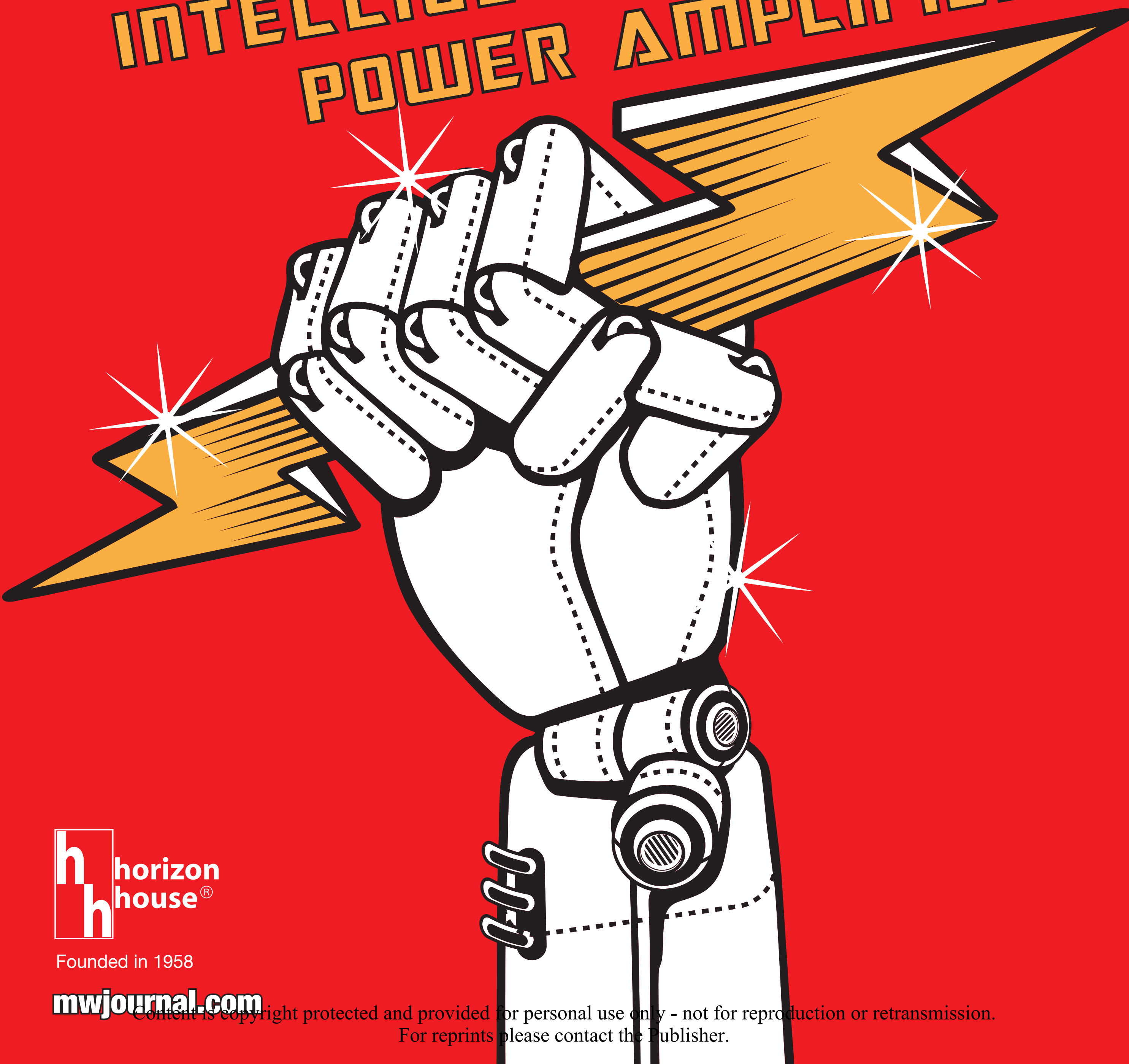

horizon house®
Founded in 1958
mwjournal.com

Maximize Precious Metal Scrap Recoveries

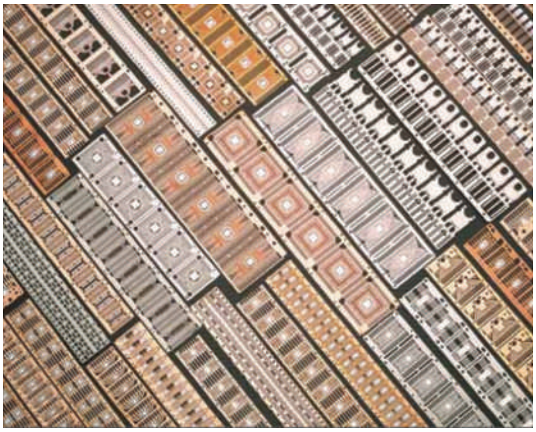

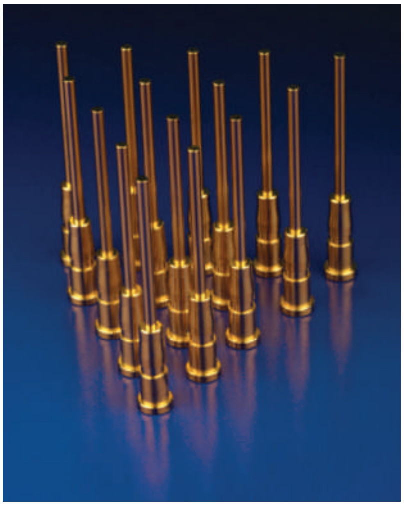

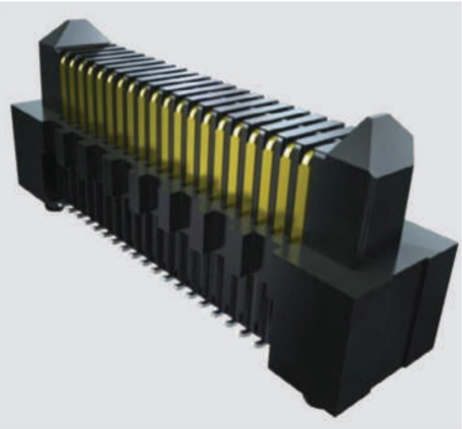

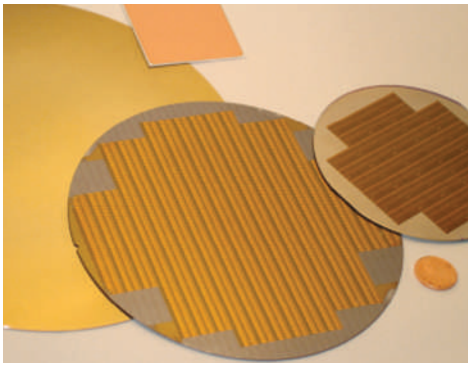

- ISO certified plant & laboratory
- Fully insured and permitted facility, ITAR compliant
- Can accept and process most precious metal containing haz. waste items
- Capability to treat high grade and lower grade precious metal bearing items
- Processes include: thermal reduction, milling, screening, blending, melting & shredding
- Payment flexibility: wire transfers, physical metal & pool account credits
- Pricing options
- Open transparent reporting
- Logistics assistance shipping materials

Metals Recycled:
Gold, Silver, Platinum, Palladium, Rhodium, Ruthenium, Iridium and Copper.

We supply 50 gallon drums or 5 gallon pails depending on your material types and grades.

Knowledgeable staff to ensure our clients reclamation needs are met.

Call us today to get the most out of your metal!

QML

Professional Precious Metal Recovery

Corporate Office (401) 490-4555 Plant Operations (401) 762-0094 sales@qml.us www.qml.us

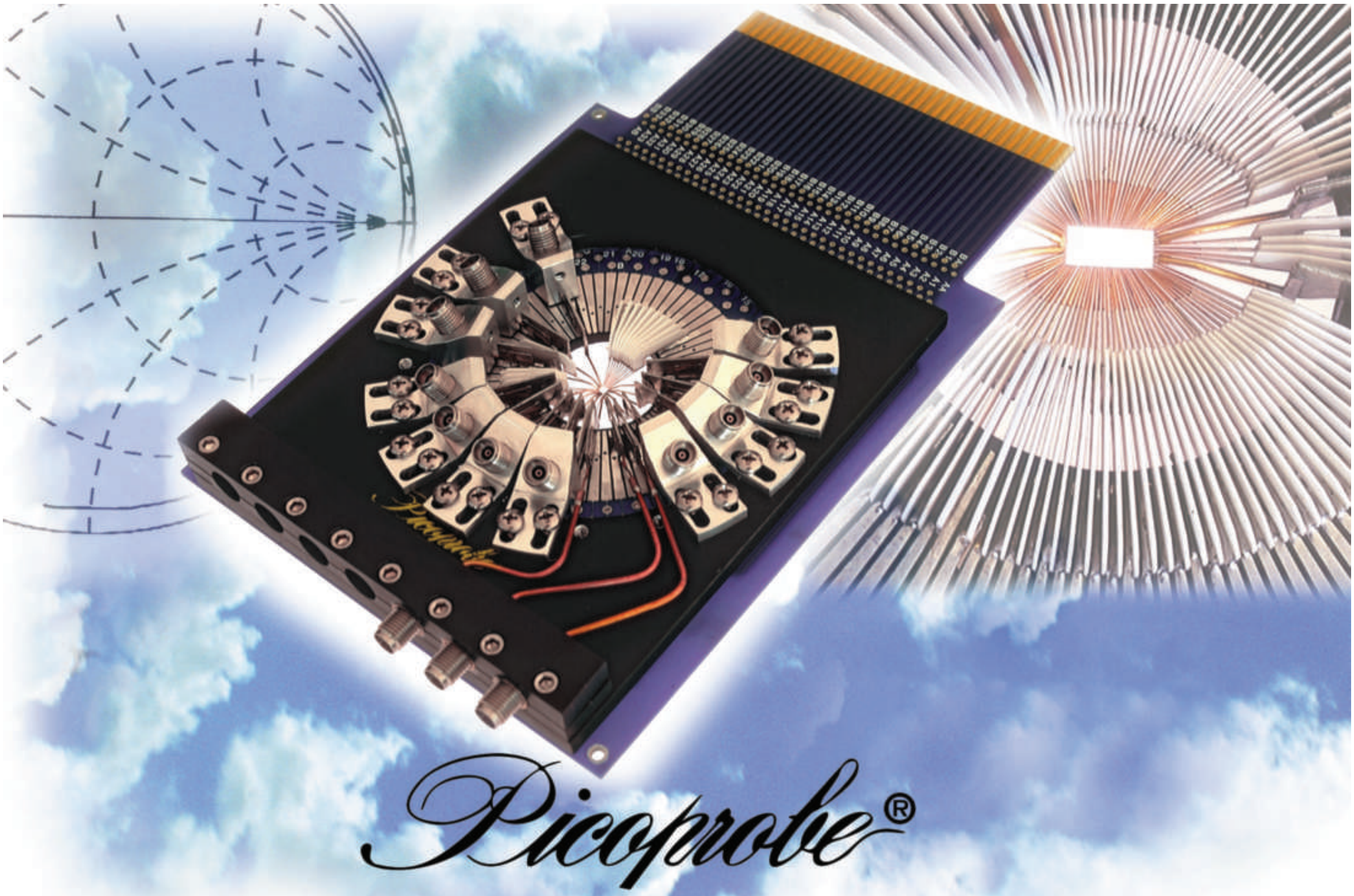

Picoprobe®

Picoprobe elevates probe cards to a higher level…

(…110 GHz to be exact.)

Since 1981, GGB Industries, Inc., has blazed the on-chip measurement trail with innovative designs, quality craftsmanship, and highly reliable products. Our line of custom microwave probe cards continues our tradition of manufacturing exceptional testing instruments.

Through unique modular design techniques, hundreds of low frequency probe needles and a variety of microwave probes with operating frequencies from DC to 40, 67, or even 110 GHz can be custom configured to your layout.

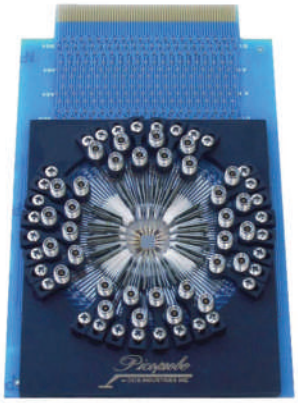

Our patented probe structures provide the precision and ruggedness you require for both production and characterization testing. And only Picoprobe® offers the lowest loss, best match, low inductance power supplies, and current sources on a single probe card.

Our proven probe card design technology allows full visibility with inking capability and ensures reliable contacts, even when probing non-planar structures.

Not only do you get all the attractive features mentioned, but you get personal, professional service, rapid response, and continuous product support--all at an affordable price so your project can be completed on time and within budget.

Typical Specs	10GHz	20GHz	40GHz
Insertion Loss	0.6 dB	0.8 dB	1.3 dB
Return Loss	22 dB	18 dB	15 dB

For technical assistance, custom product designs, or off-the-shelf delivery,call GGB Industries, Inc., at (239) 643-4400.

GGB INDUSTRIES, INC. • P.O. BOX 10958 • NAPLES, FL 34101

Telephone (239) 643-4400 • Fax (239) 643-4403 • E-mail email@ggb.com • www.picoprobe.com

DC TO MMWAVE

Preferred by 20,000+

More than Just a Supplier

Selection and Solutions

- 27 product lines from one source
- 7500+ models in stock and growing
- Coverage from VHF to mmWave
- Custom components, integrated systems and test solutions with fast turnaround

Service

- Global presence, local service
- Accessible engineering and support
- Same-day shipping and on-time delivery
- Short lead times and low minimums

Peace of Mind

- Award-winning quality excellence
- Easy troubleshooting and RMA process
- Supply chain security through the life of your system—no EOL target

Constant Innovation

- Relentless investment in new products and design capabilities
- 400+ catalog introductions per year
- Patented technologies

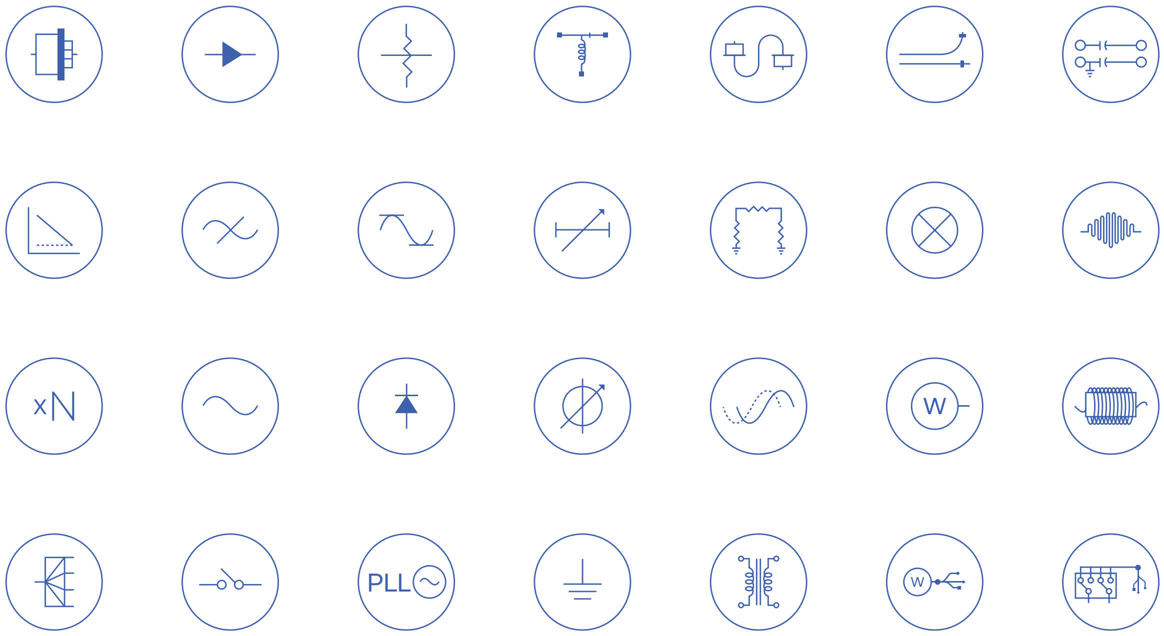

Mini-Circuits®

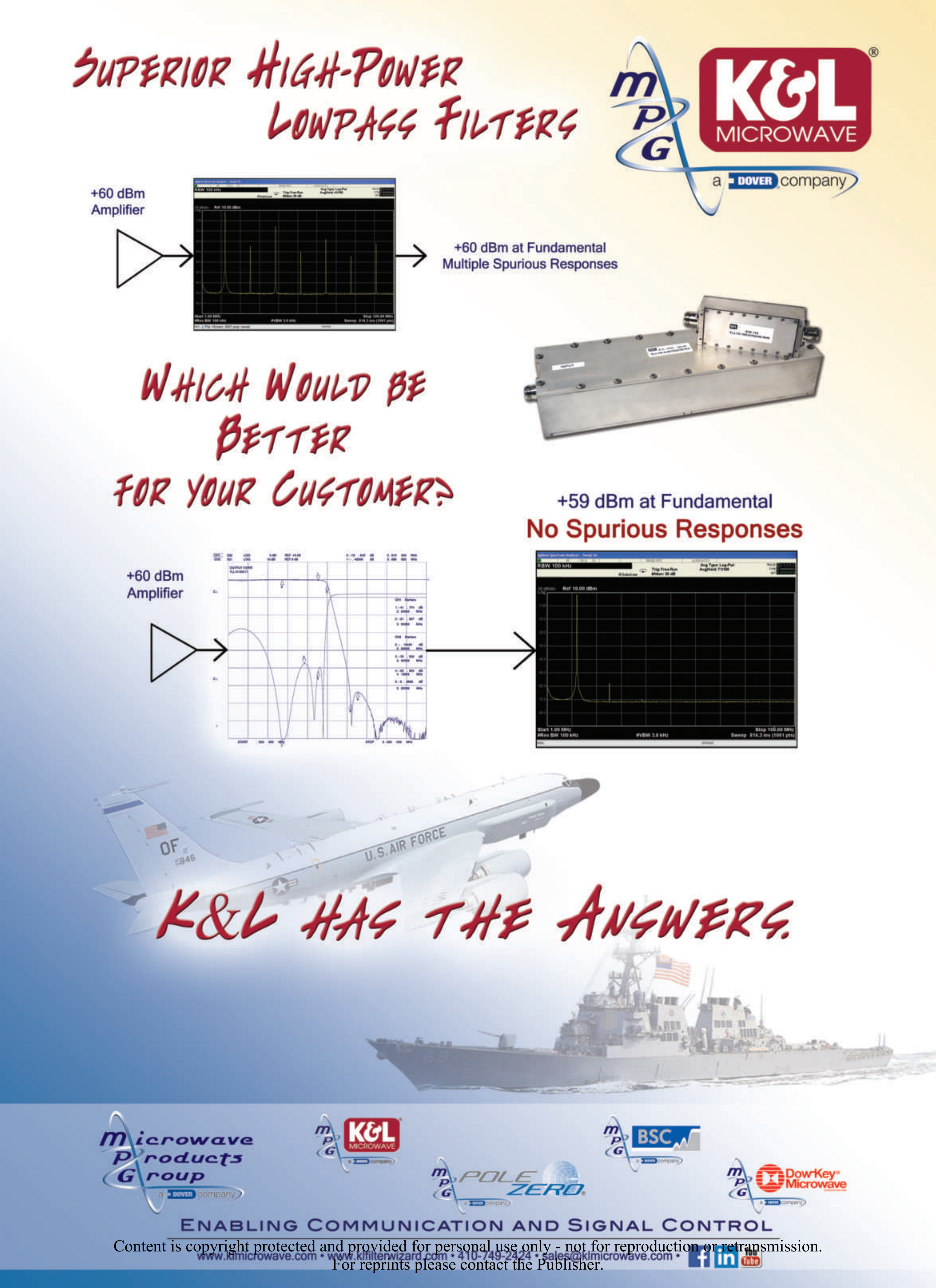
Superior High-Power Lowpass Filters
K&L Microwave
a Dover company
+60 dBm Amplifier
+60 dBm at Fundamental
Multiple Spurious Responses
Which Would be Better for your Customer?
+59 dBm at Fundamental
No Spurious Responses
+60 dBm Amplifier
U.S. AIR FORCE
K&L has the Answers.
Microwave Products Group
a Dover company
K&L Microwave
BSC
Pole Zero
Dow-Key Microwave
Enabling Communication and Signal Control
www.klmicrowave.com • www.klfilterwizard.com • 410-749-2424 • sales@klmicrowave.com •


RF-LAMBDA
THE LEADER OF RF BROADBAND SOLUTIONS
BROADBAND SSPA / EMC BENCHTOP
SOLID STATE POWER AMPLIFIER
0.1-22GHZ
ULTRA BROADBAND SSPA
RFLUPA01M22GA
4W 0.1-22GHZ
RFLUPA0218GB
20W 1-19GHZ
300W 6-18GHZ SOLID STATE BROADBAND
400W 8-11GHZ
SOLID STATE BROADBAND
0.1-6GHZ VHZ,
UHF, L, S, C BAND
RFLUPA02G06GC
100W 2-6GHZ
RFLUPA0706GD
30W 0.7-6GHZ
MADE IN USA
6-18GHZ C, X, KU BAND
RFLUPA08G11GA
50W 8-11GHZ
RFLUPA0618GD
60W 6-18GHZ
RFLUPA06G12GB
25W 6-12GHZ
18-50GHZ K, KA, V BAND
RFLUPA18G47GC
2W 18-47GHZ
RFLUPA27G34GB
15W 27-34GHZ
RFLUPA47G53GA2
10W 47-53GHZ
RFLUPA27G34GB
30W 18-40GHZ
BENCHTOP RF MICROWAVE SYSTEM POWER AMPLIFIER
RAMP00G06GA- 30W 0.01-6GHZ
RAMP39G48GA- 4W 39-48GHZ
RAMP01G22GA- 8W 1-22GHZ
RAMP27G34GA- 8W 27-34GHZ
www.rflambda.com 1-888-976-8880 San Diego, CA, US Ottawa, ONT, Canada
sales@rflambda.com 1-972-767-5998 Carrollton, TX, US Frankfurt, Germany

Microwave Journal

April 2021
Vol. 64 • No. 4
Amplifiers & Oscillators
mwjournal.com

CONTENTS

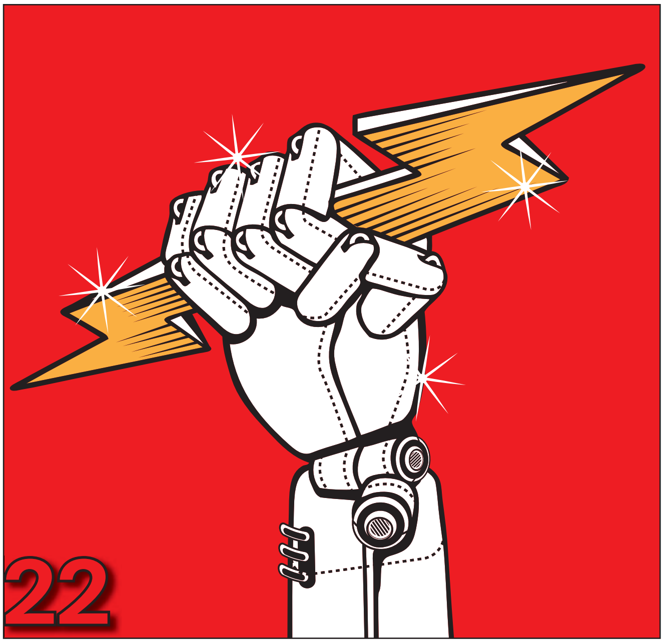

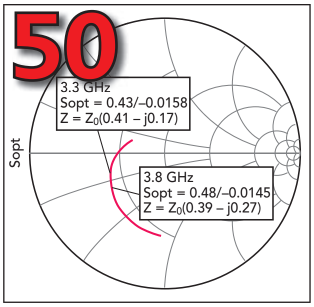

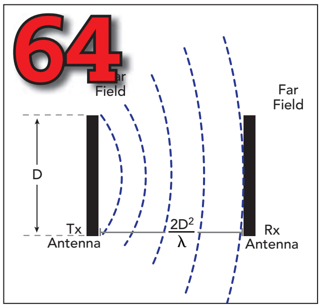

online spotlight

Look for this month's exclusive article online at mwjournal.com

Cover Feature

Technical Features

Application Note

Special Report

THIS MONTH: Our cover story is written by Mitsubishi Electric and features how artificial intelligence (AI) and machine learning (ML) technologies are becoming pervasive in our daily lives, empowering devices ranging from smart speakers to thermostats, self-driving cars to robots and social networks to banking systems. Learn how some are envisioning a future communication system that brings the hyper-connected experience to every corner of life.

64 YEARS OF PUBLISHING EXCELLENCE


Has Amplifier Performance or
Delivery Stalled Your Program?
Noise Figure In Select Frequency Bands
Noise Figure (dB)
5.00
4.50
4.00
3.50
3.00
2.50
2.00
1.50
1.00
0.50
0.00
4.5dB
4.0dB
2.8dB
2.8dB
2.5dB
1.8dB
1.5dB
1.3dB
1.2dB
0.9dB
1.2dB
0.7dB
0.7dB
0.5dB
0.35dB
0 2 4 6 8 10 12 14 16 18 20 22 24 26 28 30 32 34 36 38 40 42 44 46 48 50
Frequency (GHz)
B&Z TECHNOLOGIES
Innovating to Excel
www.bnztech.com

Microwave Journal

CONTENTS

mwjournal.com

Product Features

Tech Briefs

Departments

Microwave Journal (USPS 396-250) (ISSN 0192-6225) is published monthly by Horizon House Publications Inc., 685 Canton St., Norwood, MA 02062. Periodicals postage paid at Norwood, MA 02062 and additional mailing offices.

POSTMASTER: Send address corrections to Microwave Journal, PO Box 1028, Lowell, MA 01853 or e-mail mwj@e-circ.net.com. Subscription information: (978) 671-0446. This journal is issued without charge upon written request to qualified persons working in the RF & microwave industry. Other subscriptions are: domestic, $120.00 per year, two-year subscriptions, $185.00; foreign, $200.00 per year, two-year subscriptions, $370.00; back issues (if available) and single copies, $10.00 domestic and $20.00 foreign. Claims for missing issues must be filed within 90 days of date of issue for complimentary replacement.

STAFF

EXECUTIVE EDITORIAL OFFICE
685 Canton Street, Norwood, MA 02062
Tel: (781) 769-9750
FAX: (781) 769-5037
e-mail: mwj@mwjournal.com

EUROPEAN EDITORIAL OFFICE
16 Sussex Street, London SW1V 4RW, England
Tel: Editorial: +44 207 596 8730 Sales: +44 207 596 8740
FAX: +44 207 596 8749

SUBSCRIPTION SERVICES
Send subscription inquiries and address changes to:
Tel: (978) 671-0446
e-mail: mwj@e-circ.net

BPA WORLDWIDE

www.mwjournal.com

Printed in the USA

Microwave Journal ONLINE

Visit us @ mwjournal.com

eLEARNING CENTER

EW in Space
Sponsored by: Rohde & Schwarz 4/20

Optimized Silicon Wafers: The Ultimate Solution for Improved RF Filter and Device Performance
Sponsored by: OKMETIC 4/21

Topic: Defense and Radar
Sponsored by: RFMW and Qorvo 4/28

Executive Interview

Brian Deutsch, CEO of **Pivotal Commware**, describes how the firm's proprietary Holographic Beam Forming technology improves the coverage of 5G mmWave networks and how the company will use a recent $50 million investment.

Catch *Frequency Matters*, the industry update from *Microwave Journal*,
microwavejournal.com/FrequencyMatters

Join Us Online

Follow us
@Pathindle
@MWJGary
@MWJEditor

Join us at the RF and Microwave Community

Become a fan at facebook.com/microwavejournal

WHITE PAPERS

Coilcraft — Broadband Chokes for Bias Tee Applications

Copper Mountain Technologies — Automatic Fixture Removal from VNA Measurements

Rohde & Schwarz (Make ideas real) —
- Automated ADAS Test System Trial with Radar Sensors and Electromagnetic Interference
- Improving R&S®FSWP Measurement Speed
- R&S®GSASLP Satellite Link Planner / R&S®GSACSM Communications System Monitoring

TE connectivity — Outdoor Surveillance: A Powerful Trend for a Safer Society

FEATURED eBooks

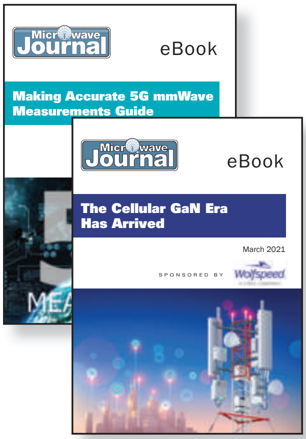

mwjournal.com/ebooks

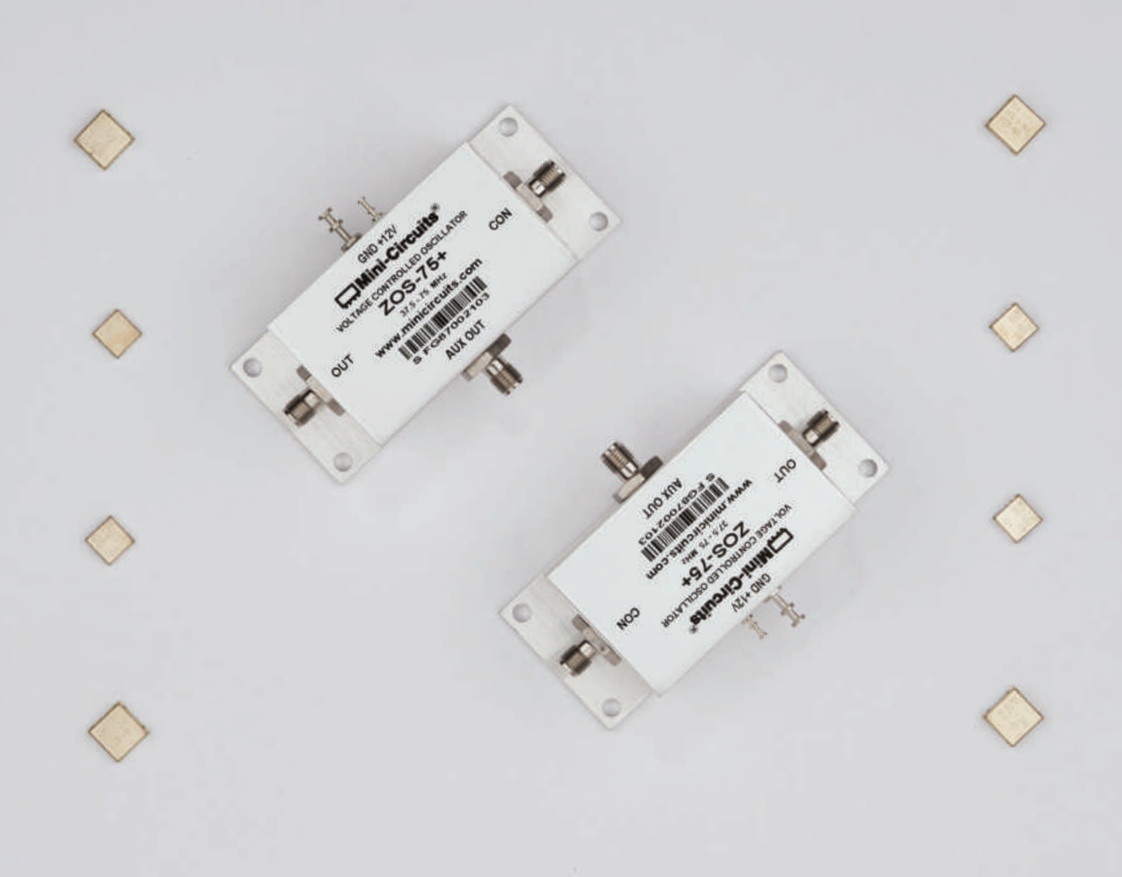

3 MHZ TO 11 GHZ

Voltage Controlled Oscillators

The Industry's Widest Selection

- Wide selection in stock and cost-effective custom designs
- Spot frequency, narrow, medium and wideband—up to 1.5 octaves
- Better phase noise than IC oscillators, as low as -111 dBc/Hz @ 1 kHz offset
- Available in SMT, connectorized and plugin formats
- Sizes as small as 0.175 x 0.175 x 0.075"

Special Features

- Linear tuning
- Dual VCOs in shared housing
- 5V PLL implementation
- Coupled auxiliary output
- Separate modulation port

Mini-Circuits®

MAY

MARK YOUR CALENDAR

ONLINE PANEL 5/18 — RF/Microwave Test and Component Solutions for New Space
www.mwjournal.com

18-20 IEEE Texas Symposium WMCS
ONLINE
https://texassymposium.org

24-27 CS MANTECH 2021 Orlando
Orlando, Fla.
www.csmantech.org

JUNE

7-9 RFIC
Atlanta, Ga.
&
ONLINE
www.rfic-ieee.org

7-10 IMS Connecting Minds. Exchanging Ideas. Atlanta 2021
Atlanta, Ga.
www.ims-ieee.org/ims2021

7-9 MILITARY SPACE USA June 7th-9th 2021 Los Angeles
WWW.MILSPACEUSA.COM
ONLINE
www.smi-online.co.uk/defence/northamerica/milspace-usa

10 ARFTG
Atlanta, Ga.
www.arftg.org

14-23 IEEE ICC®
ONLINE
https://icc2021.ieee-icc.org/

15-17 PCB EAST 2021 Conference & Exhibition
Marlborough, Mass.
https://pcbeast.com/

20-25 IMS Connecting Minds. Exchanging Ideas. Atlanta 2021 — VIRTUAL EVENT
www.ims-ieee.org/ims2021

FOR DETAILS, VISIT MWJOURNAL.COM/EVENTS

ComingEvents

CALL FOR PAPERS
AMTA 2021
April 23, 2021

German Microwave Conference 2022
October 18, 2021

mwjournal.com

APRIL

electronica China
April 14-16 • Shanghai, China
https://electronica-china.com/en/

AMTA
April 22 • Online
https://www.amta.org/i4a/pages/index.cfm?pageid=3491

2021 IEEE Conference on Technologies for Sustainability (SusTech)
April 22-24 • Online
ieee-sustech.org

IEEE Women in Engineering International Leadership Conference
April 27-30 • Online
ieee-wie-ilc.org

IEEE WAMICON
April 28-29 • Online
www.ieeewamicon.org

MAY

IEEE Texas Symposium on Wireless and Microwave Circuits and Systems
May 18-20 • Online
https://texassymposium.org

CS Mantech
May 24-27 • Orlando, Fla.
www.csmantech.org

JUNE

IEEE RFIC 2021
June 7-9 • Atlanta, Ga. + Online
www.rfic-ieee.org

IEEE MTT-S IMS2021
June 7-10 • Atlanta, Ga.
June 20-25 • Virtual Event
www.ims-ieee.org/ims2021

Military Space USA
June 7-9 • Online
www.smi-online.co.uk/defence/northamerica/milspace-usa

ARFTG Microwave Measurement Conference
June 10 • Atlanta, Ga.
www.arftg.org

IEEE International Conference on Communications (ICC)
June 14-23 • Online
icc2021.ieee-icc.org

PCB East
June 15-17 • Marlborough, Mass.
www.pcbeast.com

IEEE 7th World Forum on Internet of Things (WF-IoT)
June 20-24 • New Orleans, La. + Online
https://wfiot2021.iot.ieee.org/

MilSatCom USA
June 23-24 • Online
www.smi-online.co.uk/defence/northamerica/MilSatCom-USA

MWC Barcelona
June 28-July 1 • Barcelona, Spain
www.mwcbarcelona.com

JULY

Satellite 2021
July 26-29 • Washington D.C.
www.satshow.com

IEEE EMC+SIPI 2021
July 27-August 13 • Online
www.emc2021.emcss.org

AUGUST

DesignCon 2021
August 16-18 • San Jose, Calif.
www.designcon.com/en/home.html

SEPTEMBER

IEEE PIMRC 2021
September 13-16 • Online
https://pimrc2021.ieee-pimrc.org/

OCTOBER

PCB West 2021
October 5-8 • Santa Clara, Calif.
www.pcbwest.com

Space Tech Expo USA
October 6-8 • Long Beach, Calif.
www.spacetechexpo.com

5G Antenna Conference
October 13 • Online
www.antennasonline.com

AMTA 2021
October 24-29 • Daytona Beach, Fla.
www.amta2021.org

Apply Online at www.eravant.com/careers

NOW HIRING!

Application Engineers
Design Engineers
Product Engineers
Test Engineers

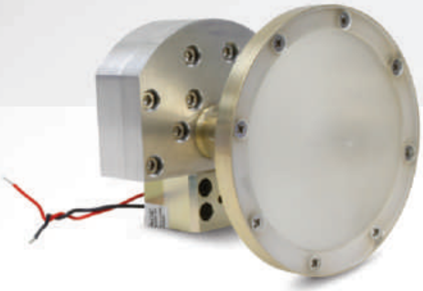

Ka Band Dual Channel Radar Sensor
SSS-35310-22L-D2 is Ka Band lens antenna-based Doppler sensor head for long-range moving target speed and direction detection applications. The operating frequency of the sensor is 35 GHz, the antenna gain is 22 dBi and system gain is 40 dB. This model can support large scale production.

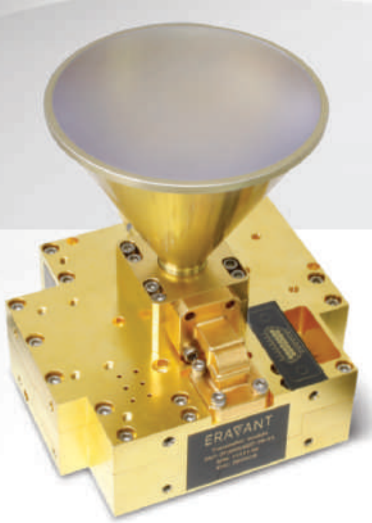

Space Qualified Integrated TX Module
SSK-ST2730253027-28-C1 is a Ka Band compact transmitter module operating at 26.8 GHz. This product is designed and manufactured for small satellite applications. The module incorporates a phase locked oscillator and an integrated 23 dBi circular polarized lens corrected antenna which delivers +50 dBm EIRP. Many modules are in orbit.

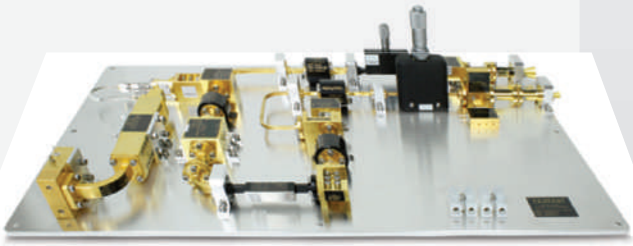

V & D Band Dual Transceiver
SSK-SC1246031010-1506-HU1 is a dual-band transceiver sub-assembly to cover both V & D Band operations. The trasnmitter portion upconverts 7.125-8 GHz into 57-64 GHz with +15 dBm output power. The receiver is D band and has a typical conversion loss of 0 dB in the frequency range of 114-128 GHz

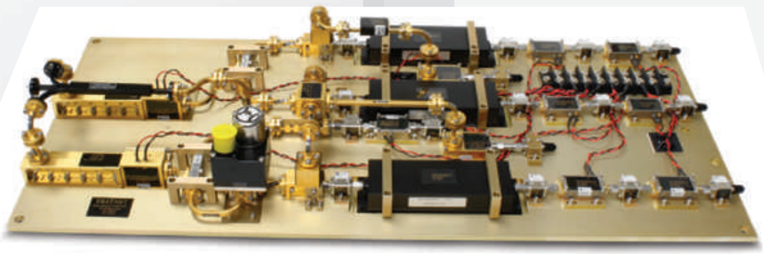

E Band Dual Channel Downconverter
SSK-SR723843-12-C1 is an E band, dual-channel down converter. It takes a 72 or 84 GHz signal at -100 dBm power and down converts them to 6 GHz. The system incorporates LNAs to minimize noise figure. The LO uses an external source at 9.75 GHz and an internal 8x multiplier to reach 78 GHz. The mixers can be pumped. Total system gain is 100 dB.

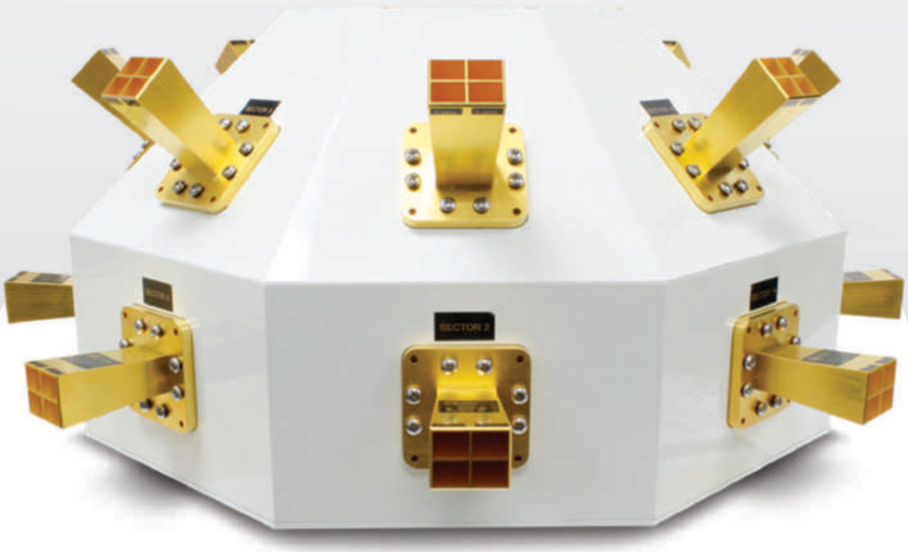

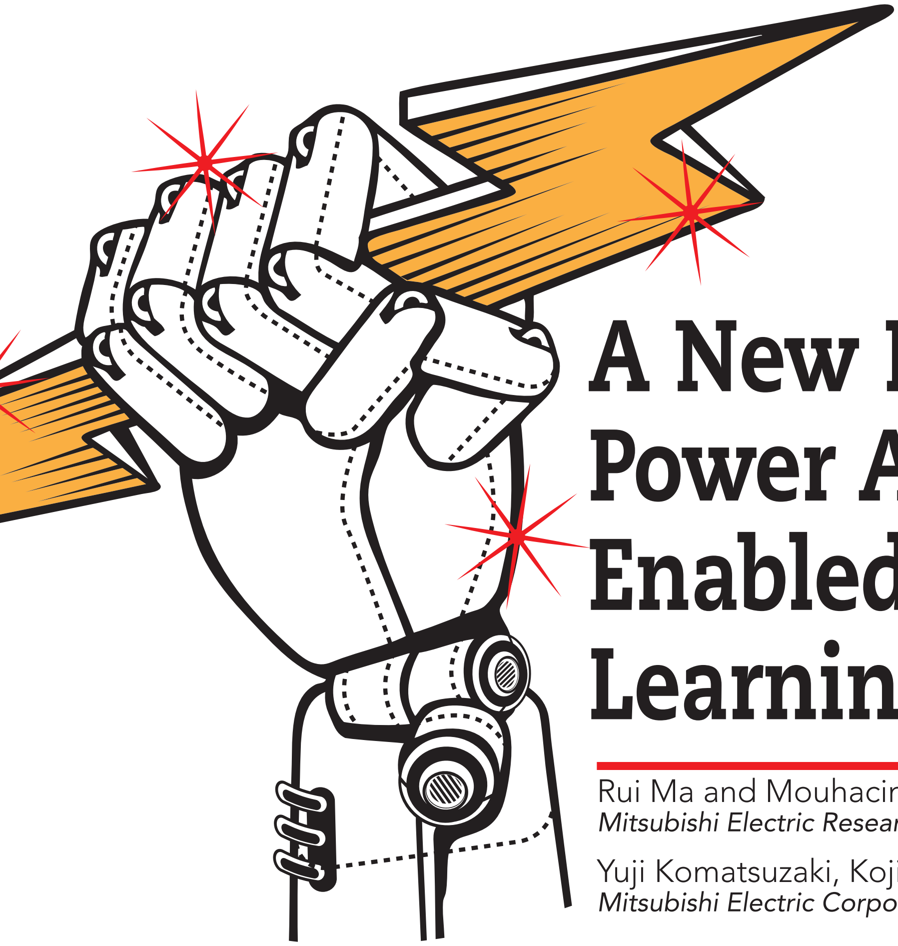

A New Frontier for Power Amplifiers Enabled by Machine Learning

Rui Ma and Mouhacine Benosman
Mitsubishi Electric Research Laboratories, Cambridge, Mass.

Yuji Komatsuzaki, Koji Yamanaka and Shintaro Shinjo
Mitsubishi Electric Corporation, Kamakura, Japan

Artificial intelligence (AI) and machine learning (ML) technologies are pervasive in our daily life empowering devices ranging from smart speakers to thermostats, self-driving cars to robots and social networks to banking systems. In wireless communications, ML has been recently applied across all layers including network planning, spectrum sensing, channel modeling, security and even the smart applications running on our mobile devices. Meanwhile, some are envisioning a future communication system that brings the hyper-connected experience to every corner of life in beyond 5G and 6G.[1] Application and deployment of AI technology for next-generation wireless communications have the profound potential to improve the end-to-end experience and reduce both the CAPEX and OPEX of networks.[2] AI becomes a necessary tool for delivering reliable and versatile services to connect hundreds of billions of machines and humans.

Improving radio hardware performance of radio access network, particularly, RF power amplifiers (PAs), has been a long-lasting challenge with ever-increasing system demands. In the past decades, RF engineers have spent numerous efforts to enhance PAs figure of merits such as power efficiency, gain, bandwidth and linearity. They came up with many brilliant solutions. Nevertheless, as the complexities of advanced PA circuits, modules and systems keep increasing, it becomes even more challenging and time consuming to design, operate and optimize PAs for highly dynamic signals with fast varying envelopes, dynamic network traffic and beam dependent radio environments such as massive-MIMO. However, such challenging use cases are becoming very common for modern mobile communications.

This article focuses on the recent studies of introducing ML for radio frequency PAs' online operational conditions optimization, primarily at sub-6 GHz frequency of 5G. Two demonstrators of advanced PA architectures are designed with cutting edge 0.15 μm GaN high electron mobility transistor (HEMT) technology, namely: a digital Doherty power amplifier (DDPA) and an innovative digitally assisted ultra-wideband mixed mode dual-input PA based on frequency-periodic load modulation (FPLM). For both examples, compact data-driven ML techniques are applied to significantly boost PAs performance. Combined with innovative hardware design, AI and ML can become a powerful tool to assist RF engineers dealing with sophisticated PAs design and operating challenges.

DIGITAL TO INTELLIGENT DOHERTY PA

Doherty PAs have been the workhorse for cellular base station radio transmitters[3] thanks to its relatively simple topology and attractive average power efficiency for amplifying signals with high peak-to-average power ratio (PAPR > 6 dB). Due to its active load pulling principles and analog nature, Doherty PAs still suffer from several key limitations such as non-optimal power splitting ratio, phase alignment and peaking amplifier turning-ON, especially over wide RF bands and input power levels.

COAXIAL DIRECTIONAL COUPLERS

RLC has the exact solution you're looking for.

Our complete line of Directional Couplers covers cellular, octave and broadband frequencies.
Designs include micro-strip, stripline and airline for high power applications.

- Frequencies from 10 MHz to 40 GHz
- Power ratings up to 500 watts average
- Custom design & packaging
- Low loss, high directivity
- Single or dual directional
- Low coupling variation
- Surface mount
- Directional detectors
- Very low passive intermodulation designs
- Standard connector types
- Waveguide

For more detailed information on Directional Couplers and Directional Detectors, visit our web site.

RLC ELECTRONICS, INC.

83 Radio Circle, Mount Kisco, New York 10549 • Tel: 914.241.1334 • Fax: 914.241.1753
E-mail: sales@rlcelectronics.com • www.rlcelectronics.com

ISO 9001:2000 CERTIFIED

VISA MasterCard

RLC is your complete microwave component source...
Switches, Filters, Power Dividers, Terminations, Attenuators, DC Blocks, Bias Tees & Detectors.

To overcome such difficulties, various modified design methods and architectures including Advanced Doherty Alignment module and DDPA were proposed by eliminating the conventional analog-based power splitting circuitry (i.e., Wilkinson divider). Instead, these designs are feeding dual-input RF signals directly to the Carrier and Peaking amplifiers of the Doherty PA, respectively.[4,5] Hence, the circuit can independently control input signals amplitudes and phases with better results. ***Figure 1*** provides a comparison of a Doherty PA and its modified version as dual-input DDPA. The input network change is highlighted in the figure.

Multi-input Doherty PA can be digitally controlled by following a set of derived closed-form equations, which approximate a pre-determined static power splitting ratio and phase imbalance between Carrier and Peaking amplifiers. Alternatively, it can be done by offline brute force search, finding an optimum input signal condition for high efficiency or high output power.[5-7] However, these two approaches have several limitations in practice: (1) derived mathematical equations only provide an approximation of highly non-linear relationships within a PA (i.e., using arctan function), (2) bias voltages optimization is not included but critical and (3) open-loop implementation does not capture the device-to-device variation or operating condition changes (i.e., ambient temperature). Consequently, manual tuning is still required to account for the dynamics of real systems and condition variations. Because of the large searching space of variables, brute force searching is inefficient for practical implementations.

Very recently, there have been new ML data-driven online optimization methods proposed and demonstrated. In an initial study shown by simulation,[9] a Simultaneous Perturbation Stochastic Approximation (SPSA) algorithm was applied to optimize the input power splitting ratio, phase offset and gate bias voltages at the same time for the Carrier and Peaking amplifiers of a dual-input Doherty PA using ADS and SystemVue software. The algorithm is here:

Algorithm 1 SPSA based optimization of digital DPA

Input: $\theta = [Vgs_m, Vgs_p, \phi, \alpha]$; % *Initial control parameters*
Input: $\theta_L = [Vgs_{mL}, Vgs_{p,L}, \phi_L, \alpha_L]$; % *Lower bound*
Input: $\theta_U = [Vgs_{mU}, Vgs_{p,U}, \phi_U, \alpha_U]$; % *Upper bound*
Input: c, λ_0 γ *and* γ_1; % *perturbation parameters*
Output: θ^* % *Optimal control parameters*

while *adaptation==True* **do**
  while *converge==False* **do**
    $k{+}{+}$
    clip θ between θ_L and θ_U
    $c_k = \frac{c}{k\gamma}$
    $\lambda_k = \frac{\lambda}{(\lambda_0 + k)^{\gamma}}$
    $\Delta = Bernouli(1, p)$; % *Bernouli perturbation*
    $\theta_+ = theta + c_k \cdot \Delta$; % *+ve perturbation*
    $\theta_- = theta - c_k \cdot \Delta$; % *-ve perturbation*
    Determine $C(\theta_-)$ and $C(\theta_+)$
    Calculate: $g = \frac{(C(\theta_+) - C(\theta_-))}{2 \cdot c_k \cdot \Delta}$
    Update: $\theta = \theta - \lambda_k \cdot g$
  end while
  Obtain optimal control parameter, θ^*
end while

It formulates digital DDPA real-time optimization as an adaptive online control problem by searching for an optimum solution for a user defined cost function consisting of several PAs figure of merits (a weighted sum of power, gain, efficiency and linearity etc.), as depicted by ***Figure 2***. Different hyper-parameters and initial conditions of optimization were tested. As a result, optimal points of power added efficiency can be found between 60 to 70 percent with many closely spaced local minimum points. A further development with a lab test bench, shown in ***Figure 3***, is a proof-of-concept and engineering demonstration that was implemented.[10]

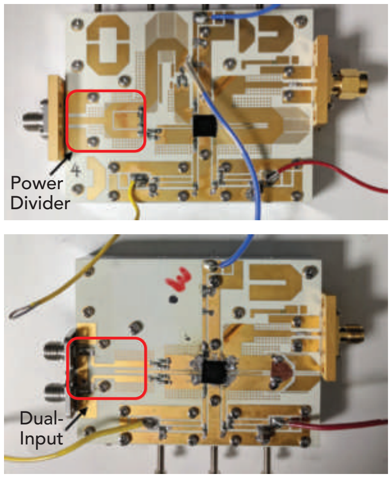

Fig. 1 A wideband Doherty power amplifier[8] and its modified version for dual-input Doherty power amplifier. The modified input power divider is outlined.

One setup implemented a model-free optimization method with simulated annealing (SA) and extremum seeking (ES), as shown in ***Figure 4***.[10] The combination of SA and ES makes the system optimization efficient. SA captures the random and abrupt variation in the system mainly due to frequency and input power level variations, where ES captures slow variation in the model such as temperature.

The compactness of the ML algorithm adopted here is quite different from the general deep learning ML category, such as deep neural network, in the sense that it neither requires massive training data nor powerful computation power and memory. This is an important feature for efficient implementation of RF front-end applications. ***Figure 5*** shows DDPA online auto-tuning of performance including output power, gain, power added efficiency via adaptive control of gate bias voltages (Vg_main, Vg_peak) and input power splitting ratio (α: how much power distributed to Peaking amplifier from total input) and phase imbalance (ΔΦ) using SA and ES. The optimization goal is to search for an optimal control parameters θ* maximizing cost function Q(θ), which is expressed as the weighted sum of PA performance of interest: $\theta^* = \mathrm{argmax}Q(\theta)$, $\theta \in U$, where θ is a vector of the amplifier tuning parameters defined as θ = [Vg_main, Vg_peak, ΔΦ, α].

As shown in Figure 5, it takes approximately 40 iterations for SA to perform random exploration with quick convergence, limited mainly by the interface communication of the test instruments. SA is then followed by ES algorithm for a fine tuning to account for effects such as temperature changes. The program is written in MATLAB and running on a PC controlling the measurement setup depicted in Figure 3. Significant performance en-

AnaPico Inc.
of Switzerland

We make
the difference

World Class RF & Microwave Test Instruments

VECTOR SIGNAL GENERATORS UP TO 40 GHZ
With Fast Control Port (FCP)

- Frequency ranges from 10 MHz to 4, 6, 12, 20 or 40 GHz
- 500 MS/s sampling rate, up to 512 MS deep internal playback memory
- Switching / settling time 200 ns
- Low phase noise: -145 dBc/Hz at 1 GHz and 20 kHz offset
- Fast Control Port for high-speed data streaming and agile control
- Single- and multi-channel models, bench-top and 19'' rack-mountable forms
- Applications: Quantum Computing, RADAR, EW, Avionics (DME, VOR, ILS), Etc.

BNC
Berkeley Nucleonics

For US Customers:
Call: 800-234-7858
Email: rfsales@berkeleynucleonics.com
Visit: https://tinyurl.com/u9wdx2w

AnaPico
of Switzerland

For Non-US Customers:
Email: rfsales@anapico.com
Visit: www.anapico.com

hancement in DDPA over a wider frequency range and different input power range (in particular lower input power range) has been observed compared with single input conventional Doherty PA thanks to the auto-tuning procedure. Over a 15 percent efficiency boost and 2 to 3 dB gain is realized without using digital predistortion (DPD). The algorithm is also able to figure out a reasonable tradeoff among these conflicting PA performance targets by assigning different weights in Q(θ). It must be mentioned that dedicated DPD schemes were not used.[10]

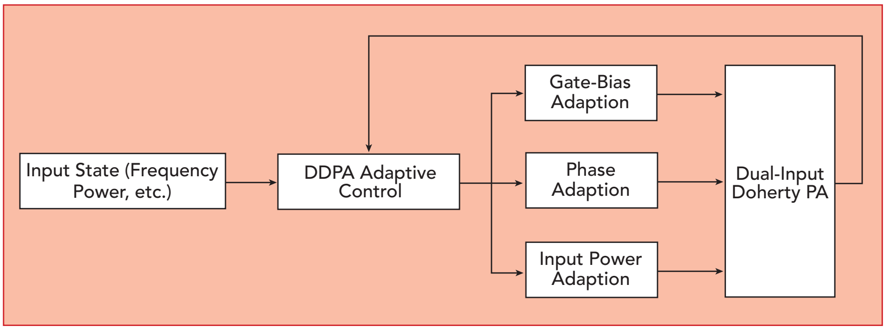

Fig. 2 Online optimization of dual-input Doherty PA.

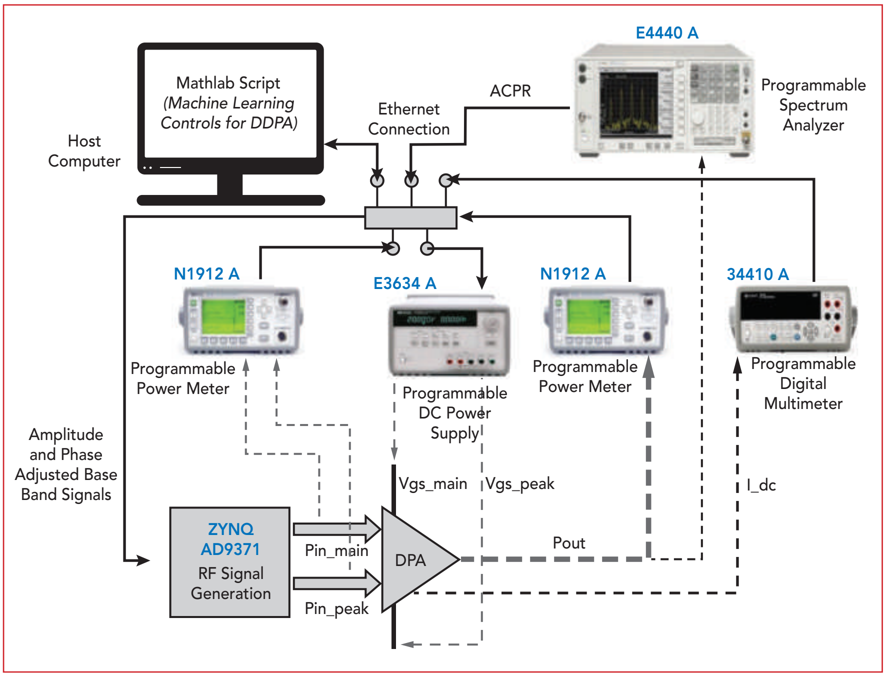

Fig. 3 Testbench of dual-input digital Doherty PA with machine learning online optimization.

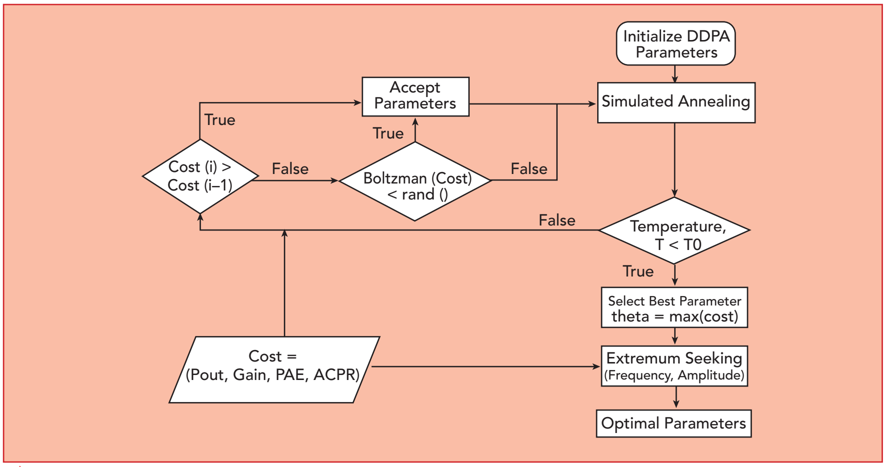

Fig. 4 Model-free machine learning algorithms used for DDPA optimization.[10]

DIGITALLY ASSISTED FREQUENCY-PERIODIC LOAD MODULATION PA

Doherty PAs in practice are limited in terms of RF bandwidth, due to many factors such as device parastics, power combiner and phase alignment challenges. An innovative mixed mode ultra-wideband FPLM PA has been proposed to achieve high power efficiency over multiple contiguous frequency bands, enabled by a digitally assisted dual-input AI module. It provides automatic optimum signal combination, magnitude and phase of dual-input signals. ***Figure 6*** illustrates several types of load modulations, such as a virtual open stub Doherty, Outphasing, general Doherty and anti-phasing Outphasing spanned over a 3x RF frequency range ($0.5f_0$~$1.5f_0$, f_0 denotes the design center frequency). Very distinct and proper input signal's amplitude and phase relationships are necessary for this amplifier to behave as Doherty and Outphasing modes over five different frequency ranges.

A new output combiner was also proposed by absorbing devices capacitances into part of the equivalent transmissions and providing differently desired output power combining functions for above mentioned five frequency ranges, respectively. The design details can be found in Y. Komatsuzaki et al.[11]

Figure 7 shows the FPLM GaN PA prototype consisting of two bare die chips with 0.15 μm HEMTs. Similar AI algorithms shown in Figure 4 have been adopted to auto-tuning the two RF input signals amplitude and phases based on a user defined cost function. The bias voltages of these two HEMTs are at pinch-off and not tuned during the optimizations. Without manual interaction and specifying the specific PA operation modes, the AI module is able to autotune the dual-channel transceivers parameters on the fly and achieves the desired PA modes with high efficiency. ***Figure 8*** shows the measured FPLM PA average ef-

A Quantic Company

- Amplifiers - Solid State
- Attenuators - Variable/ Programmable
- Bi-Phase Modulators
- Couplers (Quadrature, 180, Directional)
- Detectors - RF / Microwave
- DLVAs, ERDLVAs & SDLVAs
- Filters & Switched Filter Banks
- Form, Fit, Functional Products & Services
- Frequency Converters
- Frequency Sources
- Frequency Discriminators & IFM
- Frequency Synthesizers
- Gain & Loss Equalizers
- Integrated MIC/MMIC Assemblies (IMAs)
- IQ Vector Modulators
- Limiters - RF / Microwave
- Log Amps
- Miscellaneous Products
- Monopulse Comparators
- Multifunction Integrated Assemblies (IMAs)
- Phase Shifters & Bi-Phase Modulators
- Power Dividers/Combiners (Passive & Active)
- Pulse Modulators - SPST
- Rack & Chassis Mount Products
- Receiver Front Ends & Transceivers
- Single Side Band Modulators
- SMT & QFN Products
- Switch Matrices
- Switch Filter Banks
- Switches - Solid-State
- Systems - Radar Sense & Avoid
- Systems - Fly Eye Radar
- Threshold Detectors
- USB Products

Planar Monolithics Industries, Inc.

High Power Limiters up to 62 GHz

PMI offers a variety of mmWave Limiters capable of withstanding an input power level up to 200 W CW / 1 kW peak for military and industrial applications. PMI's limiters offer low loss, fast recovery along with low RF leakage levels and broadband coverage to 62 GHz. 2-IN-1 Dual Use Connectorized or Surface Mount Designs. More available at: https://www.pmi-rf.com/categories/limiters


LM-10M9G-100CW-1KWP-SFF


LM-10M35G-15DBM-4W-292FF
LM-10M50G-18DBM-4W-24FF
LM-10M62G-20DBM-1W-24FF


LM-20M18G-100W-15DBM


LM-0R3G8G-14-100W-SFF
LM-150M5G-200CW-2KWPK-AGAL

PMI Model No.	Freq Range (GHz)	Insertion Loss (dB)	Input Power	Leakage Power (dBm)	Recovery Time	Size (Inches) / Connectors
LM-10M9G-100CW-1KWP-SFF https://www.pmi-rf.com/product-details/lm-10m9g-100w-1kwp-sff	10 MHz - 9	2.0	100 W CW, 10 MHz to 8.0 GHz 80 W CW at 9.0 GHz	+20	100 ns	1.86" x 0.65" x 0.38" SMA (F) Field Removable
LM-10M35G-15DBM-4W-292FF https://www.pmi-rf.com/product-details/lm-10m35g-15dbm-4w-292ff	10 MHz - 35	4.0	Up to 25 W CW & Up to 50 W Peak 1 µs PW, 1% duty cycle	+18	150 ns	0.53" X 0.70" X 0.26" 2.92mm (F) Field Removable and SMT (Drop-In)
LM-10M50G-18DBM-4W-24FF https://www.pmi-rf.com/product-details/lm-10m50g-18dbm-4w-24ff	10 MHz - 50	2.5	4 W CW & 20 W peak, PW 1 µs to 10 µs, 1% duty cycle	+18	100 ns	0.53" X 0.70" X 0.26" 2.92mm (F) Field Removable and SMT (Drop-In)
LM-10M62G-20DBM-1W-24FF https://www.pmi-rf.com/product-details/lm-10m62g-20dbm-1w-24ff	10 MHz - 62	4.0	Up to 1.5 W CW & Up to 10 W Peak PW 1 µs, 1% duty cycle	+22	100 ns	0.53" X 0.70" X 0.26" 2.4mm (F) Field Removable and SMT (Drop-In)
LM-20M18G-100W-15DBM https://www.pmi-rf.com/product-details/lm-20m18g-100w-15dbm	20 MHz - 18	2.6	100 W CW Max 1 kW Peak Min @ +85 °C 1 µs Pulse Width, 0.1% duty cycle	+20	100 ns	0.90" x 0.38" x 0.38" SMA (M) / SMA (F)
LM-150M5G-200CW-2KWPK-AGAL https://www.pmi-rf.com/product-details/lm-150m5g-200cw-2kwpk-agal	0.15 - 5	2.0	200 W CW (+53 dBm) 2 kW Peak (+63 dBm) 25 µs PW, 5% duty cycle	+20	100 ns	1.00" x 0.68" x 0.35" SMA (F) Field Removable
LM-0R3G8G-14-100W-SFF https://www.pmi-rf.com/product-details/lm-0r3g8g-14-100w-sff	0.3 - 8	2.2	100 W CW (+50 dBm) +50 dBm Peak, 25 µs PW, 5% duty cycle	+15	100 ns	1.00" x 0.68" x 0.35" SMA (F) Field Removable
LM-10M14G-100W-1KWP-SFF-OPT17 https://www.pmi-rf.com/product-details/lm-10m14g-100w-1kwp-sff-opt17	1 - 7	2.0	100 W CW Max, (-55 °C to +85 °C) 1 kW Peak, 1 µs PW, 1% duty cycle	+17	100 ns	0.90" x 0.38" x 0.38" SMA (M) / SMA (F)
LM-2G4G-15-100W-SFF https://www.pmi-rf.com/product-details/lm-2g4g-15-100w-sff	2 - 4	1.5	100 W CW (+50 dBm) 250 W Peak (+54 dBm) 1 ms PW, 10% duty cycle	+21	1 µs	1.00" x 0.68" x 0.35" SMA (F) Field Removable
LM-2G18G-18-20W-1KWP-SFF https://www.pmi-rf.com/product-details/lm-2g18g-18-20w-1kwp-sff	2 - 18	2.6	+43 dBm CW +50 dBm 10% DC, 40 µs PW	+18	100 ns	1.00" x 1.00" x 0.40" SMA (F) Field Removable
LM-18G40G-SMT-1 https://www.pmi-rf.com/product-details/lm-18g40g-smt-1	18 - 40	4	20 W peak, 440 - 670 ns PW, PRF 600 - 900 kHz, 40% Duty Cycle	+14	250 ns	0.27" x 0.198" x 0.016" surface mount / drop-in carrier


LM-10M14G-100W-1KWP-SFF-OPT17


LM-2G4G-15-100W-SFF


LM-2G18G-18-20W-1KWP-SFF

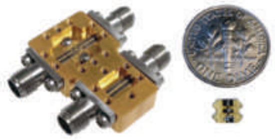
LM-18G40G-SMT-1

West Coast Operation:
4921 Robert J. Mathews Pkwy, Suite 1
El Dorado Hills, CA 95762 USA
Tel: 916-542-1401, Fax: 916-265-2597

East Coast Operation:
7311-F Grove Road
Frederick, MD 21704 USA
Tel: 301-662-5019, Fax: 301-662-1731

sales@pmi-rf.com • www.pmi-rf.com

ISO9001-2015 REGISTERED

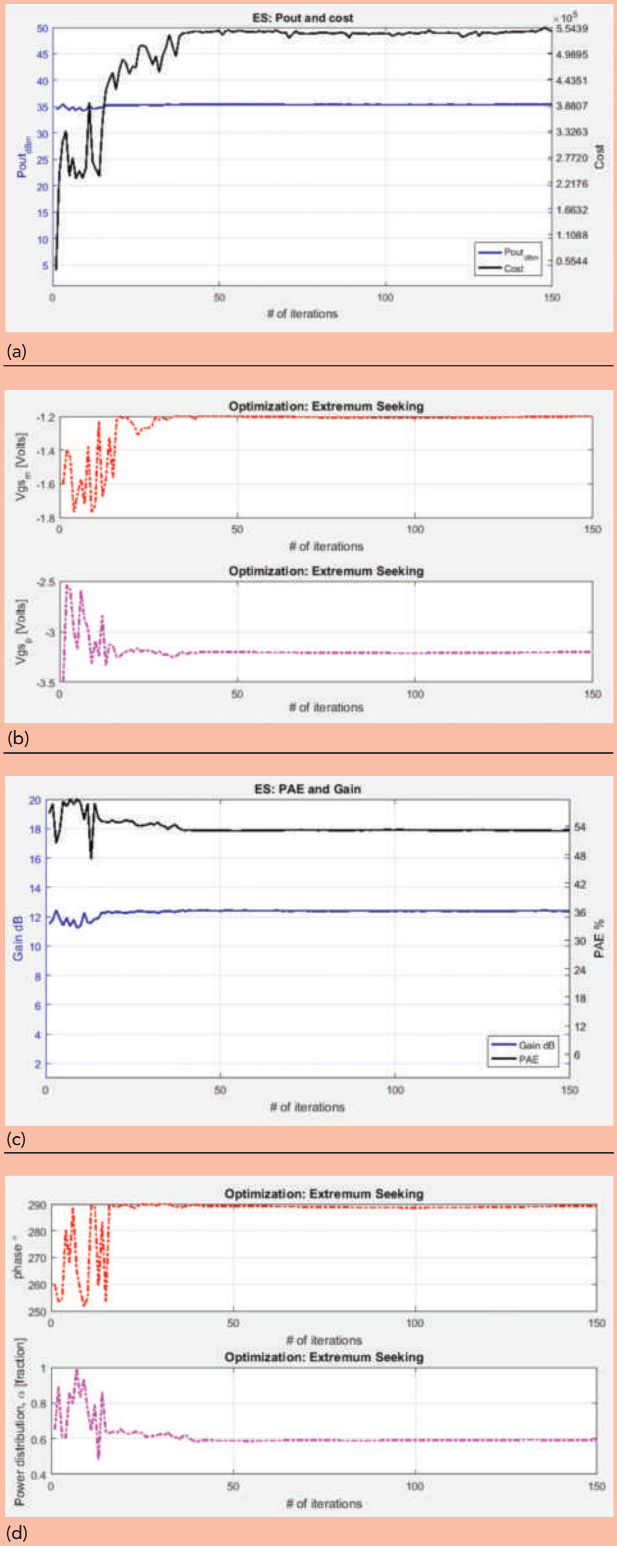

Fig. 5 DDPA performance with online auto-tuning of control parameter: Pout and defined cost function (a), gate bias voltages for main and peaking amplifier (b), PAE and Gain (c) and input phase imbalance and power splitting ratio (d).

ficiency (6 dB back-off) over the whole band.

A detailed analysis of the operating mode at each frequency range is omitted here but can be found in Komatsuzaki et al.[11] Digital assistance is able to fully use the FPLM PA's design potential and handle its sophisticated control and optimization thus offering the state-of-the-art efficiency performance over 110 percent fractional bandwidths, as compared in ***Table 1***.

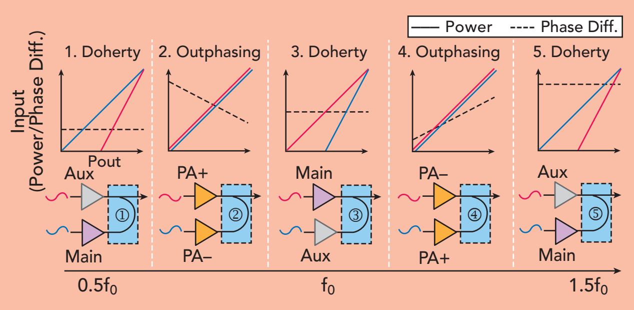

Fig. 6 Concept of a frequency-periodic load modulated (FPLM) PA with controlled dual-input signal over frequency, and f_0 being the center frequency.

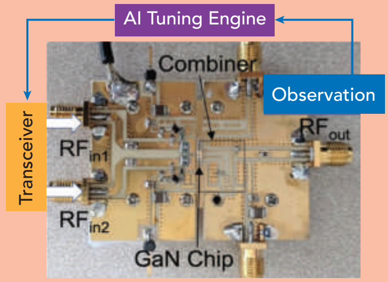

Fig. 7 Prototype of a dual-input FPLM GaN PA under AI digitally assisted operation.

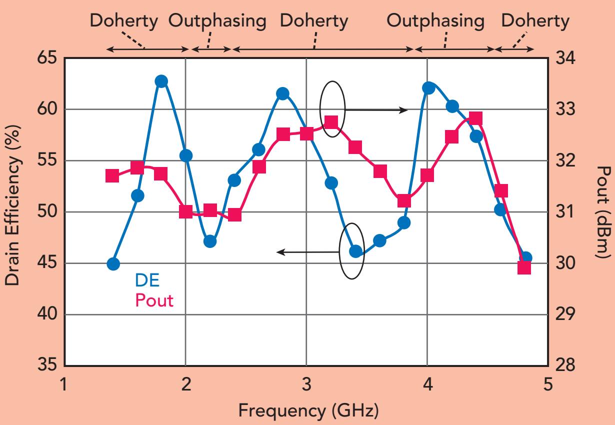

Fig. 8 Measurement of the prototype dual-input FPLM PA.

A History of Proving that Performance Barriers are Made to be *SHATTERED*

Marki® microwave

1991
Marki Microwave is founded by Ferenc and Christine Marki

1998
Support for US Army Longbow Missile Program with high performance carrier mixer

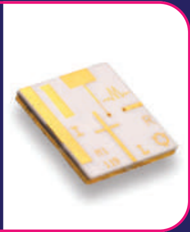

2000


Purchase of 10,000 square-foot space for headquarters and manufacturing in Morgan Hill, CA

2002


4-lag correlator for ASIAA to detect "big bang" radiation

2004
Introduction of the T3 Mixer – Still the best mixer on the planet

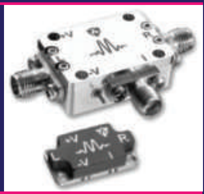

2007
Dr. Christopher Marki joins to develop new and complementary product lines

2013


Introduction of the Microlithic mixer – solving the mixer paradox

2016
- Dr. Christopher Marki becomes CEO
- 10,000 square foot expansion to support unprecedented growth
- Release of MMIC IQ Mixers, Nonlinear Transmission lines, Equalizers & Diode Limiters

2017
- Company grows past 100 employees
- Accelerating the innovation in MMIC mixers with the world's first MMIC T3 mixer, broadband triple-balanced MMIC mixer and multi-octave MMIC mixer

2018
Release of over 50 new products including Marki's first space-grade MMIC product

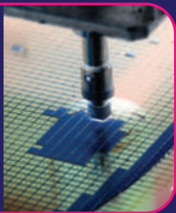

2020


Breaking 100GHz barrier and safely maintained production throughout COVID-19

2021


Expansion to a 60,000 square foot facility in Morgan Hill

Since 1991, Marki Microwave has invented technologies that empower the RF and microwave industry to design faster, simplify production, eliminate complexity and shatter performance barriers.

SHATTERING PERFORMANCE BARRIERS SINCE 1991 — 30 YEARS

To view our comprehensive catalog, visit

TABLE 1

COMPARISON OF SUB-6 GHz HIGH EFFICIENCY WIDEBAND AMPLIFIERS

Ref.	Year	Freq (GHz)	Fractional BW (%)	Efficiency (%)	Pout (dBm)	Configuration	Backoff
[12]	2012	3 to 3.6	18	38 to 56	37 to 38	Doherty	6 dB (CW)
[7]	2013	1 to 3	100	48 to 68	37.1 to 38.9	Doherty-Outphasing	6 dB (CW)
[13]	2017	0.9 to 2.15	82	32 to 36	30.0 to 30.7	Envelope Tracking	6 dB (CW)
This work [11]	2019	1.4 to 4.8	110	45 to 62	29.9 to 32.8	FPLM PA	6 dB (CW)

SUMMARY

The reported applications show that compact data-driven AI techniques can assist in unlocking the full potential of new high performance PAs for flexible and wideband wireless applications. Even after deployment in the field, these devices can adapt to changing operating conditions. Integrating cutting edge GaN semiconductor device technology, circuit design innovation and AI (digital assisted auto-tuning together with digital front-end including digital predistortion[14]) will facilitate a solution of agile and superior performance RF front-ends. It is worth pointing out that the proposed methodology is not only applicable for cellular transmitters, but also for mobile handset and general RF applications (such as microwave industrial heating), in which RF hardware/amplifiers are the key device dominating the system-level performance. Its adaptability and intelligence make AI-assisted RF front-end modules a highly promising solution for future radios.■

References

1. 6G Vision Whitepaper, *The Next Hyper Connected Experience for All*, Samsung Research, July 2020.
2. X. Zhou et al., "Intelligent Wireless Communications Enabled by Cognitive Radio and ML," *China Communications*, December 2018, pp. 16–48.
3. F. H. Raab et al., "Power Amplifiers and Transmitters for RF and Microwave," *IEEE Transactions on Microwave Theory and Techniques*, Vol. 50, No. 3, March 2002, pp. 814–826.
4. A. Ahmed et al., "Line-up Efficiency Improvement Using Dual Path Doherty Power Amplifier," *2013 European Microwave Conference*, 2013, pp. 275–278.

5. R. Darraji et al., "Doherty Goes Digital: Digitally Enhanced Doherty Power Amplifiers," *IEEE Microwave Magazine*, Vol. 17, No. 8, August 2016. pp. 41–51.
6. R. Darraji and F. M. Ghannouchi, "Digital Doherty Amplifier with Enhanced Efficiency and Extended Range," *IEEE Transactions on Microwave Theory and Techniques*, Vol. 59, No. 11, November 2011, pp. 2898–2909.
7. C. M. Andersson et al., "A 1–3 GHz Digitally Controlled Dual-RF Input Power-Amplifier Design Based on a Doherty-Outphasing Continuum Analysis," *IEEE Transactions on Microwave Theory and Techniques*, Vol. 61, No. 10, Oct. 2013, pp. 3743–3752.
8. Y. Komatsuzaki et al., "3.0–3.6 GHz Wideband, Over 46% Average Efficiency GaN Doherty Power Amplifier with Frequency Dependency Compensating Circuits," *IEEE Topical Conference on RF/Microwave Power Amplifiers for Radio and Wireless Applications (PAWR)*, 2017, pp. 22–24.
9. S. Niu et al., "Stochastically Approximated Multi Objective Optimization of Dual Input Digital Doherty Power Amplifier," *IEEE 10th International Workshop on Computational Intelligence and Applications (IWCIA)*, 2017, pp. 147–152.
10. R. Ma et al., "Machine-Learning Based Digital Doherty Power Amplifier," *IEEE International Symposium on Radio-Frequency Integration Technology (RFIT)*, 2018, pp. 1–3.
11. Y. Komatsuzaki et al., "A Novel 1.4-4.8 GHz Ultra-Wideband, Over 45% High Efficiency Digitally Assisted Frequency-Periodic Load Modulated Amplifier," *IEEE MTT-S International Microwave Symposium (IMS)*, 2019, pp. 706–709.
12. J. M. Rubio et al., "3–3.6-GHz Wideband GaN Doherty Power Amplifier Exploiting Output Compensation Stages," *IEEE Transactions on Microwave Theory and Techniques*, Vol. 60, No. 8, Aug. 2012, pp. 2543–2548.
13. S. Sakata et al., "An 80 MHz Modulation Bandwidth High Efficiency Multi-Band Envelope-Tracking Power Amplifier Using GaN Single-Phase Buck-Converter," *IEEE MTT-S International Microwave Symposium (IMS)*, 2017, pp. 1854–1857.
14. M. Mengozzi et al., "A. GaN Power Amplifier Digital Predistortion by Multi-Objective Optimization for Maximum RF Output Power," *Electronics*, 2021, https://doi.org/10.3390/electronics10030244.

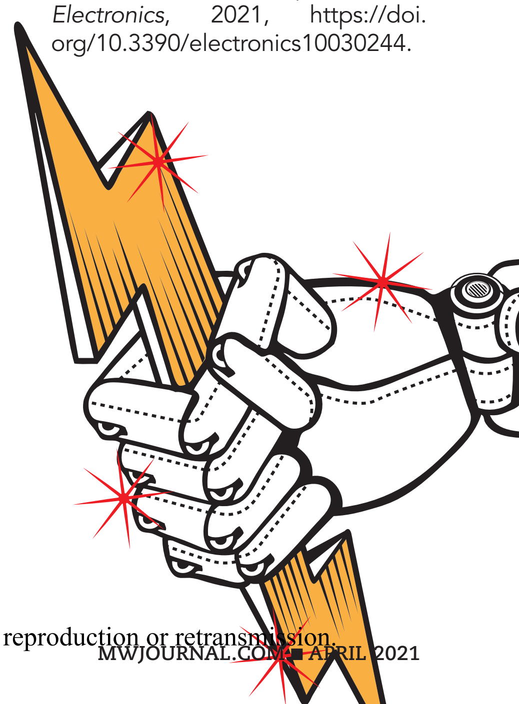

RF Amplifiers and Sub-Assemblies for Every Application

Delivery from Stock to 2 Weeks ARO from the catalog or built to your specifications!

- Competitive Pricing & Fast Delivery
- Military Reliability & Qualification
- Various Options: Temperature Compensation, Input Limiter Protection, Detectors/TTL & More
- Unconditionally Stable (100% tested)

ISO 9001:2000 and AS9100B CERTIFIED

OCTAVE BAND LOW NOISE AMPLIFIERS

Model No.	Freq (GHz)	Gain (dB) MIN	Noise Figure (dB)	Power-out @ P1-dB	3rd Order ICP	VSWR
CA01-2110	0.5-1.0	28	1.0 MAX, 0.7 TYP	+10 MIN	+20 dBm	2.0:1
CA12-2110	1.0-2.0	30	1.0 MAX, 0.7 TYP	+10 MIN	+20 dBm	2.0:1
CA24-2111	2.0-4.0	29	1.1 MAX, 0.95 TYP	+10 MIN	+20 dBm	2.0:1
CA48-2111	4.0-8.0	29	1.3 MAX, 1.0 TYP	+10 MIN	+20 dBm	2.0:1
CA812-3111	8.0-12.0	27	1.6 MAX, 1.4 TYP	+10 MIN	+20 dBm	2.0:1
CA1218-4111	12.0-18.0	25	1.9 MAX, 1.7 TYP	+10 MIN	+20 dBm	2.0:1
CA1826-2110	18.0-26.5	32	3.0 MAX, 2.5 TYP	+10 MIN	+20 dBm	2.0:1

NARROW BAND LOW NOISE AND MEDIUM POWER AMPLIFIERS

Model No.	Freq (GHz)	Gain (dB) MIN	Noise Figure (dB)	Power-out @ P1-dB	3rd Order ICP	VSWR
CA01-2111	0.4 - 0.5	28	0.6 MAX, 0.4 TYP	+10 MIN	+20 dBm	2.0:1
CA01-2113	0.8 - 1.0	28	0.6 MAX, 0.4 TYP	+10 MIN	+20 dBm	2.0:1
CA12-3117	1.2 - 1.6	25	0.6 MAX, 0.4 TYP	+10 MIN	+20 dBm	2.0:1
CA23-3111	2.2 - 2.4	30	0.6 MAX, 0.45 TYP	+10 MIN	+20 dBm	2.0:1
CA23-3116	2.7 - 2.9	29	0.7 MAX, 0.5 TYP	+10 MIN	+20 dBm	2.0:1
CA34-2110	3.7 - 4.2	28	1.0 MAX, 0.5 TYP	+10 MIN	+20 dBm	2.0:1
CA56-3110	5.4 - 5.9	40	1.0 MAX, 0.5 TYP	+10 MIN	+20 dBm	2.0:1
CA78-4110	7.25 - 7.75	32	1.2 MAX, 1.0 TYP	+10 MIN	+20 dBm	2.0:1
CA910-3110	9.0 - 10.6	25	1.4 MAX, 1.2 TYP	+10 MIN	+20 dBm	2.0:1
CA1315-3110	13.75 - 15.4	25	1.6 MAX, 1.4 TYP	+10 MIN	+20 dBm	2.0:1
CA12-3114	1.35 - 1.85	30	4.0 MAX, 3.0 TYP	+33 MIN	+41 dBm	2.0:1
CA34-6116	3.1 - 3.5	40	4.5 MAX, 3.5 TYP	+35 MIN	+43 dBm	2.0:1
CA56-5114	5.9 - 6.4	30	5.0 MAX, 4.0 TYP	+30 MIN	+40 dBm	2.0:1
CA812-6115	8.0 - 12.0	30	4.5 MAX, 3.5 TYP	+30 MIN	+40 dBm	2.0:1
CA812-6116	8.0 - 12.0	30	5.0 MAX, 4.0 TYP	+33 MIN	+41 dBm	2.0:1
CA1213-7110	12.2 - 13.25	28	6.0 MAX, 5.5 TYP	+33 MIN	+42 dBm	2.0:1
CA1415-7110	14.0 - 15.0	30	5.0 MAX, 4.0 TYP	+30 MIN	+40 dBm	2.0:1
CA1722-4110	17.0 - 22.0	25	3.5 MAX, 2.8 TYP	+21 MIN	+31 dBm	2.0:1

ULTRA-BROADBAND & MULTI-OCTAVE BAND AMPLIFIERS

Model No.	Freq (GHz)	Gain (dB) MIN	Noise Figure (dB)	Power-out @ P1-dB	3rd Order ICP	VSWR
CA0102-3111	0.1-2.0	28	1.6 Max, 1.2 TYP	+10 MIN	+20 dBm	2.0:1
CA0106-3111	0.1-6.0	28	1.9 Max, 1.5 TYP	+10 MIN	+20 dBm	2.0:1
CA0108-3110	0.1-8.0	26	2.2 Max, 1.8 TYP	+10 MIN	+20 dBm	2.0:1
CA0108-4112	0.1-8.0	32	3.0 MAX, 1.8 TYP	+22 MIN	+32 dBm	2.0:1
CA02-3112	0.5-2.0	36	4.5 MAX, 2.5 TYP	+30 MIN	+40 dBm	2.0:1
CA26-3110	2.0-6.0	26	2.0 MAX, 1.5 TYP	+10 MIN	+20 dBm	2.0:1
CA26-4114	2.0-6.0	22	5.0 MAX, 3.5 TYP	+30 MIN	+40 dBm	2.0:1
CA618-4112	6.0-18.0	25	5.0 MAX, 3.5 TYP	+23 MIN	+33 dBm	2.0:1
CA618-6114	6.0-18.0	35	5.0 MAX, 3.5 TYP	+30 MIN	+40 dBm	2.0:1
CA218-4116	2.0-18.0	30	3.5 MAX, 2.8 TYP	+10 MIN	+20 dBm	2.0:1
CA218-4110	2.0-18.0	30	5.0 MAX, 3.5 TYP	+20 MIN	+30 dBm	2.0:1
CA218-4112	2.0-18.0	29	5.0 MAX, 3.5 TYP	+24 MIN	+34 dBm	2.0:1

LIMITING AMPLIFIERS

Model No.	Freq (GHz)	Input Dynamic Range	Output Power Range Psat	Power Flatness dB	VSWR
CLA24-4001	2.0 - 4.0	-28 to +10 dBm	+7 to +11 dBm	+/- 1.5 MAX	2.0:1
CLA26-8001	2.0 - 6.0	-50 to +20 dBm	+14 to +18 dBm	+/- 1.5 MAX	2.0:1
CLA712-5001	7.0 - 12.4	-21 to +10 dBm	+14 to +19 dBm	+/- 1.5 MAX	2.0:1
CLA618-1201	6.0 - 18.0	-50 to +20 dBm	+14 to +19 dBm	+/- 1.5 MAX	2.0:1

AMPLIFIERS WITH INTEGRATED GAIN ATTENUATION

Model No.	Freq (GHz)	Gain (dB) MIN	Noise Figure (dB)	Power-out @ P1-dB	Gain Attenuation Range	VSWR
CA001-2511A	0.025-0.150	21	5.0 MAX, 3.5 TYP	+12 MIN	30 dB MIN	2.0:1
CA05-3110A	0.5-5.5	23	2.5 MAX, 1.5 TYP	+18 MIN	20 dB MIN	2.0:1
CA56-3110A	5.85-6.425	28	2.5 MAX, 1.5 TYP	+16 MIN	22 dB MIN	1.8:1
CA612-4110A	6.0-12.0	24	2.5 MAX, 1.5 TYP	+12 MIN	15 dB MIN	1.9:1
CA1315-4110A	13.75-15.4	25	2.2 MAX, 1.6 TYP	+16 MIN	20 dB MIN	1.8:1
CA1518-4110A	15.0-18.0	30	3.0 MAX, 2.0 TYP	+18 MIN	20 dB MIN	1.85:1

LOW FREQUENCY AMPLIFIERS

Model No.	Freq (GHz)	Gain (dB) MIN	Noise Figure dB	Power-out @ P1-dB	3rd Order ICP	VSWR
CA001-2110	0.01-0.10	18	4.0 MAX, 2.2 TYP	+10 MIN	+20 dBm	2.0:1
CA001-2211	0.04-0.15	24	3.5 MAX, 2.2 TYP	+13 MIN	+23 dBm	2.0:1
CA001-2215	0.04-0.15	23	4.0 MAX, 2.2 TYP	+23 MIN	+33 dBm	2.0:1
CA001-3113	0.01-1.0	28	4.0 MAX, 2.8 TYP	+17 MIN	+27 dBm	2.0:1
CA002-3114	0.01-2.0	27	4.0 MAX, 2.8 TYP	+20 MIN	+30 dBm	2.0:1
CA003-3116	0.01-3.0	18	4.0 MAX, 2.8 TYP	+25 MIN	+35 dBm	2.0:1
CA004-3112	0.01-4.0	32	4.0 MAX, 2.8 TYP	+15 MIN	+25 dBm	2.0:1

CIAO Wireless can easily modify any of its standard models to meet your "exact" requirements at the Catalog Pricing.

Visit our web site at **www.ciaowireless.com** for our complete product offering.

Ciao wireless

Ciao Wireless, Inc. 4000 Via Pescador, Camarillo, CA 93012
Tel (805) 389-3224 Fax (805) 389-3629 sales@ciaowireless.com

New Quantum Receiver the First to Detect Entire Radio Frequency Spectrum

A new quantum sensor can analyze the full spectrum of radio frequency and real-world signals, unleashing new potentials for soldier communications, spectrum awareness and electronic warfare. Army researchers built the quantum sensor, which can sample the radio frequency spectrum—from 0 to 20 GHz—and detect AM and FM radio, Bluetooth, Wi-Fi and other communication signals.

The Rydberg sensor uses laser beams to create highly-excited Rydberg atoms directly above a microwave circuit, to boost and hone in on the portion of the spectrum being measured. The Rydberg atoms are sensitive to the circuit's voltage, enabling the device to be used as a sensitive probe for the wide range of signals in the RF spectrum.

"All previous demonstrations of Rydberg atomic sensors have only been able to sense small and specific regions of the RF spectrum, but our sensor now operates continuously over a wide frequency range for the first time," said Dr. Kevin Cox, a researcher at the U.S. Army Combat Capabilities Development Command, now known as DEVCOM, Army Research Laboratory. "This is a really important step toward proving that quantum sensors can provide a new, and dominant, set of capabilities for our soldiers, who are operating in an increasingly complex electromagnetic battlespace."

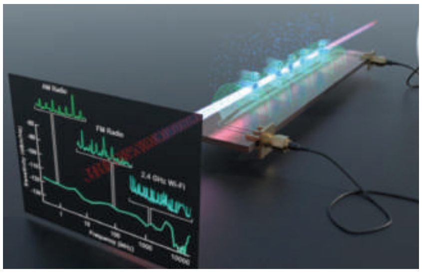

Rydberg Receiver (Source: U. S. Army Illustration)

The Rydberg spectrum analyzer has the potential to surpass fundamental limitations of traditional electronics in sensitivity, bandwidth and frequency range. Because of this, the lab's Rydberg spectrum analyzer and other quantum sensors have the potential to unlock a new frontier of Army sensors for spectrum awareness, electronic warfare, sensing and communications—part of the Army's modernization strategy.

"Devices that are based on quantum constituents are one of the Army's top priorities to enable technical surprise in the competitive future battlespace," said Army researcher Dr. David Meyer. "Quantum sensors in general, including the one demonstrated here, offer unparalleled sensitivity and accuracy to detect a wide range of mission-critical signals."

The researchers plan additional development to improve the signal sensitivity of the Rydberg spectrum analyzer, aiming to outperform existing state-of-the-art technology.

Developing Advanced Military GPS Receivers and Chips

BAE Systems received a $247 million contract from the U.S. Space Force's Space and Missile Systems Center to design and manufacture an advanced military GPS receiver and next-generation semiconductor. The technology will provide positioning, navigation and timing capabilities to warfighters so they can execute missions in challenging electromagnetic environments.

GPS Receiver (Source: BAE Systems)

The Military GPS User Equipment Increment 2 Miniature Serial Interface program will provide improved capabilities for size-constrained and power-constrained military GPS applications, including precision-guided munitions and battery-powered handheld devices. The program will focus on the certification of an advanced application-specific integrated circuit and the development of an ultra-small, low-power GPS module. Both products will work with the next-generation military M-Code signal technology, which provides reliable GPS data with anti-jamming and anti-spoofing capabilities to protect against electronic warfare threats.

Leonardo's Drink-Can-Sized Decoy Launched from GA-ASI MQ-9

Following its successful testing and entry into service with the U.K.'s Royal Air Force, the unique BriteCloud capability is now being evaluated for use by U.S. Armed Forces.

Leonardo and General Atomics Aeronautical Systems Inc. are working together to bring the world-class protection offered by Leonardo's BriteCloud expendable active decoy to operators of the MQ-9 remotely piloted aircraft system. The joint activity is addressing the growing market need to protect the high-value unmanned aircraft from modern, radar-guided threats as they carry out their missions.

Progress has already been made, with a number of BriteCloud rounds successfully launched from an MQ-9 in an aircraft survivability 'carriage and release' trial, designed to ensure that the decoy can be dispensed safely from the platform's new self-protect pod. Discussions are underway concerning further tests with live rounds to demonstrate that BriteCloud can effectively protect

For More Information Visit mwjournal.com for more defense news.

the MQ-9 against the most advanced RF threats.

BriteCloud is a next-generation decoy, protecting aircraft from the latest radar-guided threats. The industry's first, and currently only, such product proven to work effectively, BriteCloud packs sophisticated jamming technology into a package the size of a drink can, allowing it to be fired from an aircraft in the same manner as a flare. Designed and manufactured in the U.K., it was first adopted for service by the Royal Air Force following an extensive testing campaign. As a unique capability, it is now being evaluated by the U.S. Armed Forces under the U.S. Foreign Comparative Test program.

DARPA Initiates Design of LongShot Unmanned Air Vehicle

DARPA's LongShot program, which is developing an air-launched unmanned air vehicle (UAV) with the ability to employ multiple air-to-air weapons, has awarded contracts to General Atomics, Lockheed Martin and Northrop Grumman for preliminary Phase I design work. The objective is to develop a novel UAV that can significantly extend engagement ranges, increase mission effectiveness and reduce the risk to manned aircraft.

LongShot (Source: DARPA)

Current air superiority concepts rely on advanced manned fighter aircraft to provide a penetrating counter air capability to effectively deliver weapons. It is envisioned that LongShot will increase the survivability of manned platforms by allowing them to be at standoff ranges far away from enemy threats, while an air-launched LongShot UAV efficiently closes the gap to take more effective missile shots.

"The LongShot program changes the paradigm of air combat operations by demonstrating an unmanned, air-launched vehicle capable of employing current and advanced air-to-air weapons," said DARPA program manager Lt. Col. Paul Calhoun. "LongShot will disrupt traditional incremental weapon improvements by providing an alternative means of generating combat capability."

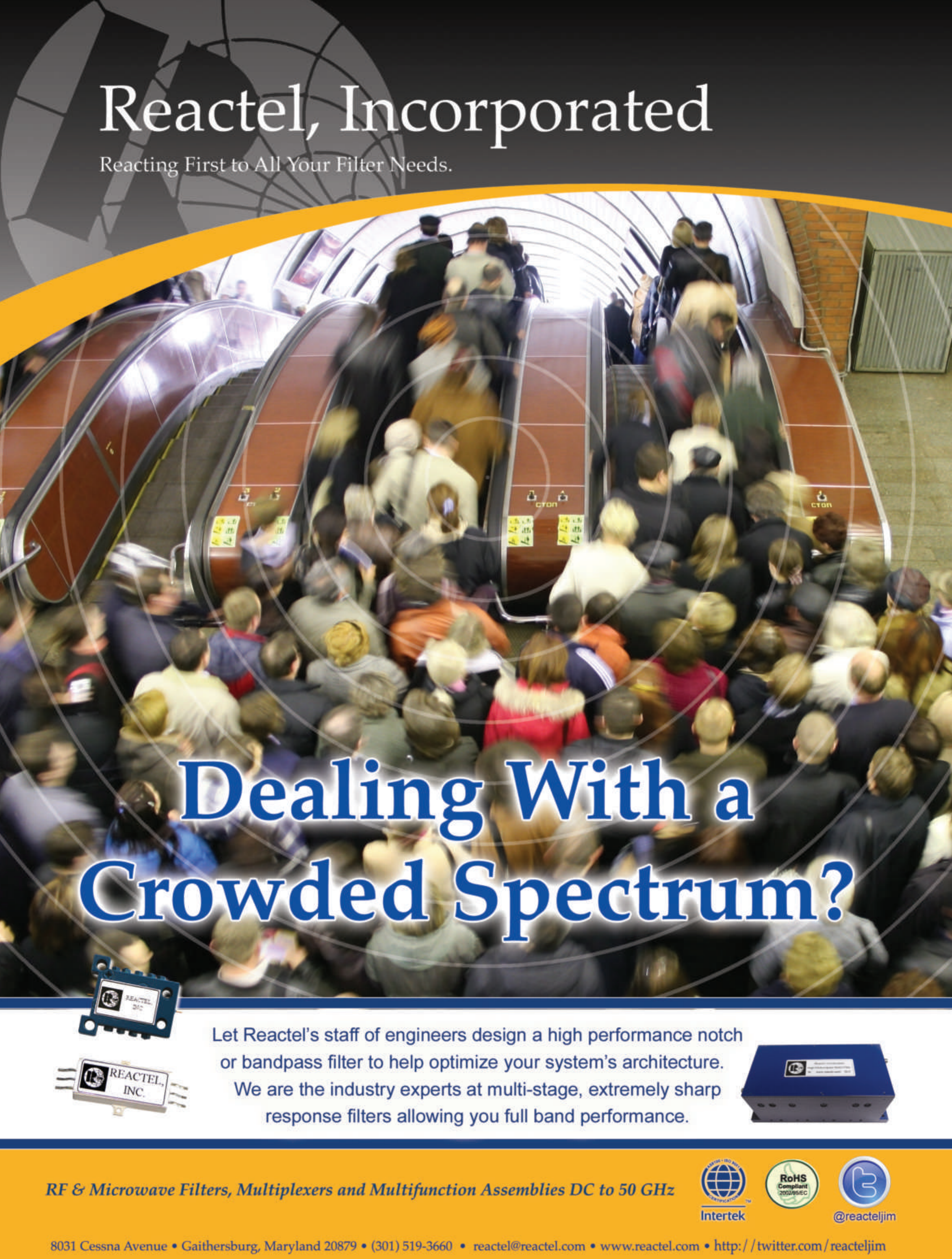
Reactel, Incorporated
Reacting First to All Your Filter Needs.
Dealing With a Crowded Spectrum?
REACTEL, INC.
Let Reactel's staff of engineers design a high performance notch or bandpass filter to help optimize your system's architecture. We are the industry experts at multi-stage, extremely sharp response filters allowing you full band performance.
RF & Microwave Filters, Multiplexers and Multifunction Assemblies DC to 50 GHz
Intertek
RoHS Compliant
@reacteljim
8031 Cessna Avenue • Gaithersburg, Maryland 20879 • (301) 519-3660 • reactel@reactel.com • www.reactel.com • http://twitter.com/reacteljim

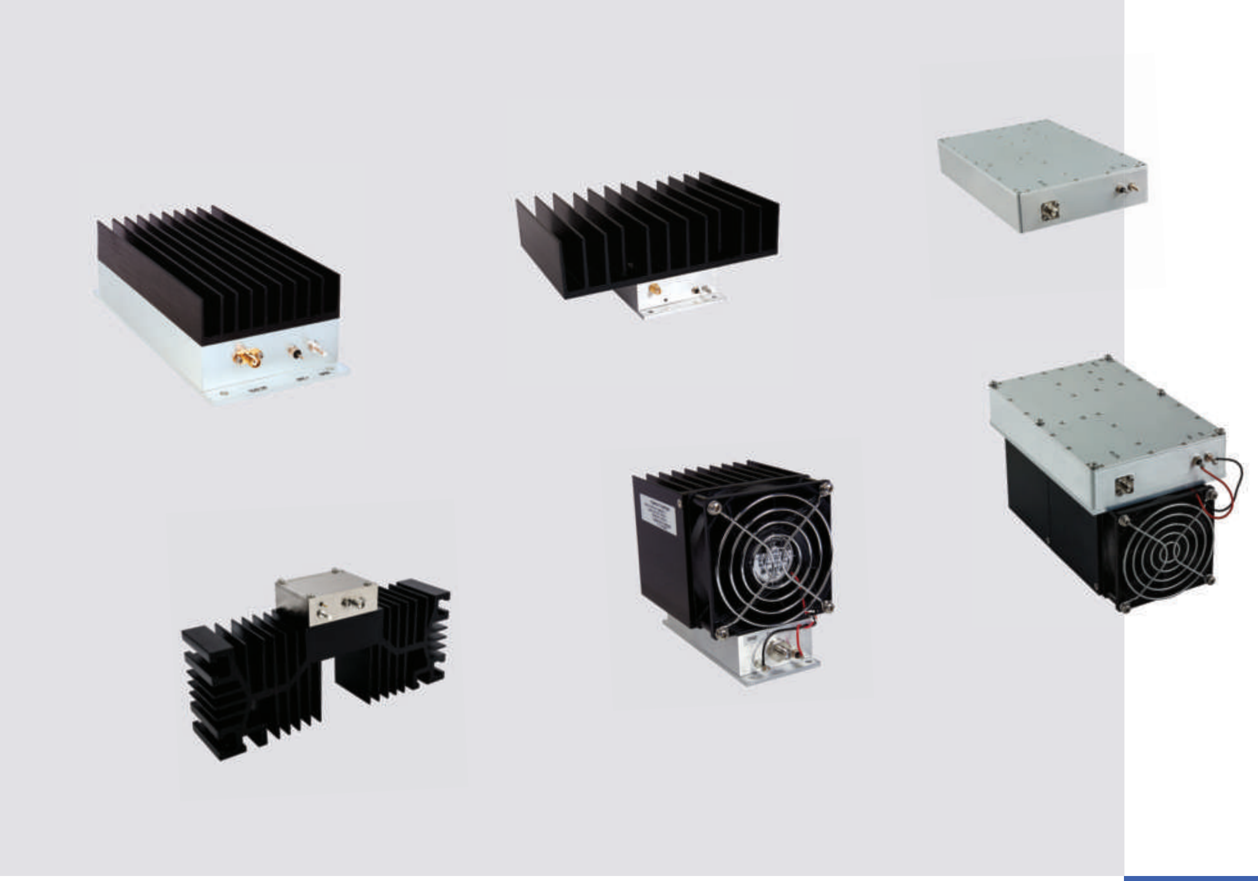

FCC Announces Winning Bidders in C-Band Auction

The Federal Communications Commission (FCC) recently announced the winning bidders and the final bid totals in Auction 107—commonly referred to as the C-Band auction. Auction 107 net winning bids totaled $81,114,481,921 and gross winning bids totaled $81,168,677,645. Twenty-one bidders won all of the available 5,684 licenses.

"It is essential to America's economic recovery that we deliver on the promise of next-generation wireless services for everyone, everywhere," said FCC Acting Chairwoman Jessica Rosenworcel. "This auction reflects a shift in our nation's approach to 5G toward mid-band spectrum that can support fast, reliable and ubiquitous service that is competitive with our global peers. Now we must work fast to put this spectrum to use in service of the American people."

The five bidders with the largest total gross winning bid amounts from both the clock and assignments phases were Cellco Partnership: $45,454,843,197, AT&T Spectrum Frontiers LLC: $23,406,860,839, T-Mobile License LLC: $9,336,125,147, United States Cellular Corporation: $1,282,641,542 and NewLevel II, L.P.: $1,277,395,688. The five bidders winning the largest number of licenses were Cellco Partnership with 3,511, AT&T Spectrum Frontiers LLC with 1,621, United States Cellular Corp. with 254, T-Mobile License LLC with 142 and Canopy Spectrum LLC with 84. The Public Notice summarizes auction results and announces deadlines for payments and the filing of long-form applications, as well as other post-auction procedures needed for the prompt issuance of licenses.

Cellular IoT Connections to Reach 3.5 Billion by 2030

According to recent research from Strategy Analytics, 5G comprised less than 1 percent of IoT connections in 2020 but will rise to 40 percent overall connections by 2030. The majority of 5G connections will not be significant until 2026, with 4G remaining the dominant technology over the forecast period.

2020 witnessed slower than expected growth due to the COVID-19 pandemic, with a slight increase in overall connections. Strategy Analytics expects similar connection growth rates in 2021, with the pandemic highlighting the need for investment in telehealth, especially remote patient monitoring and diagnostics.

Andrew Brown, executive director of Enterprise and IoT Research at Strategy Analytics, said, "The adoption of 5G will likely happen in different stages in the largest markets, with enhanced mobile broadband reaching mass adoption first, ultra-reliable and low latency communication gaining traction soon afterward and massive machine type communication (mMTC) showing the longest tail. Adoption will be determined not only by application needs, but by the availability of 5G chipsets, the speed and coverage of 5G network deployments, as well as the evolution of regulations. Even as 5G develops, 4G will continue to co-exist, provide extensive coverage at lower cost and remain very important in the IoT."

David Kerr, senior vice president of the Global Wireless Practice at Strategy Analytics added, "The tipping point for 5G in IoT occurs when support for mMTC, a price decline in hardware and widespread network coverage, sees NB IoT and Cat M folded into 5G standards and devices. For this reason, we think the pivot to 5G in IoT will be a gradual one, rather than a dramatic shift."

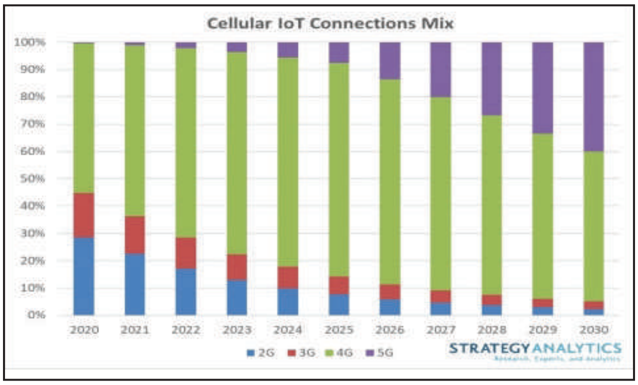

Cellular IoT Connections Mix (Source: Strategy Analytics)

LPWA Connectivity to Remain Dominant Across Smart City Segments

Despite the important investments in 5G networks, the uptake of 5G across smart city segments will remain very low over the next five years. ABI Research predicts that of all cellular smart city connections, 75 percent will ride on LPWA LTE networks (Cat 1, Cat M, NB IoT) in 2026, with around only 1.6 percent powered by 5G, accounting for less than 10 million connections globally.

"Next to the time needed to deploy 5G networks globally, there are two main reasons for the low uptake of 5G in smart cities applications," said Dominique Bonte, vice president of End Markets and Verticals at ABI Research. "First, there is a high proportion of fixed lines, including fiber for connecting non-mobile applications like commercial buildings, signage, ITS, kiosks, smart electricity, gas meters and surveillance. Second, where cellular is used, LPWA technologies are favored. This is due to the low bandwidth requirements for telemetry type applications such as smart streetlights,

For More Information Visit mwjournal.com for more commercial market news.

smart parking, metering and smart bins, many of which are also connected via non-cellular, proprietary LPWA connectivity such as LoRa."

However, in the longer term, new 5G use cases will emerge across a wide range of smart city segments, mostly centered around low latency, mission-critical services:

- Remote monitoring and control of unmanned assets like drones, robots and driverless vehicles
- ITS applications like Intelligent Cooperative Traffic Lights and Emergency Vehicle Preemption
- Remote healthcare services in ambulances
- AI-base surveillance and security monitoring
- Low latency edge cloud applications for demand-response and active security solutions.

5G Network Densification and mMIMO Will Drive Cellular Infrastructure Spending

Massive MIMO (mMIMO) is proving to be the catalyst that will fuel infrastructure vendor revenue in the foreseeable future. This is especially the case in the Asia Pacific region, where mobile network operators are expected to deploy 28.3 million units representing more than 78 percent of the total mMIMO market by 2026, despite banning of Chinese vendors in the Western World. According to a new report published by ABI Research, the installed base mMIMO market is expected to grow at a compound annual growth rate of 63.8 percent between 2020 to 2026 and reach US$58.2 billion by 2026. Furthermore, 5G densification and mMIMO will account for approximately 73 percent of the outdoor revenue reaching US$97.3 billion by 2026.

"mMIMO enables mobile network operators to offer best-in-class service to end users while leveraging cell site infrastructure and spectrum assets acquired for 5G," said Johanna Alvarado, senior analyst at ABI Research. "The adoption of different configurations depends on multiple factors such as user density, cell site characteristics, local regulations and clutter features."

In addition, in-building wireless will represent approximately 22 percent of the total mobile network infrastructure revenue in the world market, reaching US$34.4 billion by 2026. "Protocols such as 5G NR-Unlicensed, Citizens Broadband Radio Systems, Licensed Shared Access and locally licensed spectrum will fuel the acceleration of small cell deployments in the enterprise domain," added Alvarado.

ERAVANT

FORMERLY SAGE MILLIMETER

BROADBAND AMPLIFIERS | DC to 95 GHz

MODULAR | COMPACT BENCHTOP | BENCHTOP

SAGE Millimeter is now Eravant, a change that renews our commitment to the millimeterwave industry. Since 2011, we have been delivering quality products and energizing the customer experience to meet the needs of RF engineers working on the technology of the future.

1 mm Connectorized Broadband Amplifiers
Eravant has developed 1 mm connectorized broadband amplifiers to support this trend up to 95 GHz. The widest bandwidth model is offered to cover 0.5 to 80 GHz under the model number SBB-0528031512-1F1F-S1.

Benchtop Amplifiers
Offers convenience and stable lab test setup for standard test requirements. Comes with an AC power adapter for immediate DC power hook up. Standard models are offered to cover many broadband and waveguide bands.

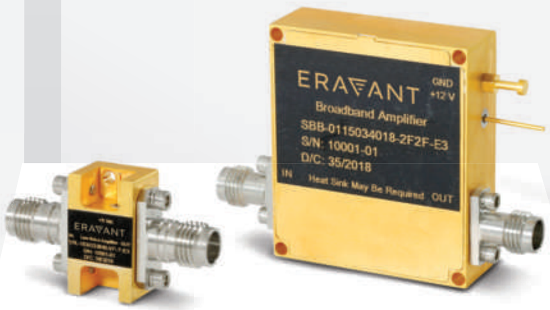

Compact Benchtop Amplifiers
Offers convenience and flexible lab test setup alternatives with its light weight, small size, and easy orientation. Comes with an AC power adapter for immediate DC power hook up. Standard models are offered to cover 0.01 to 26.5 GHz, 0.01 to 40 GHz, 0.01 to 50 GHz, and 0.01 to 70 GHz.

Low Noise and Power Broad Bandwidth Amplifiers
Eravant offers broad bandwidth amplifiers in three focuses, gain boosting, power and low noise figure. The amplifiers offer gain in the range of 15 to 50 dB and as low as 2 dB noise figure or up to 1 watts P-1dB output power.

WWW.ERAVANT.COM

www.eravant.com 501 Amapola Avenue Torrance, CA 90501
T: 424-757-0168

Adapters • Amplifiers • Antenna Feeds • Antennas • Attenuators • Bias Tees • Cable Assemblies • Corner Reflectors • Couplers • DC Blocks • Detectors • Ferrite Devices • Filters • Frequency Converters • Frequency Multipliers • Limiters • Magic Tees • Mixers • Noise Sources • Oscillators • Phase Shifters • Power Dividers • Radar Sensors • Subassemblies • Switches • Termination Loads • Test Equipment • Test Hardware & Accessories • [illegible] • Waveguide Sections

Around the **Circuit**

Barbara Walsh, Multimedia Staff Editor

IN MEMORIAM

Professor Tatsuo Itoh passed away on March 4, 2021. Dr. Itoh was a Fellow of the IEEE, a member of the Institute of Electronics and Communication Engineers of Japan and Commissions B and D of USNC/URSI. He served in many capacities in the IEEE MTT-S Society such as the editor of IEEE Transactions on Microwave Theory and Techniques from 1983 to 1985; president of the Microwave Theory and Techniques Society in 1990; editor-in-chief of IEEE Microwave and Guided Wave Letters from 1991 through 1994; and elected as an Honorary Life Member of MTT Society in 1994. He was the chairman of Commission D of International URSI for 1993 to 1996 and served on advisory boards and committees of a number of organizations. He served as Distinguished Microwave Lecturer on Microwave Applications of Metamaterial Structures of IEEE MTT-S 2004 through 2006.

Tatsuo Itoh received a Ph.D. in Electrical Engineering from the University of Illinois, Urbana, in 1969. After working for University of Illinois, SRI and University of Kentucky, he joined the faculty at the University of Texas at Austin in 1978, where he became a professor of Electrical Engineering in 1981. In September 1983, he was selected to hold the Hayden Head Centennial Professorship of Engineering at The University of Texas. In January 1991, he joined the University of California, Los Angeles as Professor of Electrical Engineering and holder of the TRW Endowed Chair in Microwave and Millimeter Wave Electronics (currently Northrop Grumman Endowed Chair). He received a number of awards including IEEE Third Millennium Medal in 2000 and IEEE MTT Distinguished Educator Award in 2000. He was elected as a member of National Academy of Engineering in 2003. Itoh has 400 journal publications, 820 refereed conference presentations and has written 48 books/book chapters in the area of microwaves, mmWaves, antennas and numerical electromagnetics. He generated 70 Ph.D. students and will be remembered for inspiring and mentoring many in our industry.

▲ *Tatsuo Itoh*

MERGERS & ACQUISITIONS

Infinite Electronics announced that it has been acquired by **Warburg Pincus** from Genstar Capital. The investment will support Infinite's geographic and product line expansion, entry into new, high-growth markets and enhanced digital capabilities. Terms of the transaction were not disclosed. Infinite Electronics offers a broad range of components, assemblies and wired/wireless connectivity solutions, serving the aerospace, defense, industrial, government, consumer electronics, instrumentation, medical and telecommunications markets. Infinite's proprietary brands include Pasternack, Fairview Microwave, L-com, MilesTek, Aiconics, KP Performance Antennas, PolyPhaser, Transtector, RadioWaves, ShowMe Cables, INC Installs, Integra Optics and NavePoint.

COLLABORATIONS

LitePoint announced that **Morse Micro**, developer of the smallest Wi-Fi HaLow single-chip solution, has standardized on the LitePoint IQxel-MW for design verification of its Wi-Fi HaLow system-on-chip family. Customers and manufacturing partners integrating Morse Micro's Wi-Fi HaLow SoC based on IEEE 802.11ah into their IoT design will be able to use the IQxel-MW to test the wireless functionality of their product, helping bring the design to market.

ACHIEVEMENTS

NASA's Mars Perseverance Rover finally touched down on Mars on February 18, 2021. Smiths Interconnect provides the Mars Perseverance Rover with high performance ruggedized cPCI 2 mm connectors addressing NASA's need for a high reliability connector solution to meet the mechanical, electrical and environmental performance requirements. Designed to be the most sophisticated rover NASA has built, the Mars Perseverance Rover will use advanced systems to explore the diverse geological landscape, discover ancient habitats, gather rock and soil samples that will be returned to Earth and demonstrate cutting-edge technology for future human exploration.

Keysight Technologies Inc. continues to maintain its leading support of 5G device acceptance test plans as mandated by U.S. carriers, helping to accelerate the rollout of 5G new radio services in both NSA and SA mode. Since December 2018, Keysight has maintained consistent and wide-ranging support of validated test cases specific to U.S. mobile operators' 5G device acceptance plans. Continuous support of validated U.S. carrier acceptance test cases has enabled 5G mobile device vendors to rapidly verify that new 5G devices operate as intended on a carrier's network.

Rohde & Schwarz has joined the **FiRa Consortium** as an associate member. FiRa, short for "fine ranging," is an organization dedicated to growing the ultra-wideband (UWB) ecosystem by ensuring interoperability between multiple devices through compliance and certification programs. The FiRa Consortium focuses on three core UWB services: hands-free access control, location based services and device-to-device services that rely on the latest UWB-based secure ranging technology specified by the IEEE 802.15.4z. The advantages of

For More Information For up-to-date news briefs, visit mwjournal.com

Exceptional Phase Noise

Dielectric Resonator Oscillator

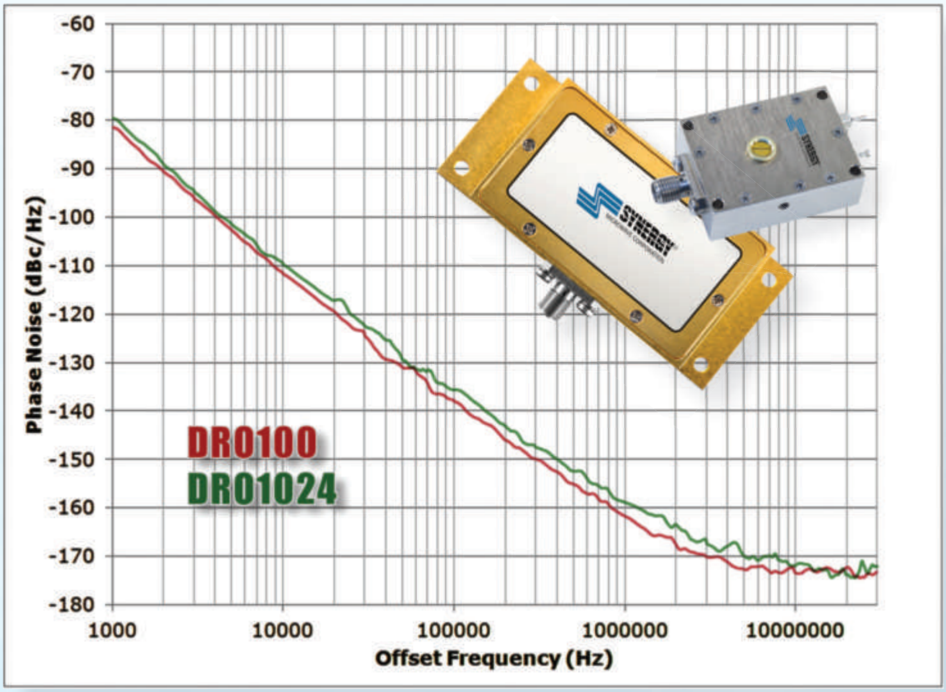

Available In Surface Mount.

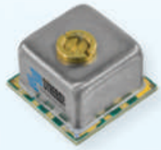

SDRO Series
0.75" x 0.75 x 0.53"

RoHS ***Patented Technology***

Model	Frequency (GHz)	Tuning Voltage (VDC)	DC Bias (VDC)	Typical Phase Noise @ 10 kHz (dBc/Hz)
Surface Mount Models				
SDRO800-8	8.000	1 - 10	+8.0 @ 25 mA	-110
SDRO900-8	9.000	1 - 10	+8.0 @ 25 mA	-112
SDRO1000-8	10.000	1 - 15	+8.0 @ 25 mA	-107
SDRO1024-8	10.240	1 - 15	+8.0 @ 25 mA	-105
SDRO1118-7	11.180	1 - 12	+5.5 - +7.5 @ 25 mA	-104
SDRO1121-7	11.217	1 - 12	+5.5 - +7.5 @ 25 mA	-106
SDRO1130-7	11.303	1 - 12	+5.5 - +7.5 @ 25 mA	-106
SDRO1134-7	11.340	1 - 12	+5.5 - +7.5 @ 25 mA	-107
SDRO1250-8	12.500	1 - 15	+8.0 @ 25 mA	-104
Connectorized Models				
DRO80	8.000	1 - 15	+7.0 - +10 @ 70 mA	-114
DRO8R95	8.950	1 - 10	+7.0 - +10 @ 38 mA	-109
DRO100	10.000	1 - 15	+7.0 - +10 @ 70 mA	-111
DRO1024	10.240	1 - 15	+7.0 - +10 @ 70 mA	-109
DRO1024H	10.240	1 - 15	+7.0 - +10 @ 70 mA	-115
KDRO145-15-411M	14.500	*	+7.5 @ 60 mA	-100

* Mechanical tuning only ±4 MHz

Talk To Us About Your Custom Requirements.

SYNERGY® MICROWAVE CORPORATION

Phone: (973) 881-8800 | Fax: (973) 881-8361
E-mail: sales@synergymwave.com | Web: www.synergymwave.com
Mail: 201 McLean Boulevard, Paterson, NJ 07504

the UWB standard include centimeter-accurate location measurements, allowing for doors to open when approached with a UWB device or bringing positioning functionality to indoor environments. UWB also features secure device-to-device data communications with very low power requirements.

Modelithics announced that it has crossed another milestone in the history of the company. As of March 1, 2021, Modelithics celebrated 20 years of establishment. What began as a small spinout startup from the University of South Florida has risen to stand tall as the industry leader in RF, microwave and mmWave measurements and measurement-based modeling of RF and microwave components and semiconductor devices. Since 2001, Modelithics has provided precision measurement and modeling services with unmatched accuracy. Modelithics has set a standard for excellence in RF/microwave model development and support.

ERZIA, along with the 12 other trans-European Consortium partners of the Hi-SIDE (formerly Hi-FLY) project, an EU-funded Research and Innovation program which was started in January 2018, recently celebrated the achievement of a major milestone with the completion and publication of detailed design descriptions for elements of the project's high speed data chain (HSDC). The designs, which meet all the rigorous requirements for space flight and satellite application, were made available for all elements of the HSDC, including but not limited to onboard network, data compression, storage, protection and transmission. These design descriptions constitute the capstone achievement in the most recent phase of the project, which has an anticipated end during 2021.

CONTRACTS

Elbit Systems Ltd. announced that it was awarded an approximately $300 million contract by a country in Asia to provide Hermes 900 Unmanned Aircraft Systems (UAS). The contract will be performed over a period of five years. Under the contract, the company will provide its Hermes 900 UAS and associated subsystems, as well as maintenance and support services. The Hermes 900 UAS has been selected to date, by 12 countries, attesting to its competitive edge that combines technological sophistication, reliability, open architecture and a solid growth path.

Meggitt PLC has secured a $5.8 million radome contract with **BAE Systems** to enable advanced radar technology on the Royal Air Force's Typhoon fight jet. These technologies will equip RAF Typhoons with wideband electronic attack in addition to traditional radar functions. BAE Systems and Leonardo are on contract to deliver the European Common Radar Systems Mk 2 (ECRS Mk 2) which equips RAF pilots with the ability to locate, identify and suppress enemy air defenses using high-powered jamming. The newly designed Meggitt radome is a broader bandwidth radome while still protecting from environmental effects and preventing electromagnetic interference for the AESA Radar system's operational modes.

Comtech Telecommunications Corp. announced that its Santa Clara, Calif.-based subsidiary, **Comtech Xicom Technology Inc.**, has received a follow-on order for $1.6 million for Ka-Band solid-state power amplifiers (SSPAs) that use state-of-the-art GaN technology for an in-flight connectivity (IFC) application. Comtech offers advanced technology solutions that enable people to stay connected wherever they are. The Comtech portfolio offers both Ku-Band and Ka-Band products for IFC applications. Comtech Xicom Technology Inc. manufactures a wide variety of tube-based and SSPAs for military and commercial satellite uplink applications.

PEOPLE

▲ *Theodore (Ted) S. Rappaport*

Theodore (Ted) S. Rappaport, the David Lee/Ernst Weber Professor of Electrical and Computer Engineering at the NYU Tandon School of Engineering and the founding director of the research center NYU WIRELESS, was elected to the **National Academy of Engineering (NAE)**. Election to the NAE—part of the 158-year-old National Academies of Science, Engineering and Medicine—is among the highest professional distinctions accorded to an engineer. The NAE specifically cited Rappaport's contribution to the characterization of radio frequency propagation in mmWave bands for cellular communications networks. This marks the second consecutive year in which someone from NYU WIRELESS has been elected to NAE.

▲ *Carsten Gralla*

Spectrum Instrumentation GmbH has announced that **Carsten Gralla** has joined its expanded executive team as managing director. Gralla holds a degree in mechanical engineering and is seen as a major asset to the business. Having previously worked in both large and small organizations, he brings a wealth of experience in all areas of commerce. This includes production, IT, international sales, marketing and quality management. As MD, Carsten will work with company founder and CEO Gisela Hassler as well as CTO Oliver Rovini, guiding and controlling all facets of the company's operations.

▲ *NXTCOMM Board of Directors*

Following successful validation tests of its next-generation Ku-Band antenna design, **NXT Communications**

Corp. announced formation of a new Board of Directors to help guide the next phase of its growth and commercial market introduction. Coming from the technology, aerospace, manufacturing, retail and satellite sectors, the board brings more than a century of experience and leadership to address the connectivity challenge. The board members include **Robert (Scott) Zimmer**, Board chairman, NXTCOMM, **David Horton**, CEO, NXTCOMM, **Stephen Newell**, chief commercial officer, NXTCOMM, **Curtis C. Reusser**, Board member, NXTCOMM and **Lawrence Soriano**, president, Western Pioneer Inc.

PLACES

pSemi®, a **Murata** company focused on semiconductor integration, is opening a design center in Chennai, India, to support the company's growing demand for semiconductor products for 5G and IoT applications. The India office will establish a base for a strong engineering team developing design innovations for cellular RF front-end modules, sensor systems-on-a-chip and power management ICs. The design center, which includes labs and office space, is located at Level 9, Olympia Teknos Park, No. 28 SIDCO Industrial Estate, Guindy, Chennai. The new design center supports pSemi's product growth in 5G, wireless connectivity, power management and sensors, with increased content in smartphones and mobile applications.

Intelliconnect (Europe) Ltd. a U.K. based specialist manufacturer of RF, waterproof and cryogenic connectors and cable assemblies, has moved to a larger facility at the Corby Innovation Hub following sales growth of 30 percent in 2020. The move to a 6,400-foot site provides the space required for their immediate increase in production requirements and provides additional space for future expansion. Despite enormous supply chain, delivery and logistics challenges during 2020 Intelliconnect have introduced a number of key new products including high density connector blocks and high specification cable products and capitalized on a number of significant opportunities in cryogenic, defense, medical and marine applications worldwide. Growth markets include wireless communications, IoT and Industry 4.0, quantum computing and research.

REP APPOINTMENT

Richardson Electronics Ltd. announced the expansion of its product portfolio with a new range of microwave filters from its established partner **3RWave**. Located in the Republic of Korea, 3Rwave has just over 300 filter types that are representative of the company's design capability with ceramic, cavity and LC types as well as substrate integrated waveguide and microstrip products.

INVITED PAPER

Model-Based Optimization Outperforms LNA Datasheet Specifications

Chris DeMartino, Hugo Morales and Larry Dunleavy
Modelithics Inc., Tampa, Fla.

It is possible in certain instances to improve the performance of a design that uses a MMIC low noise amplifier (LNA), using the same concepts for discrete transistor LNA designs. In this article, a design using a MMIC LNA is optimized over a 5G frequency band to achieve a lower noise figure than specified on the device datasheet.

An LNA is a critical component typically found in any receiver chain. Its purpose is to amplify an extremely weak signal captured by the receiver's antenna, adding minimal noise power to the signal. An LNA's noise figure is an important parameter enabling a designer to determine whether a given LNA is suitable for a requirement. Noise figure is the decibel representation of noise factor, a measure of the degradation in the signal-to-noise ratio as a signal passes through a network. LNAs are available as MMICs from various manufacturers, and it is often possible to purchase a MMIC LNA with the performance needed for a requirement, rather than having to design an LNA using a discrete transistor. The MMIC LNA can then be incorporated into the overall design by mounting it on a printed circuit board, following the manufacturer's instructions. In contrast, designing an LNA with a discrete transistor generally requires more effort than using a MMIC because discrete transistor LNA design involves creating appropriate matching networks so the amplifier achieves the desired performance.

To illustrate, ***Figure 1*** shows a single-stage amplifier design consisting of an input matching network, a transistor and output matching network. The minimum noise figure is achieved when the source reflection coefficient (Γ_S) is properly selected; the value of Γ_S achieving the minimum noise figure is known as Γopt. Γopt, with the minimum noise figure, Fmin, and the equivalent normalized noise resistance, r_n, are provided by the manufacturer of the transistor or can be determined experimentally.[1] In general, the goal when designing an LNA with a discrete transistor is to design the input matching network to achieve the lowest noise figure from the transistor and design the output matching network to help the LNA meet the requirements for output return loss, gain, gain flatness and other parameters.[1,2]

Compared to a discrete transistor LNA design, purchasing a MMIC LNA internally matched to 50 Ω seems easier because there is no need to design any matching networks. Instead, the MMIC is simply inserted into a 50 Ω environment following the manufacturer's instructions, which is obviously quicker and acceptable in many cases. However, it may be possible to optimize the performance of the MMIC LNA by exploiting the same concepts used for a discrete transistor LNA design. A MMIC LNA may be specified to operate over a wide frequency range, and many designers may assume the noise figure in the datasheet is the best that can be achieved; however, a MMIC LNA may achieve a lower noise figure than shown in the datasheet over a portion of the frequency band. This improved performance can be achieved by optimizing the design over the desired frequency range.

In this article, we optimized an LNA over a 5G band using the PMA-5451+ wideband MMIC LNA from Mini-Circuits. The design was simulated using Keysight Technologies' Advanced Design System (ADS) software. Modelithics models for the MMIC LNA and all passive components were used, and the Modelithics model for the PMA-5451+ was validated for both S-parameters and noise parameters, which were used to optimize the

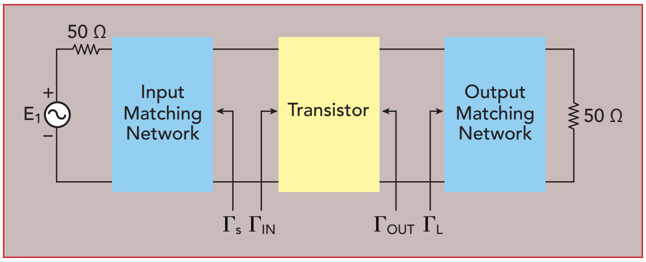

Fig. 1 Single stage LNA topology.

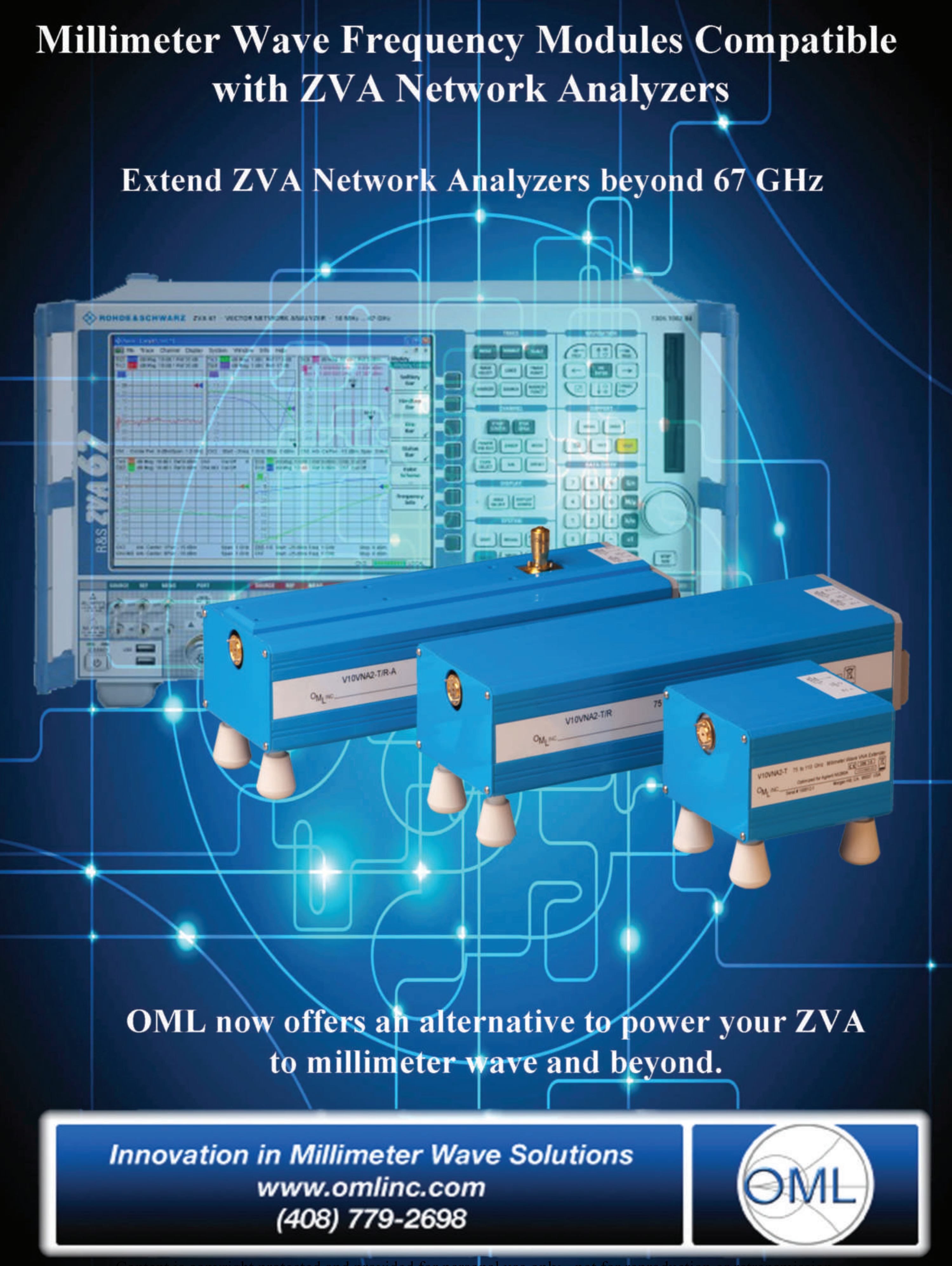
Millimeter Wave Frequency Modules Compatible with ZVA Network Analyzers
Extend ZVA Network Analyzers beyond 67 GHz
ROHDE&SCHWARZ
R&S ZVA 67
V10VNA2-T/R-A
V10VNA2-T/R
V10VNA2-T
OML now offers an alternative to power your ZVA to millimeter wave and beyond.
Innovation in Millimeter Wave Solutions
www.omlinc.com
(408) 779-2698
OML

complete design for the best noise figure over the desired frequency band. The goal was for the noise figure of the optimized LNA to be lower than the typical noise figure for the PMA-5451+ specified in the Mini-Circuits datasheet. Measured data confirmed this approach.

MMIC LNA PERFORMANCE

The Mini-Circuits PMA-5451+ MMIC LNA (see ***Figure 2***) is fabricated using an enhancement-mode PHEMT process. The operating frequency range is specified from 50 MHz to 6 GHz. Operating from a single +3 V DC power supply, the MMIC typically draws 30 mA with a 1.5 kΩ bias resistor. It is assembled in a 3 × 3 mm package. The PMA-5451+ data sheet contains a schematic of the recommended application circuit (see ***Figure 3***) and the characterization test circuit used to determine device specifications. The typical gain, noise figure and input/output return loss at +25°C are shown in ***Table 1***. The table shows the PMA-5451+ has typical noise figures of 1.3 and 1.5 dB at 3 and 4 GHz, respectively. For this design, the goal is to minimize the noise figure from 3.3 to 3.8 GHz, which is the n78 5G NR band.

Modelithics provides models for many Mini-Circuits components, including the PMA-5451+ LNA. The model is a data-based behavioral model developed from broadband S-parameters and noise parameters measured us-

Fig. 2 PMA-5451+ MMIC LNA.

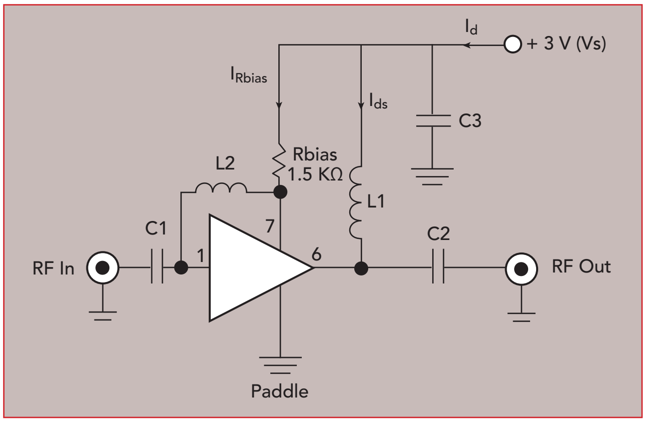

Fig. 3 PMA-5451+ application circuit.

TABLE 1

PMA-5451+ PERFORMANCE (25°C)

Parameter	*Frequency (GHz)*	*Typical Performance (dB)*
Noise Figure	0.05	1.3
	0.5	0.6
	1.0	0.8
	2.0	1.0
	3.0	1.3
	4.0	1.5
	5.0	2.0
	6.0	2.3
Gain	0.05	24.2
	0.5	22.1
	1.0	18.6
	2.0	13.7
	3.0	10.6
	4.0	8.5
	5.0	6.7
	6.0	5.3
Input Return Loss	0.05 to 0.5	8.8
	0.5 to 6.0	6.5
Output Return Loss	0.05 to 0.1	14.0
	0.1 to 6.0	19.0

HYPERLABS™

Innovation at Hyperspeed since 1992

ULTRA-BROADBAND

We offer some of the broadest band components on the market.

Our engineers are constantly working on new designs and expanding our product line.

INDUSTRY LEADING

Components that are “invisible” with regards to bandwidth roll-off and jitter performance keep pulse and eye fidelity at their best.

We design our products specifically to achieve these goals over the broadest band possible.

DEMOS AVAILABLE

Demos are in stock for most offerings, and we will get them in your lab quickly for a “hands on” evaluation.

CUSTOM DESIGNS

Don’t see exactly what you need? Our engineers may be able to help.

Many of our products can be modified or adapted to your specific needs quickly and with low minimum order quantities.

HL OREGON

13830 SW Rawhide Ct.
Beaverton, OR 97008

HL COLORADO

315 W South Boulder Rd.
Suite 206
Louisville, CO 80027

www.hyperlabs.com

NEW: 30 GHZ ULTRA-BROADBAND LINEAR AMPLIFIER

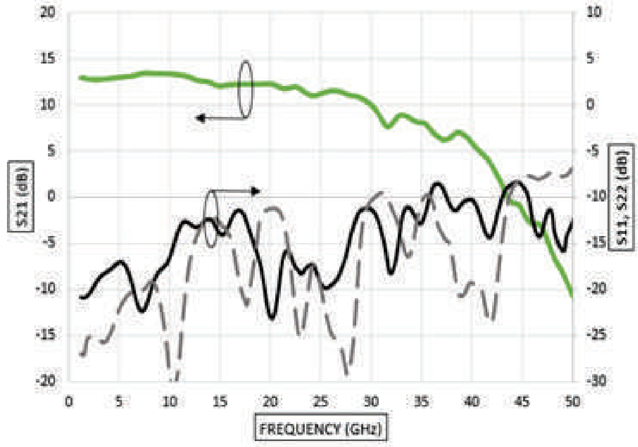

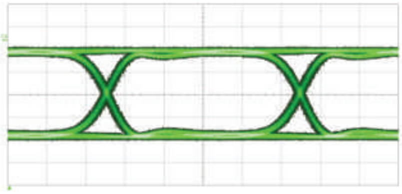

INPUT: 12.5 GBPS PRBS31 250 mV

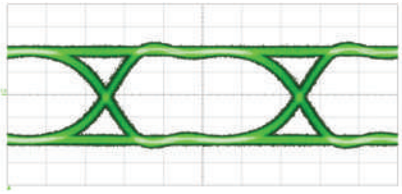

OUTPUT: 12.5 GBPS PRBS31 1100 mV

- Optimized step response with exceptional topline flatness
- Ideal for up to 32 Gbps NRZ and PAM4 data signaling
- Broadband linear gain amplifier with 13 dB gain
- 30 GHz bandwidth with exceptional gain flatness
- Lower 3 dB freqeuncy of 75 kHz
- Low deviation from linear phase (± 3 degrees)
- 1 dB gain compression point of 13 dBm
- Thermally compensated (ampl. and crossing point), 0-60° C
- Can be implemented as a general purpose gain block

ULTRA-BROADBAND BIAS TEES: NEW OFFERINGS!

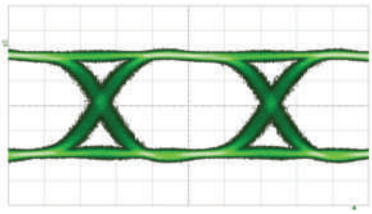

INPUT: 32 GBPS PRBS31

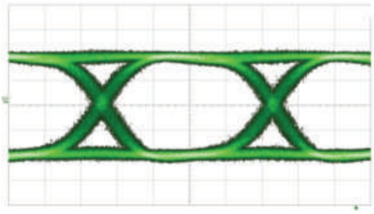

OUTPUT: 32 GBPS PRBS31

- HL9447 from 35 kHz to 67+ GHz @ 175 mA with 1.25 dB max insertion loss
- HL9547 from 50 kHz to 67+ GHz @ 400 mA with 1.5 dB max insertion loss
- HL9647 from 75 kHz to 67+ GHz @ 1000 mA with 2.0 dB max insertion loss

Visit our website for baluns, pick-off tees, power dividers, risetime filters, DC blocks, amplifiers, and more!

PUT HYPERLABS IN YOUR LAB

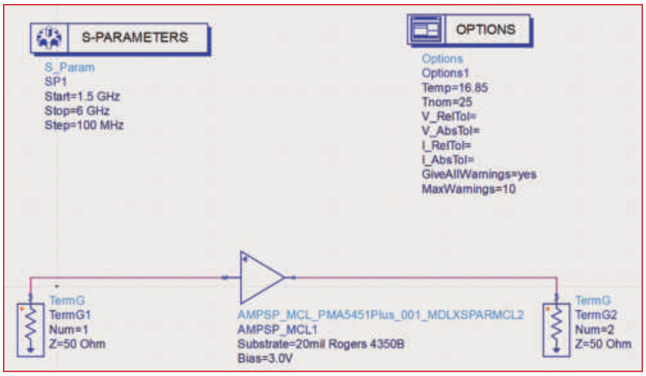

▲ Fig. 4 **ADS Modelithics PMA-5451+ model using 20 mil RO4350B substrate.**

ing a Keysight PNA-X vector network analyzer equipped with the ultra-fast noise option. The Modelithics model for the PMA-5451+ is validated for S-parameters and noise parameters at +25°C and biased at +3 V and 30 mA, predicting the S-parameters from 45 MHz to 20 GHz and noise parameters from 500 MHz to 8 GHz—beyond the operating frequency range specified by Mini-Circuits. The model includes three substrate options, since it was extracted from measurements performed using 6.6, 10 and 20 mil thick Rogers RO4350B substrates. Designers can select one of these substrates using the "Substrate" parameter. For this design, the 20 mil thick RO4350B was used. Modelithics provides a datasheet for the PMA-5451+ showing the application schematic used for model extraction. Also included are the model's S-parameters and noise parameters. The plots from the model datasheet can be replicated by simulating a schematic in ADS containing the PMA-5451+ model with 50 Ω port terminations at the input and output (see ***Figure 4***).

Simulating the schematic of Figure 4, the actual noise figure (NF50 in the model datasheet) and minimum possible noise figure (NFMin in the model datasheet) are plotted in ***Figure 5***, and ***Figure 6*** compares the simulated 50 Ω noise figure with the three substrate thicknesses available in the model. Figure 5 shows the noise figure is 1.14 dB at 3.3 GHz, rising slightly to 1.32 dB at 3.8 GHz. At these same frequencies, the minimum noise figure is 0.82 dB and 0.89 dB, respectively. At 3.3 GHz, the noise figure is 0.32 dB higher than the minimum, with a greater difference of 0.43 dB at 3.8 GHz. By designing a proper matching network, the LNA can be optimized so the noise figure is closer to the minimum values; a realistic goal is a noise figure ≤ 1.0 dB from 3.3 to 3.8 GHz.

The optimum source reflection coefficient for the minimum noise figure, known as S_{opt} in ADS, can also be determined (see ***Figure 7***) and seen in the Modelithics model. To achieve the lowest noise figure, the matching network placed at the input of the PMA-5451+ must produce a source reflection coefficient, Γ_S, closely matching S_{opt} over the frequency range of 3.3 to 3.8 GHz. ***Figure 8*** plots the $|S_{21}|$, $|S_{11}|$ and $|S_{22}|$ from the same simulation, showing the gain varies between 8.70 and 9.82 dB over the n78 band.

MMIC LNA DESIGN

The ADS schematic for the MMIC LNA design, shown in ***Figure 9***, essentially mirrors Mini-Circuits' rec-

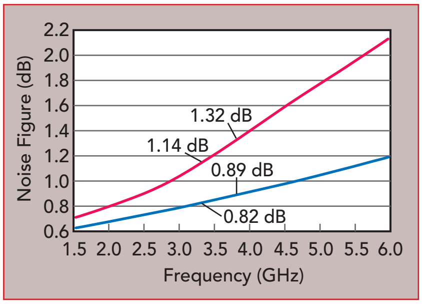

▲ Fig. 5 **Simulated 50 Ω noise figure (red) and minimum noise figure (blue).**

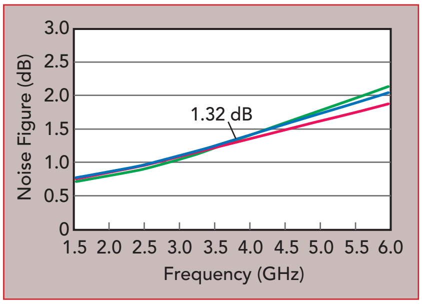

▲ Fig. 6 **Simulated 50 Ω noise figure using 6.6 mil (red), 10 mil (blue) and 20 mil (green) RO4350B substrates.**

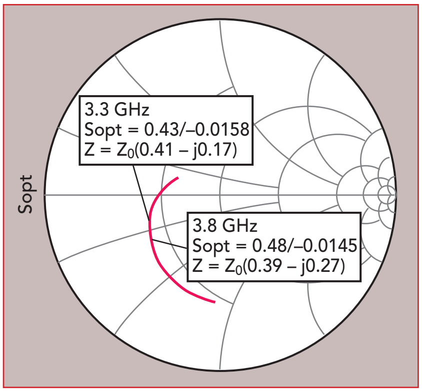

Fig. 7 Optimum source reflection coefficient for minimum noise figure, 1.5 to 6 GHz.

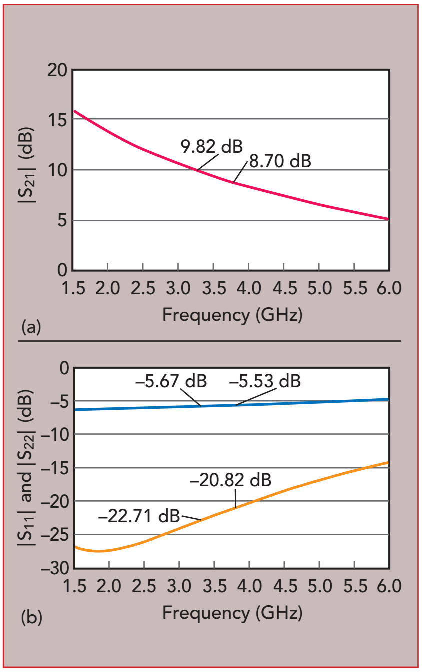

Fig. 8 Simulated $|S_{21}|$ (a), $|S_{11}|$ and $|S_{22}|$ (b).

ommended application circuit. The design includes the PMA-5451+, capacitor C1 and inductor L2 located at the input of the MMIC. These two components combined with the microstrip interconnects connecting them to the PMA-5451+ are the input matching network. The capacitor C2 and inductor L1 at the output of the MMIC are selected to achieve acceptable output return loss. The circuit also includes a 1.5 kΩ bias resistor, Rbias, setting the 30 mA bias current, and a bypass capacitor, C3.

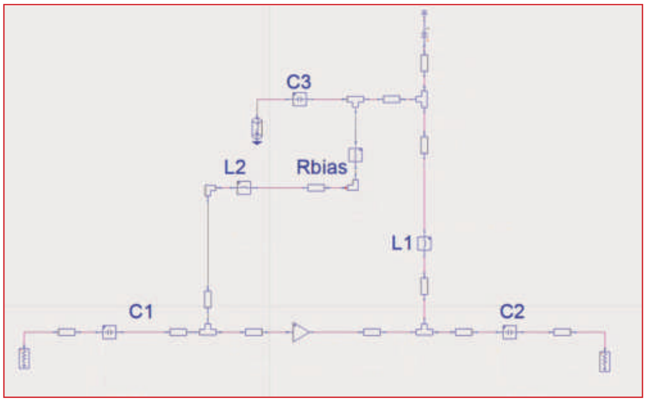

Fig. 9 ADS model of the complete LNA design.

Modelithics Microwave Global Models™ are used for the capacitors, inductors and resistor, which are all 0603 sized parts. AVX SQCS capacitors are used for C1 and C2, Würth Elektronik WE-KI inductors are used for L1 and L2, a KOA Speer RK73H 1.5 kΩ resistor is used for R_{bias} and a Murata GRM188R72A 0.1 µF capacitor is used for C3. A single Microwave Global Model covers the full range of values for a vendor's component, and since the values in these models are scalable, the models are useful for tuning or optimizing a design.

To optimize the noise figure from 3.3 to 3.8 GHz, the values of C1 and L2 must be suitably adjusted. As the lengths of the microstrip interconnects connecting C1 and L2 to the PMA-5451+ play a role in achieving the best performance, the optimization process includes tuning the lengths of the microstrip interconnects, as well as adjusting the component values. To establish a starting point for the design, the gain and noise figure of the LNA were simulated before optimizing the component values and interconnect dimensions, by setting C1 and L2 to the initial values of 100 pF and 390 nH, respectively, and the microstrip interconnect lengths to arbitrary values. At 3.8 GHz, the starting gain was just under 8 dB and the noise figure slightly greater than 1.6 dB (see ***Figure 10***).

The next step was optimizing the design to reduce the noise figure, a process made simpler using the "discrete optimization" feature within the Microwave Global Modrf/microwave instrumentation

Other ar companies: modular rf • sunar rf motion • ar europe

We're with you all the way

The **broadest bandwidth** with the **highest power** in the industry.

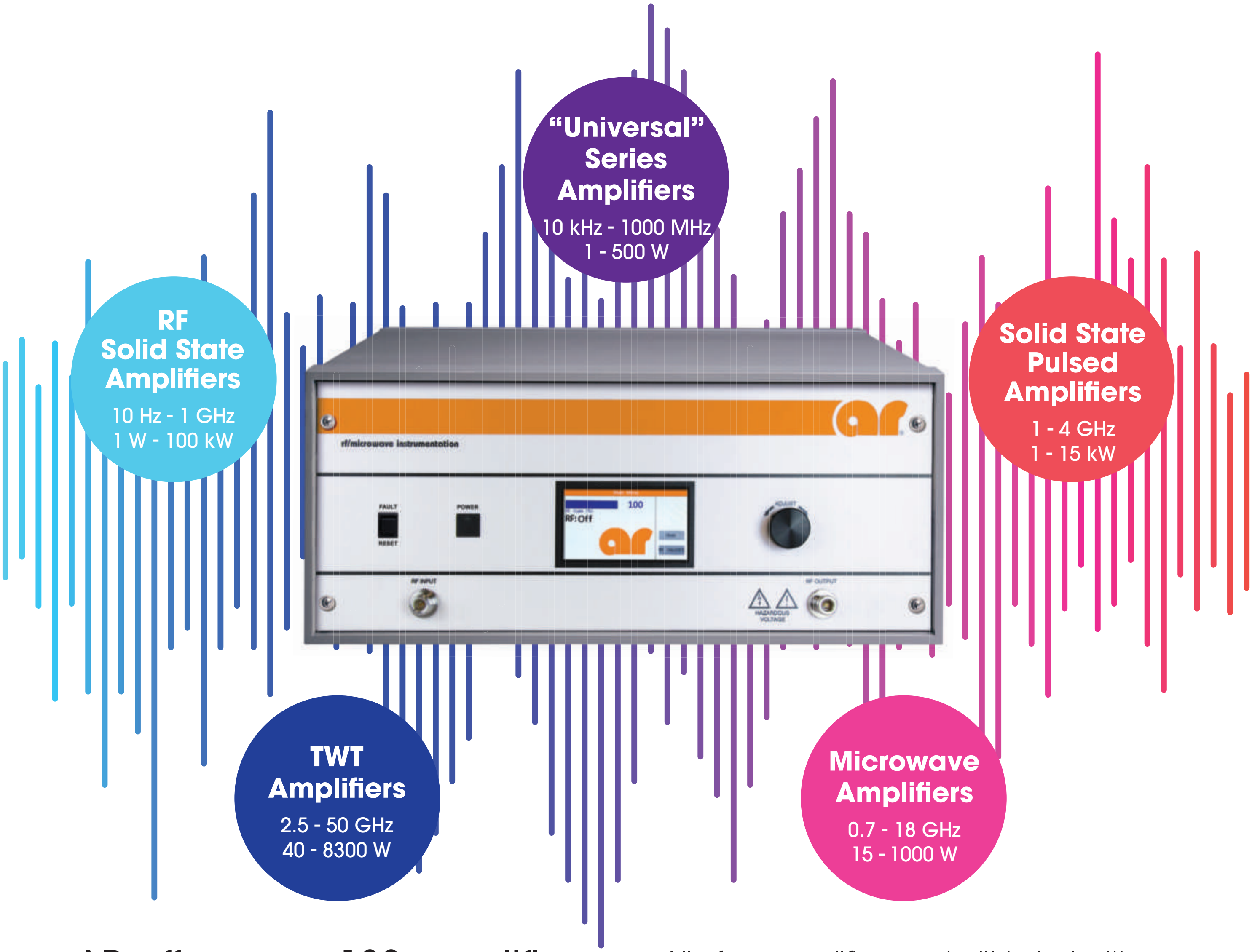

AR offers over 100 amplifiers ranging from **10 Hz - 50 GHz** and with power levels of **1 W - 100 kW**.

All of our amplifiers are built to last with the reliability that has made AR legendary. For more information on AR Amplifiers visit **www.arworld.us**.

els (see ***Figure 11***). This feature makes it possible to perform discrete optimization, where the model's part value is adjusted to the manufacturer's "real life" part value.[3] With this method, designers can indicate the range of part values within a part family to be included in the optimization. In this case, the discrete optimization feature was activated for C1 and L2, the components at the input of the PMA-5451+, to achieve the best noise figure. The optimization goal must be specified and the optimization itself configured. An optimization goal of 0.9 dB maximum noise figure—probably unrealistic—was set over the range from 3.3 to 3.8 GHz, and a discrete optimization performed, combined with tuning the microstrip interconnect lengths, to obtain the best noise figure over the n78 band. In addition, the values of the components at the output of the PMA-5451+, C2 and L1, were determined to achieve adequate output return loss. After optimization, the values were C1 = 2 pF, L2 = 27 nH, C2 = 3.6 pF and L1 = 3.3 nH (see ***Table 2***).

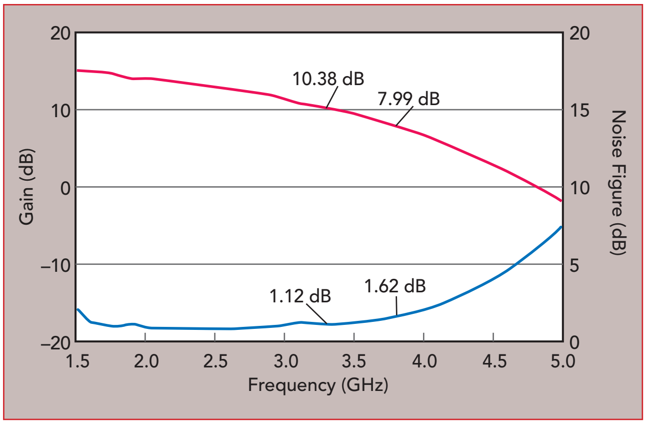

Fig. 10 Simulated gain (red) and noise figure (blue) of the unoptimized LNA design.

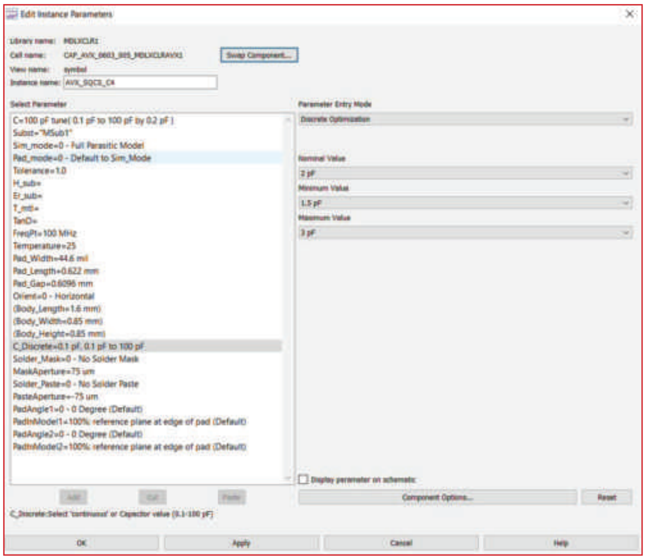

Fig. 11 Discrete elements optimized with the Modelithics passive component model parameters.

TABLE 2

FINAL COMPONENT VALUES

Component	Value	Part #
C1	2 pF	AVX SQCS
C2	3.6 pF	AVX SQCS
C3	0.1 µF	Murata GRM188R72A
L1	3.3 nH	Würth Elektronik WE-KI
L2	27 nH	Würth Elektronik WE-KI
Rbias	1.5 kΩ	KOA Speer RK73H

Figure 12 shows the simulated noise figure of the optimized LNA design, comparing it to the simulated noise figure before optimization (from Figure 10). After optimization, the simulated noise figure was < 1.0 dB from 3.3 to 3.8 GHz. ***Figure 13*** shows the simulated gain and return loss of the optimized LNA design. The stability factor was > 1 over the entire simulated frequency range from 50 MHz to 8 GHz. ***Figure 14*** compares the S_{opt} data of the PMA-5451+ model to the reflection coefficient looking into the input matching network from

ERAVANT

FORMERLY **SAGE MILLIMETER**

FREQUENCY **CONVERTERS & MULTIPLIERS**

ACTIVE | PASSIVE | MODULATORS | UPCONVERTERS | 24 to 70 GHz

SAGE Millimeter is now Eravant, a change that renews our commitment to the millimeterwave industry. Since 2011, we have been delivering quality products and energizing the customer experience to meet the needs of RF engineers working on the technology of the future.

Active Frequency Multipliers
Employs a broadband circuitry design to offer continuous frequency coverage up to full waveguide band operations. Standard offering covers the frequency range of 26.5 to 98 GHz and requires a bias voltage of +8.0 Volts.

Passive Frequency Multipliers
Employs a broadband circuitry and balanced structure to offer higher conversion efficiency and continuous frequency coverage up to full waveguide band operations. The balanced design enhances the desired harmonic output. Standard models cover the frequency range of 26.5 to 110 GHz.

Single Sideband Modulators
GaAs beam lead Schottky diode- or MMIC device-based frequency converters that use the IF frequency as a pumping source. The IF quadrature hybrid is not included in these modulators. Instead, separate I and Q ports are provided.

Balanced Upconverters
Similar to GaAs beam lead Schottky diode-based mixers, the upconverters employ a broadband circuitry and balanced structure to offer low conversion loss and harmonics for full waveguide band and broad IF bandwidth operations. Standard models cover the RF frequency range of 18 to 170 GHz and IF range up to40 GHz.

WWW.ERAVANT.COM

www.eravant.com 501 Amapola Avenue Torrance, CA 90501
T: 424-757-0168 [illegible]

Adapters • Amplifiers • Antenna Feeds • Antennas • Attenuators • Bias Tees • Cable Assemblies • Corner Reflectors • Couplers • DC Blocks • Detectors • Ferrite Devices • Filters • Frequency Converters • Frequency Multipliers • Limiters • Magic Tees • Mixers • Noise Sources • Oscillators • Phase Shifters • Power Dividers • Radar Sensors • Subassemblies • Switches • [illegible] guide Sections

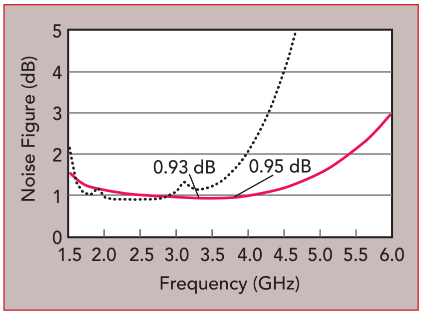

▲ Fig. 12 Simulated noise figure of the LNA before (dotted) and after (red) optimization.

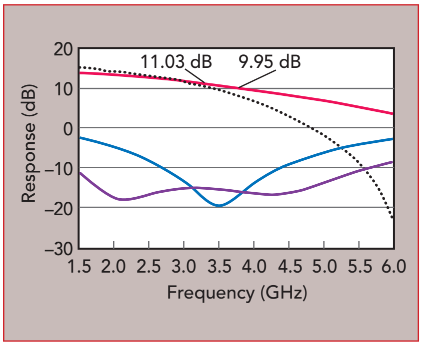

▲ Fig. 13 Simulated $|S_{21}|$ before (dashed black) and after (red) optimization, $|S_{11}|$ (blue) and $|S_{22}|$ (magenta).

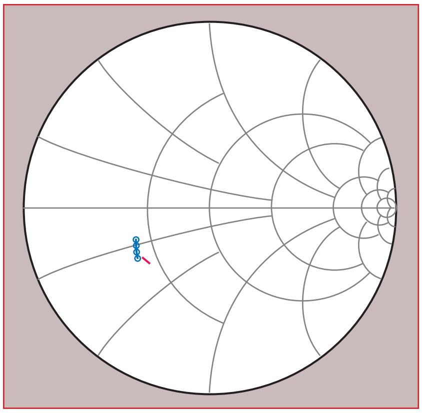

▲ Fig. 14 PMA-5451+ Sopt (blue circles) and reflection coefficient looking into the input matching network from the PMA-5451+ (red).

the PMA-5451+. To achieve optimal noise figure from 3.3 to 3.8 GHz, the source reflection coefficient should be as close as possible to S_{opt}, which is shown in the figure.

LNA MEASUREMENTS

The final step was validating the design by building and measuring the LNA; ***Figure 15*** shows one of two units that were assembled and

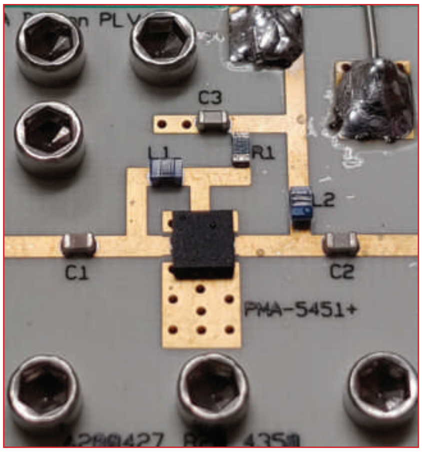

▲ Fig. 15 LNA assembly.

measured. The measured gain and return loss largely agree with the simulations (see ***Figures 16*** and ***17***). ***Figure 18*** compares the measured and simulated noise figure, including the simulated noise figure before optimization. One of the two measured LNAs had a noise figure < 1 dB from 3.3 to 3.8 GHz, while the noise figure of the second LNA was slightly higher, peaking at 1.06 dB at 3.8 GHz. We believe assembly variability

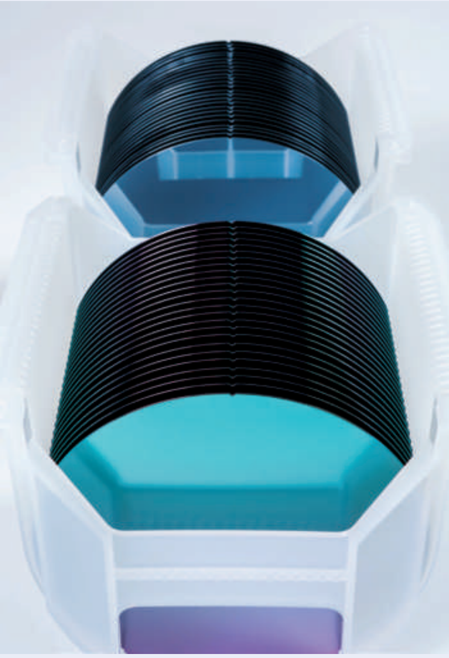

Customizable & Ultra-Flat: Game-Changing RF Silicon Wafer Technology

Introducing UF-RFSi™, a tailored silicon substrate dedicated for thin film surface acoustic wave hybrid structures. This new extension to Okmetic's RFSi™ wafer family optimizes RF filter and device performance.

As the industry's first wafer with ultra-flat properties, UF-RFSi leverages Okmetic's proprietary A-MCz®-silicon material technology to deliver improved technical performance with superior linearity, high resistivity and ultra-low loss radio frequency specifications. Boasting a TTV below 700 nanometers, the ultra-flat wafer can undergo a fully customizable wafering process, providing customers with tailored solutions and optimized configurations that meet their specific product, process and technology needs. UF-RFSi is an extension to the RFSi™ portfolio, a family of specialty wafers that reaches over 7,000 ohm-centimeters of bulk resistivities combined with advanced surface engineering.

SUPPLIER FOR TAILORED SILICON WAFERS IN 150 TO 200 MILLIMETER DIAMETER

UF-RFSi embodies over 35 years of experience supplying specialty wafers for advanced RF filters and applications alongside wafers for microelectromechanical systems and sensors. Founded in 1985, Okmetic is the seventh largest silicon wafer manufacturer in the world and a leading supplier for advanced silicon wafers in 150 to 200 millimeter diameter. Okmetic's silicon wafers provide a highly functional and reliable platform for the manufacture of various everyday applications, including smartphones, portable devices, automotive electronics, industrial process control and medical applications, IoT, as well as different solutions related to power supply and efficiency improvement:

- RFSi™ High Resistivity for RF filters and devices
- Silicon on Insulator (SOI) wafers; BSOI, C-SOI® and E-SOI®
- Advanced solutions (TSV, customized structures)
- Single Side Polished (SSP) wafers
- Double Side Polished (DSP) wafers including CAP

Okmetic has worldwide sales organizations in Europe, the United States, Japan and the Asia-Pacific region. The company is headquartered in Finland, where the majority of its silicon wafers are manufactured. Okmetic's operations rely on quality and environmental systems in line with the ISO 9001:2015, ISO 14001:2015 and IATF 16949:2016 standards. To learn more, visit www.okmetic.com.

and measurement sensitivity caused the higher noise figure and deviation from the simulation. Nonetheless, the results confirm that reducing the noise figure was achieved.

CONCLUSION

The test results demonstrate a MMIC LNA can be optimized to achieve lower noise figure than specified in the manufacturer's data sheet over a narrower frequency range. Designers can use this approach to achieve lower noise figure than specified for a MMIC. Modelithics amplifier models are well-suited for this approach because they enable designers to predict both S-parameters and noise parameters. Adding the ability to scale the model values of passive components makes it easy to optimize the passive elements to meet design goals.■

References

1. Guillermo Gonzalez, *Microwave Transistor Amplifiers: Analysis and Design*, Second Edition, Prentice Hall, New Jersey, 1997.
2. S. Akamatsu, S. Muir and L. Dunleavy, "Simulation Procedures for Successful Low Noise Amplifier (LNA) Design Using Discrete Components," *High Frequency Electronics*, 2012, pp. 22–30.
3. "Discrete Optimization with Modelithics Models in ADS," *Modelithics*, October 2018, Web, www.modelithics.com/Literature/Presentation.

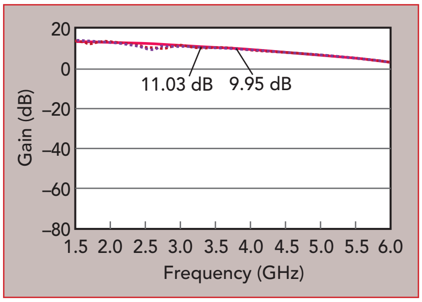

▲ Fig. 16 Measured gain of two LNAs (dashed) vs. simulated gain (red).

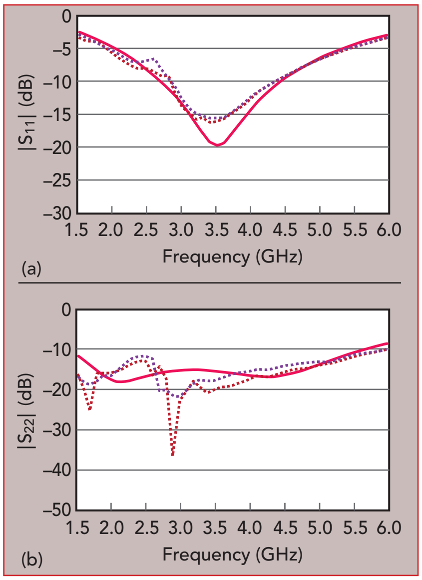

▲ Fig. 17 Measured vs. simulated $|S_{11}|$ (a) and $|S_{22}|$ (b). The dashed traces represent measurements of two LNAs; the red traces are simulated performance.

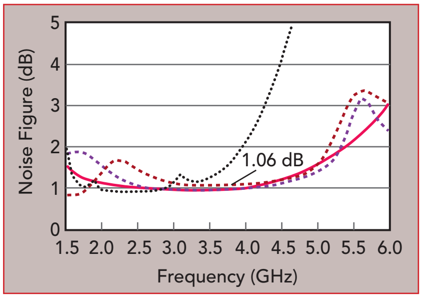

▲ Fig. 18 Measured noise figure of two LNAs (dashed) vs. simulation before (dotted black) and after (red) optimization.

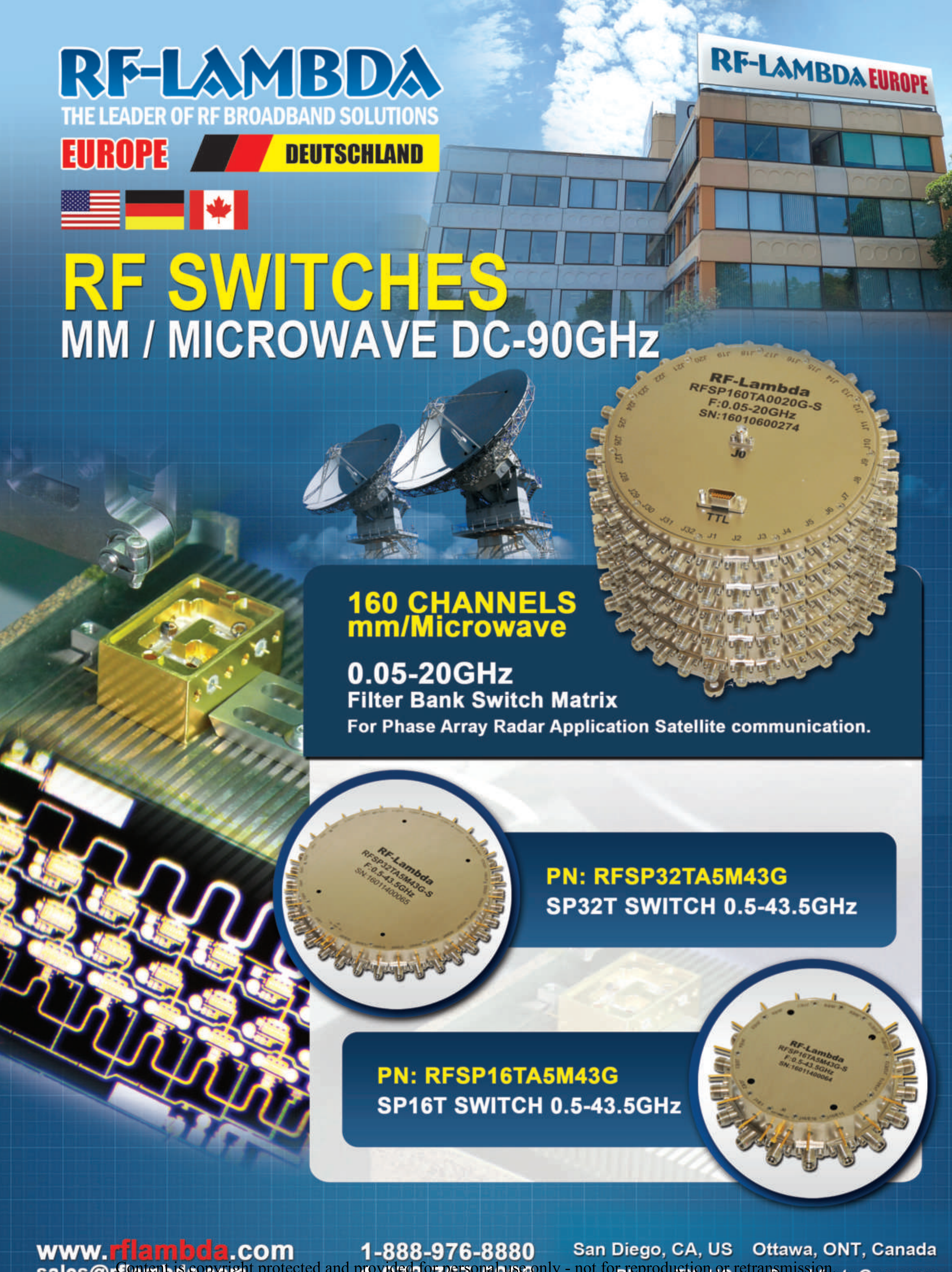
RF-LAMBDA
THE LEADER OF RF BROADBAND SOLUTIONS
EUROPE
DEUTSCHLAND
RF-LAMBDA EUROPE
RF SWITCHES
MM / MICROWAVE DC-90GHz
RF-Lambda
RFSP160TA0020G-S
F:0.05-20GHz
SN:16010600274
160 CHANNELS
mm/Microwave
0.05-20GHz
Filter Bank Switch Matrix
For Phase Array Radar Application Satellite communication.
PN: RFSP32TA5M43G
SP32T SWITCH 0.5-43.5GHz
PN: RFSP16TA5M43G
SP16T SWITCH 0.5-43.5GHz
www.rflambda.com
sales@rflambda.com
1-888-976-8880
1-972-767-5998
San Diego, CA, US
Plano, TX, US
Ottawa, ONT, Canada
Frankfurt, Germany

INVITED PAPER

RF Wireless Power: A to Z

Charles Greene
Powercast Corporation, Pittsburgh, Pa.

For many years, the capabilities of long-range wireless power have been talked about and with increasing interest. The technology is proven and is already being used today in many industries like manufacturing, building automation and hospitality. An assortment of other, short-range wireless charging technologies are on the market, including Qi (inductive coupling) and magnetic resonance. However, the focus of this article will be on the various methodologies for RF-based wireless power for powering devices over distance.

WIRELESS POWER OVER DISTANCE

RF wireless power is a technology that enables power to be sent over distance using radio waves. A transmitter uses an antenna to generate an RF field which propagates toward a receiver's antenna. The receiver captures a portion of the RF field and uses an RF to DC converter to produce usable DC to power electronics or recharge batteries. RF wireless power can be implemented in various ways and many design decisions impact the performance of the system. When all variables are considered, RF wireless power networks offer a way to remove wires and batteries from many of the devices we encounter every day.

Wireless power transmission using RF in the far field can be described using the Friis equation:

$$P_R = P_T \frac{G_T(\theta_T,\phi_T)G_R(\theta_R,\phi_R)\lambda^2}{(4\pi r)^2} \quad (1)$$

$$\left(1-|\Gamma_T|^2\right)\left(1-|\Gamma_R|^2\right)\left|\hat{\rho}_T \bullet \hat{\rho}_R\right|^2$$

where P_R is the received power, P_T is the transmitted power, $G_T(\theta_T,\phi_T)$ is the angular dependent transmitter antenna gain, $G_R(\theta_R,\phi_R)$ is the angular dependent receiver antenna gain, λ is the wavelength, r is the distance between the transmit and receive antennas, Γ_T is the transmit antenna reflection coefficient, Γ_R is the receive antenna reflection coefficient, $\hat{\rho}_T$ is the transmitter antenna polarization vector and $\hat{\rho}_R$ is the receiver antenna polarization vector. Generally, the transmitter and receiver are assumed to be matched, have the same polarization vectors and are in the main radiation beam, which simplifies the equation to:

$$P_R = P_T \frac{G_T G_R \lambda^2}{(4\pi r)^2} \quad (2)$$

This equation shows the received power is inversely proportional to the distance squared, which means if the distance doubles, the received power reduces by 4×. This can be understood considering the power is spreading over the surface area of a sphere with area $A=4\pi r^2$.

Another factor in RF wireless power transfer is the received power is proportional to the square of λ or inversely proportional to the square of the frequency. This means a low frequency signal will provide more received power than a higher frequency signal, assuming all other variables are the same. For example, consider an amplifier delivering 1 W of RF power to a transmitting antenna with a gain of 4, i.e., 4 W EIRP. A dipole antenna at a fixed distance at 915 MHz will receive about 7x more power than a dipole antenna at 2.4 GHz:

$$\frac{P_{R@915\,MHz}}{P_{R@2.4\,GHz}} \propto \left(\frac{\lambda_{915\,MHz}}{\lambda_{2.4\,GHz}}\right)^2$$

and about 40x more power than a dipole at 5.8 GHz:

$$\frac{P_{R@915\,MHz}}{P_{R@5.8\,GHz}} \propto \left(\frac{\lambda_{915\,MHz}}{\lambda_{5.8\,GHz}}\right)^2$$

AMCOM COMMUNICATIONS
The RF Power House

ISO 9001

Featured GaAs & GaN MMIC PAs

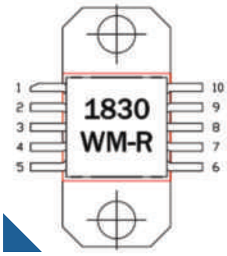

AMCOM's **AM183031WM-EM-R** is part of the GaAs MMIC power amplifier series. It has 30.5dB gain and 31.5dBm output power over the **1.6 to 3.3 GHz** band. This MMIC is in a ceramic package with both RF and DC leads at the lower level of the package to facilitate low-cost SMT assembly to the PC board.

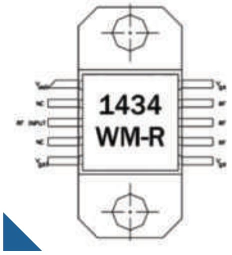

AMCOM's **AM143440WM-EM-R** is part of the GaAs HiFET MMIC power amplifier series. This high efficiency MMIC is a 2-stage GaAs pHEMT power amplifier biased at 10 to 14V. The input and inter-stage matching networks cover **1.4 to 3.4 GHz** with 20 dB of gain and 39 dBm output power.

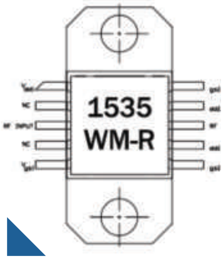

AMCOM's **AM153540WM-EM-R** is part of the GaAs HiFET MMIC power amplifier series. It is a 2-stage GaAs HIFET PHEMT MMIC power amplifier. It is fully matched to 50-ohm at both input and output, covering **1.5 to 3.5 GHz**. The MMIC has 21dB gain and 38.5dBm output power at 14V.

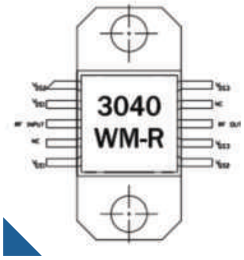

AMCOM's **AM304031WM-EM-R** is part of the GaAs MMIC power amplifier series. It has 31dB gain and 31 dBm saturated output power over the **2.6 to 4.8 GHz** band. This MMIC is in a ceramic package with both RF and DC leads.

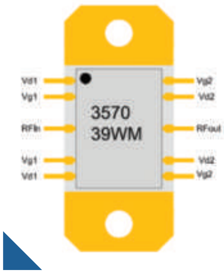

AMCOM's **AM357039WM-SN-R** is a broad-band GaAs MMIC Power Amplifier. It has a nominal CW performance of 21dB small signal gain, and 38.5dBm (7W) saturated output power over the **3.5 to 7 GHz** band.

AMCOM's **AM07511542WM-SN-R** is a broadband GaAs MMIC power amplifier. It has 25 dB small signal gain, and 42 dBm output power over the **8 to 11 GHz** band at 8V bias and a 5% pulsed operation.

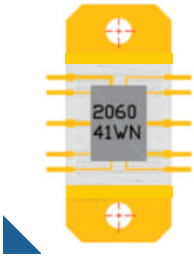

AMCOM's **AM206041WN-SN-R** is a broad-band GaN MMIC power amplifier. It has > 30 dB gain, and > 41 dBm output power over the **1.75 to 6.5 GHz** band. The AM206041WN-SN-R is in a ceramic package version with a flange and straight RF and DC leads for drop-in assembly.

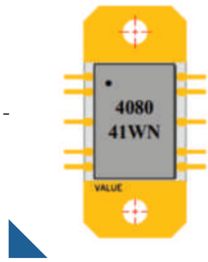

AMCOM's **AM408041WN-SN-R** is in a ceramic package with a flange and straight RF and DC leads for drop-in assembly. It has 31dB gain, and 41.5 dBm output power over the **3.75 to 8.25 GHz** band. Because of high DC power dissipation, good heat sinking is required.

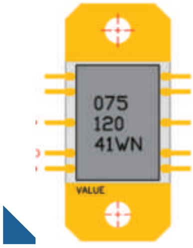

The **AM07512041WN-SN-R** is in a ceramic package with a flange and straight RF and DC leads for drop-in assembly. It has 27dB gain, and 41dBm output power over the **8.25 to 11.75 GHz** band. Because of high DC power dissipation, good heat sinking is required. The package is RoHS compliant. This MMIC is matched to 50 Ohms.

IMS
Connecting Minds. Exchanging Ideas

Atlanta 2021

Visit us at Booth1449

We are excited to participate in this years International Microwave Symposium (IMS) show that will be held in Atlanta, GA from June 6th - 11th. We have lots to show!

www.amcomusa.com

Phone 301.353.8400 - www.amcomusa.com - info@amcomusa.com

This difference in power is because the effective area of the antenna is reducing as frequency increases. The dipole antenna, typically λ/2 long, gets shorter as frequency increases, reducing the physical capture area of the antenna.

However, the power density, S, is independent of frequency:

$$S = \frac{P_T G_T}{4\pi r^2} = \frac{EIRP}{4\pi r^2} \quad (3)$$

Equation 3 shows the radiated power spreads over the surface of a sphere independent of frequency, and the effective area of the antenna, also known as capture area, determines the amount of received power. This explains why a λ/2 dipole antenna at 5.8 GHz captures less energy than a λ/2 antenna at 915 MHz under identical conditions.

The effective area of an antenna, A_e, is directly proportional to its gain:

$$A_e = \frac{G_R \lambda^2}{4\pi} \quad (4)$$

Higher gain antennas can be used to increase the capture area, but high gain antennas come at the cost of directionality. Depending on the application, precise antenna directionality is not always advantageous. One way around this potential burden is using multiple antennas and RF to DC converters to increase the overall capture area. However, this solution also increases the cost of the receiver because of the additional hardware. This shows why it is important to outline performance and project expectations prior to designing the system.

The Friis equation is only valid in the far field, so determining the boundary between the near and far field is important. One common method is to determine where the parallel ray approximation begins to break down, i.e., where the wave exiting the transmit antenna can be approximated as a plane wave impinging on the receiving antenna. A plane wave means the receiving antenna sees a constant amplitude and phase across its aperture (see ***Figure 1***). Typically, a phase error of π/8 or 22.5 degrees across the receiving aperture is considered an acceptable approximation for a plane wave, which yields the common boundary between the near and far fields given by:

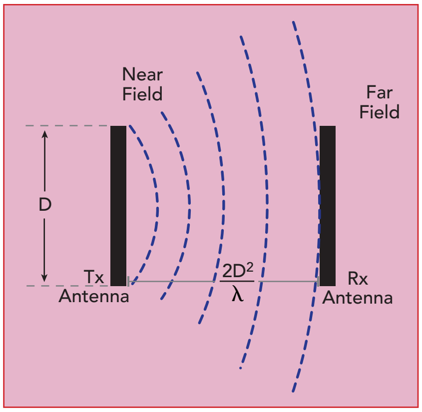

Fig. 1 **Far-field boundary where spherical waves approximate a plane wave.**

$$r > \frac{2D^2}{\lambda} \quad (5)$$

where D is the maximum dimension of the transmitting or receiving antenna or array, r is the distance between the transmitting and receiving antennas and λ is the wavelength.

BEAM FOCUSING, POWER DENSITY SPOT SIZE

In some applications, it is advantageous to focus the RF field onto a receiving antenna to maximize power throughput. This can be done several ways, usually through far-field focusing (see ***Figure 2***) or near-

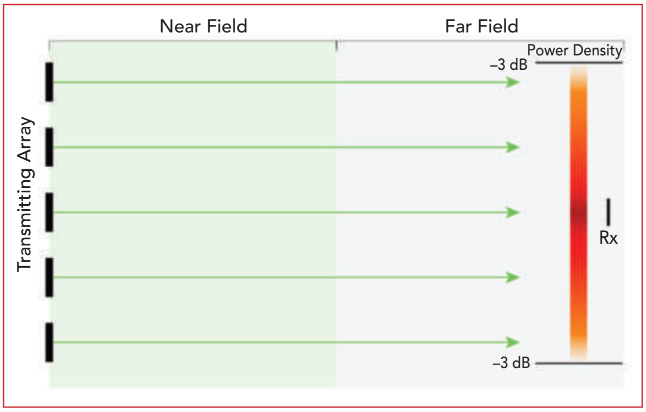

Fig. 2 **Far-field focusing.**

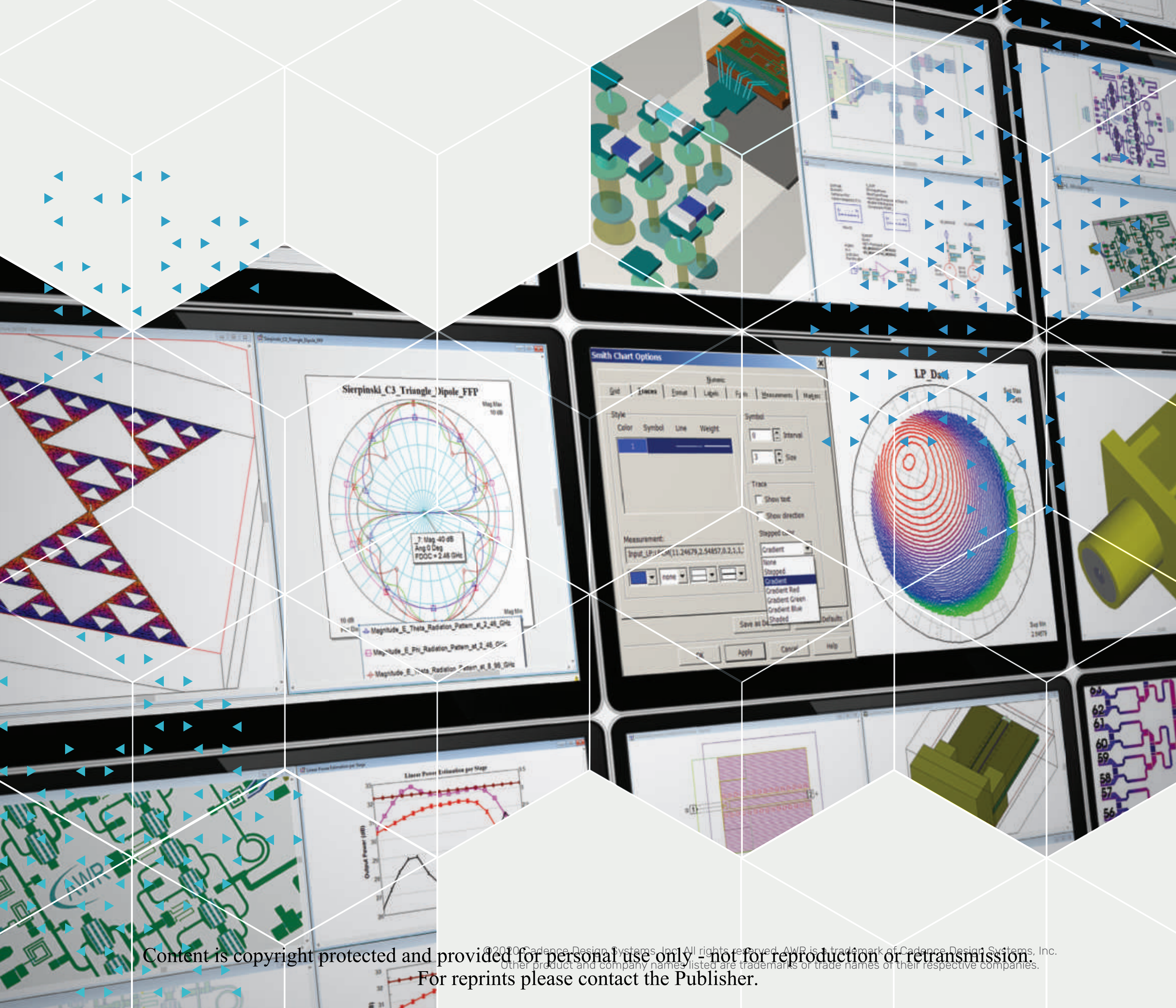

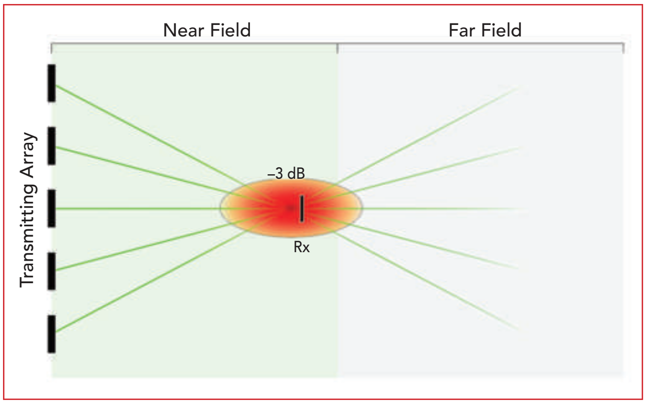

▲ **Fig. 3** Near-field focusing.

field focusing (see ***Figure 3***) of the RF power to increase power density. The far-field technique is usually referred to as beamforming or beam steering and is accomplished with a high gain antenna or by using an antenna array focused at an infinite distance to produce a directional beam. The direction of the beam is controlled by either mechanically or electronically directing the signal toward the receiving antenna. With near-field focusing, an antenna array typically focuses each antenna element to a finite point in the near field to produce a hot spot of RF power density, with the subsequent fields for each antenna diverging in the far field beyond the hot spot.

With far-field beamforming, it is important to understand the limitations of "focusing" the RF energy. The size of the beam and the focus area will always be bigger than the physical dimensions of the transmitting antenna. Focusing the rays from each antenna element at an infinite point in the far field means the rays are parallel, as seen in Figure 2. However, the ray from each antenna element will spread over distance per the far-field beamwidth specification in the datasheets of commercially available antennas. A narrow beam's aperture begins as the minimum size of the antenna and spreads as it travels. Therefore, if the transmitting array is 1 m^2, the beam will never be smaller than 1 m^2, which is important when sending RF power to a receiving antenna smaller than the transmitting antenna. While beamforming does focus more RF power to a receiving antenna, a large portion of the steered beam may be outside the desired capture area.

With near-field focusing, the rays from each antenna converge on a point in the near field to form a localized spot of high RF power density, as shown in Figure 3. The -3 dB (i.e., half power) size of the spot can be as small as slightly less than λ/2. Depending on the dimensions of the receiving antenna, the spot can be comparably sized to the receiving antenna. If the two are similarly sized, more efficient coupling can be achieved between the transmitter and receiver. However, since this solution is more closely coupled, the system should be simulated and designed as a whole, meaning both the transmit and receive antennas. Due to the proximity of the antennas, their impedances can change, and the amplitude and phase of the field across the receiving antenna aperture are likely not uniform. While far-field antennas are designed with consistent amplitude and phase across their capture areas (i.e., assuming plane waves), typical antenna design practices may not apply for near-field operation, so system simulation is vital for optimizing the performance of a near-field wireless power solution.

Both far-field and near-field focusing can provide higher throughput of RF wireless power. However, this is achieved incurring complexity, which often increases cost. A beam focusing solution may contain mechanical or electronic steering, like a motor or amplitude and phase adjusting circuitry. This increased cost makes the wireless benefits difficult to justify. As a transmitter with a single antenna and amplifier will be much smaller and significantly less expensive than a beam focusing solution, this approach is more viable for high volume applications.

BUILDING MATERIALS

As RF wireless power propagates through various dielectric materials, antennas can be embedded inside a product because line of sight between the transmitter and receiver is not necessary. This also means wire-

lessly powered sensors can be permanently embedded into building materials and placed behind walls. Typical indoor building materials like drywall are "RF friendly," as we know from the proliferation of Wi-Fi.

Considering the impact of walls on RF wireless power transfer, several properties impact power delivery. All dielectric materials have a dielectric constant (i.e., relative permittivity) and a loss tangent. Typically, a dielectric material is characterized by its loss or how it attenuates the RF signal propagating through it. This loss is related to the loss tangent of the material, which can be quite low for materials like drywall and will be greater for masonry like brick and concrete. Since the dielectric constant of the material is greater than the dielectric constant of the air inside the room, the difference creates an interface between the mediums that causes a refraction and reflection of the wave off the surface of the material.

The amount of reflected power and the angle of reflection depend on the polarization of the wave with respect to the plane of incidence and are described by the Fresnel equations. For simplicity, the following equations assume a lossless, non-magnetic dielectric:

$$R_S = \left|\frac{\sqrt{\varepsilon_1}\cos\theta_i - \sqrt{\varepsilon_2}\cos\theta_t}{\sqrt{\varepsilon_1}\cos\theta_i + \sqrt{\varepsilon_2}\cos\theta_t}\right|^2 = \left|\frac{\sqrt{\varepsilon_1}\cos\theta_i - \sqrt{\varepsilon_2}\sqrt{1-\left(\frac{\sqrt{\varepsilon_1}}{\sqrt{\varepsilon_2}}\sin\theta_i\right)^2}}{\sqrt{\varepsilon_1}\cos\theta_i + \sqrt{\varepsilon_2}\sqrt{1-\left(\frac{\sqrt{\varepsilon_1}}{\sqrt{\varepsilon_2}}\sin\theta_i\right)^2}}\right|^2 \quad (6)$$

$$R_P = \left|\frac{\sqrt{\varepsilon_1}\cos\theta_t - \sqrt{\varepsilon_2}\cos\theta_i}{\sqrt{\varepsilon_1}\cos\theta_t + \sqrt{\varepsilon_2}\cos\theta_i}\right|^2 = \left|\frac{\sqrt{\varepsilon_1}\sqrt{1-\left(\frac{\sqrt{\varepsilon_1}}{\sqrt{\varepsilon_2}}\sin\theta_i\right)^2} - \sqrt{\varepsilon_2}\cos\theta_i}{\sqrt{\varepsilon_1}\sqrt{1-\left(\frac{\sqrt{\varepsilon_1}}{\sqrt{\varepsilon_2}}\sin\theta_i\right)^2} + \sqrt{\varepsilon_2}\cos\theta_i}\right|^2 \quad (7)$$

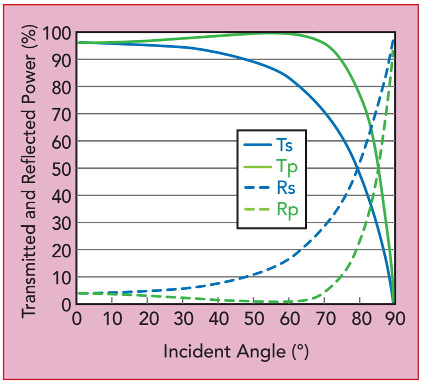

Fig. 4 Calculated transmitted and reflected power of an incident wave on a lossless, non-magnetic drywall boundary (ε_r = 2.19).

where R_S is the power reflection coefficient for the perpendicular polarization, R_P is the power reflection coefficient for the parallel polarization, θ_i is the angle of the incident wave, θ_t is the angle of the refracted wave and ϵ_1 and ϵ_2 are the dielectric constants of the two media.

Plotting these equations (see ***Figure 4***) shows the reflected and transmitted power at the interface. Incident angles less than 60 degrees enable 80 percent or more of the RF wireless power to transmit into the wall. Interestingly, with parallel polarization, 100 percent of the RF wireless power transmits into the wall at Brewster's angle.

Because a sheet of drywall is not lossless and creates two interfaces —room into the drywall and drywall to the air behind it—a simulation using Ansys HFSS helps visualize how drywall affects propagation. The scenario comprised 12.8 mm thick drywall with ε_r = 2.19, tan δ = 0.0111 and a 915 MHz transmitting dipole antenna located 0.5 m from the wall. The magnitude of the electric field (E-field) was plotted for a 4 × 2 m plane of incidence with perpendicular polarization (see ***Figure 5a***). For comparison, the simulation was repeated with the wall removed (see ***Figure 5b***). The figures show top-down views of the plane of incidence, i.e., the dipole and wall project into and out of the page.

The simulation without the wall (Figure 5b) shows smooth, even E-field rings. In Figure 5a, the portions of the rings at angles of incidence near zero (i.e., directly down from the dipole) show results similar to the no-wall example because of little reflec-

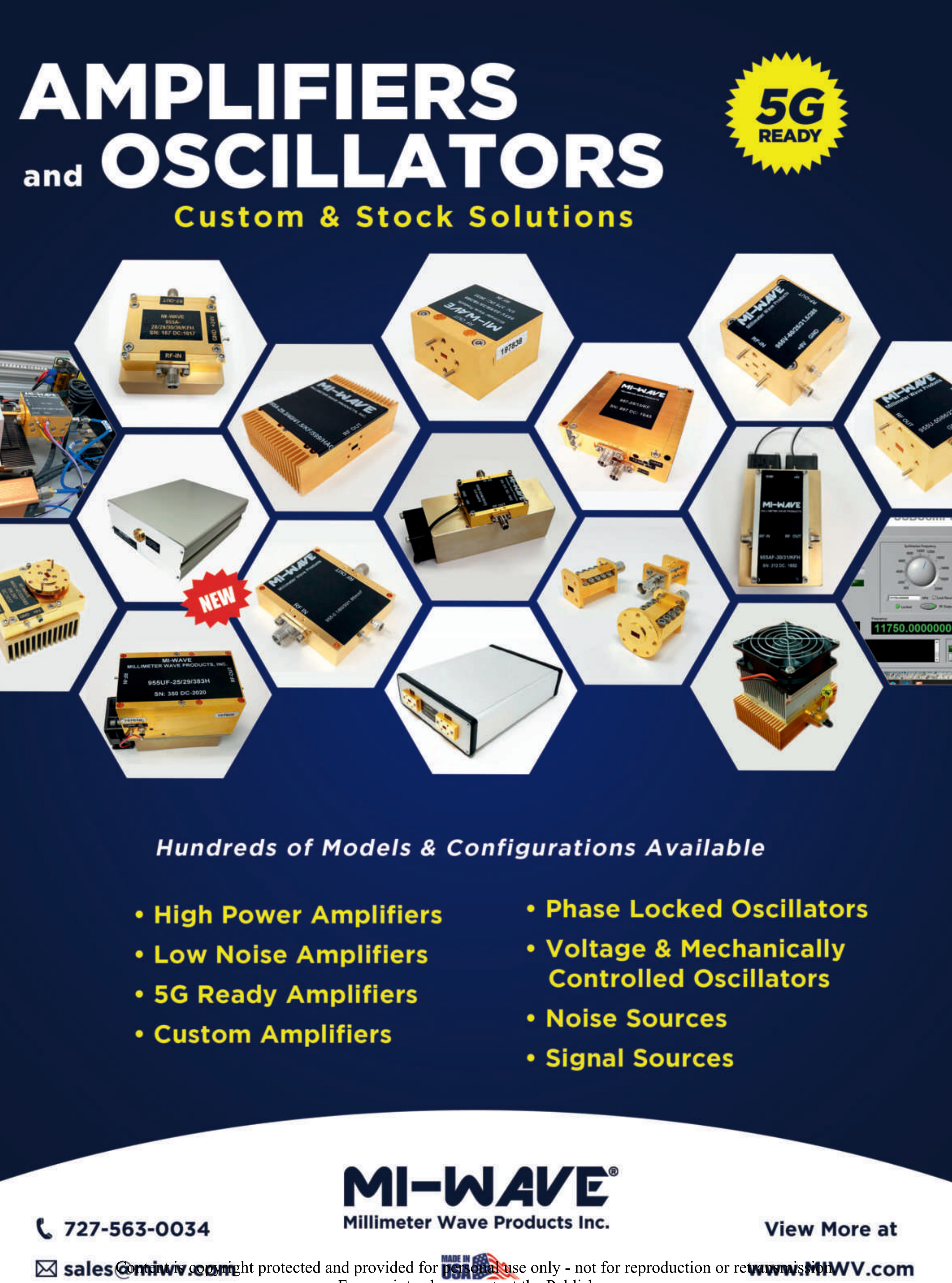
AMPLIFIERS
and OSCILLATORS
Custom & Stock Solutions
5G READY
NEW
Hundreds of Models & Configurations Available
• High Power Amplifiers
• Low Noise Amplifiers
• 5G Ready Amplifiers
• Custom Amplifiers
• Phase Locked Oscillators
• Voltage & Mechanically Controlled Oscillators
• Noise Sources
• Signal Sources
MI-WAVE®
Millimeter Wave Products Inc.
727-563-0034
View More at
www.MIWV.com

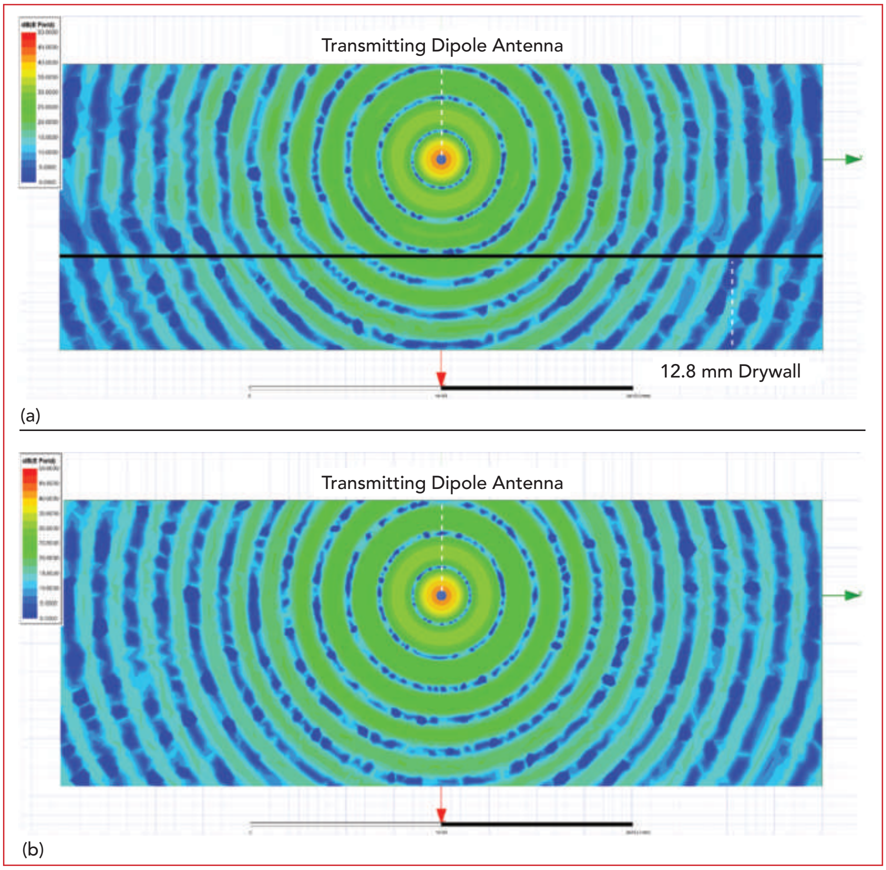

▲ Fig. 5 Top view of the E-field magnitude with (a) and without (b) drywall boundary.

tion off the drywall, i.e., due to the small angle of incidence. At steeper angles—at the far right and left of the dipole—the reflected E-field is higher, causing more distortion of the rings. The reflected waves are constructively and destructively interfering with the main E-field from the dipole. Examining both images, the two simulations share a similar E-field due to the relatively low dielectric constant of the drywall, with minimal RF reflection. The simulation confirms RF wireless power can be implemented without line of sight as long as the system is designed for it. Even with a wall separating the transmit and receive antennas, power delivery is possible, relatively unaffected by the barrier.

CONCLUSION

RF wireless power can be implemented in vastly different ways. Due to the complexity of each environment, various system parameters can be adjusted to meet the demands of an individual application. In general, lower frequency signals have greater RF power throughput. The size of the receiving product typically sets the maximum antenna size, which dictates the minimum frequency for power delivery. While it is possible to use electrically small antennas, these have a narrow bandwidth which makes them impractical for mass production from shifts in resonant frequency caused by manufacturing tolerances.

Focusing the RF in the near field or far field offer additional ways to increase throughput. However, including multiple antennas in an array with supporting electronics multiplies the cost of a deployment, so a transmitter with a single antenna and amplifier may be more advantageous for high volume applications. The presence of standard indoor building materials has minimal impact on the RF field, so multi-room RF wireless power systems are possible.

Given the design options, RF wireless power systems can be engineered to meet the different needs of many applications in many market verticals. RF wireless power is not a technology of the future; it is a technology being deployed today, with rapid expansion and mass adoption on the near-term horizon.■


ANALOG DEVICES
AHEAD OF WHAT'S POSSIBLE™
One Transceiver, Endless Radio Applications
Our industry-leading, software-defined radio solutions—including the new ADRV9002—deliver scalability, simplicity, and flexibility across all military communication applications to get you to market faster.
End-to-End Signal Chain
Wide Signal Bandwidth
Agile
Low Power
Get to market faster at analog.com/radioverse

Miniaturized Microstrip UWB Bandpass Filter with Dual Notched Bands and Improved Out-of-Band Rejection

Yong-Qin Liu
Xi'an University of Technology, Xi'an, China, Weinan Normal University, Weinan, China

Xi-Zheng Ke
Xi'an University of Technology, Xi'an, China

Gang Zhang
Weinan Normal University, Weinan, China

A miniaturized microstrip ultra-wideband (UWB) bandpass filter with dual notched bands and improved out-of-band rejection uses a modified square ring multi-mode resonator (MSRMMR). Four high-low impedance resonant cells are placed in the inner area of a conventional square ring multi-mode resonator (MMR), forming an MSRMMR to achieve harmonic suppression and size reduction. An E-shaped resonator is coupled to the MSRMMR to achieve dual notched bands.

UWB radio technology has become more popular for high speed wireless connectivity since the Federal Communications Commission's decision to permit unlicensed operation in the band from 3.1 to 10.6 GHz in February 2002.[1] UWB radio offers several advantages, such as higher data rate, lower transmit power and simplified error control coding. The UWB bandpass filter, one of the essential components of an UWB system, has received much attention in recent years. Several different designs have been proposed.[2-6] Gomez-Garcia et al.[2] directly cascaded highpass and lowpass filters, but insertion loss and overall circuit size were inevitably increased. A multilayer broadside-coupled structure has been used,[3,4] but the multilayer structure is not compatible with existing microwave integrated circuit design. Song et al.[5] used an MMR, but the filter had a narrow upper stopband. Wei et al.[6] used a three-line coupled resonator, but selectivity was not ideal. Additionally, signals from existing wireless networks such as 5.8 GHz WLAN and some 8.0 GHz satellite communication systems can interfere with UWB transmissions. To address this, UWB BPF designs with notched rejection bands are emerging.[7]

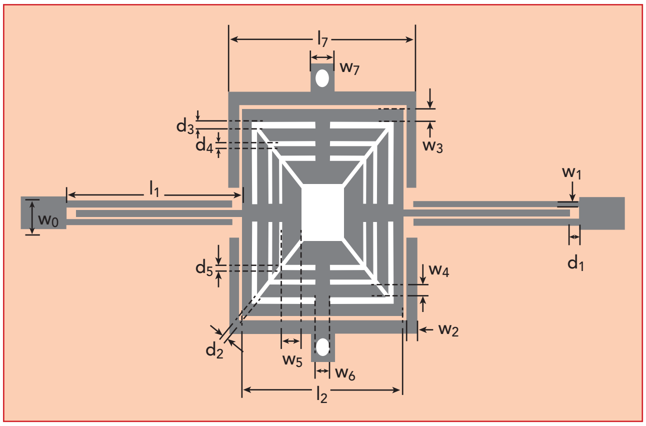

Fig. 1 Layout of the UWB bandpass filter.

Based on our previous work,[8] we introduce a new miniaturized microstrip UWB bandpass

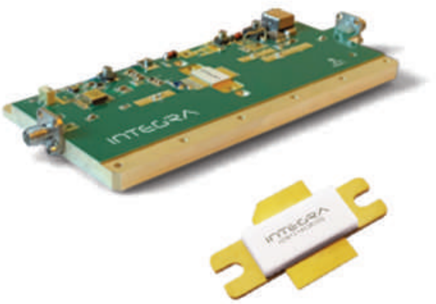
INTEGRA

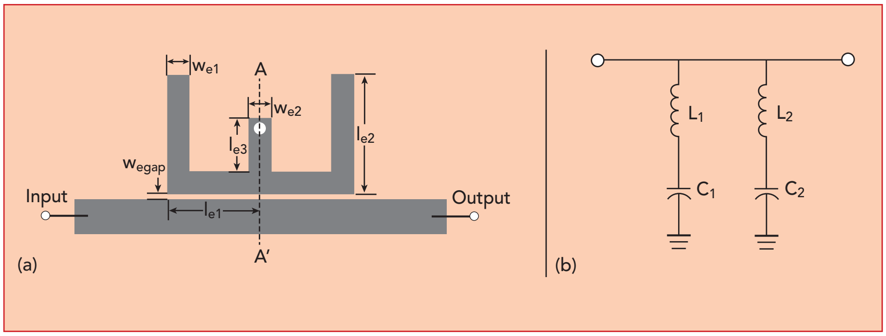

Fig. 2 Layout (a) and equivalent circuit (b) of the coupled E-shaped resonator.

filter with dual notched bands and improved out-of-band rejection using a MSRMMR. Four high-low impedance resonant cells are periodically placed within the inner area of a conventional square ring MMR. This achieves harmonic suppression and size reduction. Coupling an E-shaped resonator to the MSRMMR creates dual notched bands.

FILTER DESIGN

Four high-low impedance resonant cells are placed inside the free area of the conventional square ring MMR (see ***Figure 1***). Each unit cell comprises two high impedance and two low impedance lines, cascaded alternately. The high impedance lines are loaded only at the sites connected to the ring, creating lumped form inductances, which do not influence the per unit length inductance of the main transmission lines. The low impedance lines are loaded in parallel with the main transmission lines, which adds distributed capacitance and increases the per unit length capacitance of the main transmission lines. This type of slow-wave loading mainly increases shunt capacitance in the UWB bandpass filter.

The effective characteristic impedance Z and propagation constant β are given by:

$$Z = \sqrt{\frac{L_0}{C_0 + C_1}} \quad (1)$$

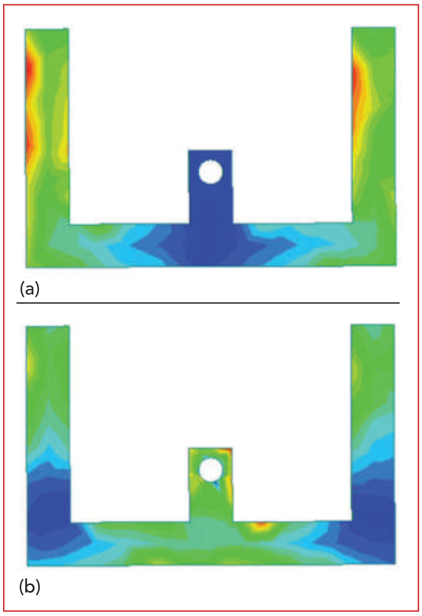

Fig. 3 E-shaped resonator simulated E-fields: odd (a) and even mode (b).

$$\beta = \sqrt{L_0\left(C_0 + C_1\right)} \quad (2)$$

where L_0 and C_0 are the distributed inductance and capacitance without loading per unit length, respectively; C1 is the effective distributed capacitance caused by the periodic loading per unit length. Equation 2 shows the propagation constant is increased by the periodic capacitive loading. An increased propagation constant means a shorter physical structure can be used to yield the required electrical length compared to a conventional transmission line. The slow-wave loading does not increase the circuit area, as it is placed within the outer square ring.[9] Therefore, a compact UWB bandpass filter with improved out-of-band rejection and good selectivity can be achieved using this slow-wave structure.

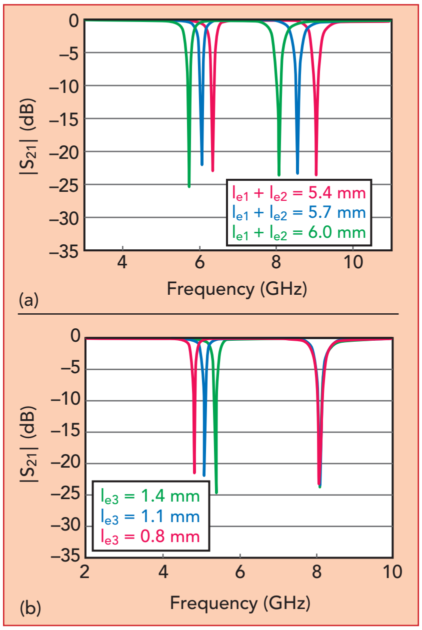

Fig. 4 Simulated $|S_{21}|$ of the coupled E-shaped resonator vs. $l_{e1} + l_{e2}$ (a) and l_{e3} (b).

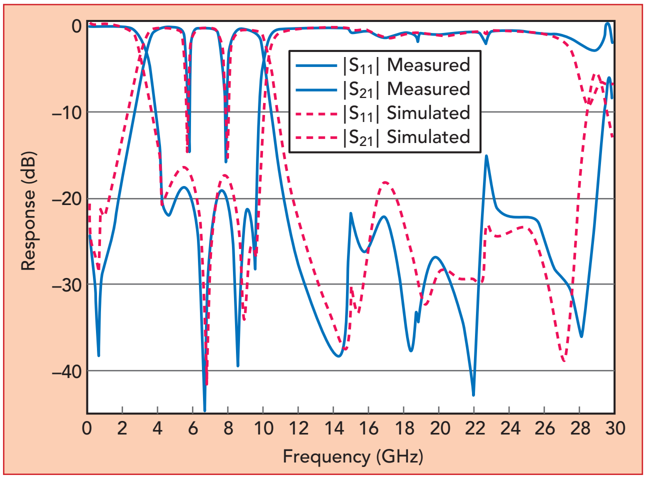

Fig. 5 Measured vs. simulated $|S_{21}|$ and $|S_{11}|$.

FILTER DESIGN WITH NOTCHED BANDS

To realize band-notched characteristics, an E-shaped resonator is added to the basic UWB bandpass filter. This structure is simple and flexible, consisting of a stepped impedance hairpin resonator centrally loaded with a shorted stub. ***Figure 2*** shows the layout of the resonator coupled to a section of the main transmission line and its equivalent circuit. Its resonant properties can be determined by even-odd mode analysis. Under excitation, the resonator's electric field (E-field) exhibits either an even or an odd mode distribution property (see ***Figure 3***). For the odd mode, the E-fields are anti-symmetric, distributed along the A-A' axis, and there is no E-field on the shorted stub, as shown in Figure 3a. For the even mode, the E-fields exhibit a symmetric distribution along the A-A' axis on both the open and shorted stub, shown in Figure 3b.

The even-odd mode resonant frequencies can be expressed as

$$f_{notch-even} = \frac{c}{\lambda_{notch-even}\sqrt{\varepsilon_{eff}}} = \frac{c}{4\left(l_{e1} + l_{e2} + l_{e3}\right)\sqrt{\varepsilon_{eff}}} \quad (3)$$

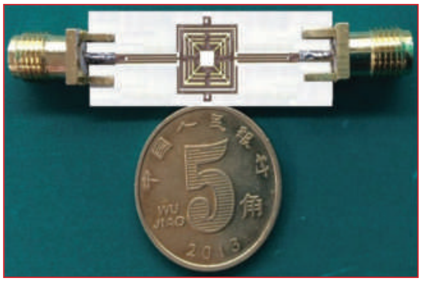

Fig. 6 Fabricated UWB bandpass filter.

ERAVANT
FORMERLY **SAGE MILLIMETER**

NOISE SOURCES | **26.5 to 170 GHz**

PRECISION CALIBRATED | CW | PULSED | TTL | MANUAL

SAGE Millimeter is now Eravant, a change that renews our commitment to the millimeterwave industry. Since 2011, we have been delivering quality products and energizing the customer experience to meet the needs of RF engineers working on the technology of the future.

Eravant's Noise Sources come standard with our high-quality faraday isolators integrated to improve the port return loss and load pull to provide more reliable and accurate noise figure measurements.

Eravant offers extended frequency noise sources. These noise sources operate outside of the standard waveguide bandwidth parameters.

For example, the WR-12 noise source can be calibrated to cover 60 to 96 GHz which is offered under model STZ-60396320-12-I1 and WR-10 can cover 65 to 116 GHz under model STZ-675312412-10-I1.

Eravant also offers High ENR version noise sources that can have an ENR specified up to 20 dB.

Noise Figure + Gain Test Extender
Eravant offer Noise Source and Gain Test Extenders to ease the millimeterwave noise figure testing from 26.5 to 170 GHz. The extenders are designed and manufactured to work with the industry standard noise figure test equipment, such as Keysight 8970A/B, N8973A, and N8975A/B.

WWW.ERAVANT.COM

www.eravant.com 501 Amapola Avenue Torrance, CA 90501
T: 424-757-0168

Adapters • Amplifiers • Antenna Feeds • Antennas • Attenuators • Bias Tees • Cable Assemblies • Corner Reflectors • Couplers • DC Blocks • Detectors • Ferrite Devices • Filters • Frequency Converters • Frequency Multipliers • Limiters • Magic Tees • Mixers • Noise Sources • Oscillators • Phase Shifters • Power Dividers • Radar Sensors • Subassemblies • Switches • ... Waveguide Sections

$$f_{notch-odd} = \frac{c}{\lambda_{notch-odd}\sqrt{\varepsilon_{eff}}} = \frac{c}{4\left(l_{e1}+l_{e2}\right)\sqrt{\varepsilon_{eff}}} \quad (4)$$

where λ_{notch} is the wavelength of the center frequency of the notched band, f_{notch} is the center frequency of the notched band, ε_{eff} is the effective dielectric constant and c is the speed of light in free space. The E-shaped resonator frequency characteristics at several dimensions were simulated to illustrate its dual-mode resonant properties (see ***Figure 4***). The frequency locations of the two notch bands move down with increasing dimensions of $l_{e1} + l_{e2}$, as shown in Figure 4a. This is because the E-fields are distributed in these two areas for both the even and odd modes. With a changing length of l_{e3}, however, only the lower band moves, as shown in Figure 4b, because there is no E-field distribution in this area for the odd mode.

TABLE 1

PUBLISHED UWB BANDPASS FILTERS

Reference	Circuit Dimension	3 dB Fractional Bandwidth (%)	Roll-Off Rate (dB/GHz)	Stopband (GHz)
3	3D	86	23	18
4	3D	138	20	25
5	2D	100	26	15
6	2D	117	15	20
7	2D	107	18	14
8	2D	98	NA	27
10	2D	110	19	20
This Work	2D	110	31	29.2

The roll-off rate is defined as $|\alpha max - \alpha min|/|fs - fc|$, where αmax is the 30 dB attenuation point, αmin is the 3 dB attenuation point, fs is the 30 dB stopband frequency and fc is the 3 dB cutoff frequency.

EXPERIMENTAL RESULTS

Simulation was performed with IE3D electromagnetic (EM) simulation software, a simulator based on the method of moments. The filter was designed on a RT/duroid® RO4350B substrate, with a dielectric constant of 3.38, thickness of 0.508 mm and loss tangent of 0.003. The dimensions of the filter (see Figure 1) were: l_1 = 8.0 mm, l_2 = 7.2 mm, w_0 = 1.1 mm, w_1 = 0.2 mm, w_2 = 0.4 mm, w_3 = 0.4 mm, w_4 = 0.3 mm, w_5 = 0.8 mm, w_6 = 0.6 mm, d_1 = 0.5 mm, d_2 = 0.2 mm, d_3 = 0.3 mm, d_4 = 0.2 mm and d_5 = 0.2 mm.

The fabricated UWB filter was measured with a Keysight Technologies N5238A vector network analyzer. The measured $|S_{21}|$ and $|S_{11}|$ are compared with the simulations in ***Figure 5***, showing good agreement. The differences between the measurements and simulation are attributed to fabrication tolerances and the SMA connectors. ***Figure 6*** shows the fabricated UWB bandpass filter, which is only 22 × 10 mm.

The passband of the fabricated filter covers 3.2 to 10.4 GHz, with a 100 percent fractional bandwidth at 6.80 GHz. The mid-band insertion loss was 0.25 dB, with return loss higher than 15 dB over the entire passband. The upper stopband stretches to 29 GHz, with insertion loss greater than 15 dB. For the two notched bands, the measured results show better than 15 dB insertion loss at 5.8 and 8.0 GHz with 3 dB FBWs of 5.9 and 4.2 percent, respectively. Comparisons with the performance of other published UWB bandpass filters are presented in ***Table 1***.

CONCLUSION

A miniaturized UWB bandpass filter achieved a wide upper stopband, good selectivity, low passband insertion loss and small size

using four high-low impedance resonant cells periodically placed in the inner area of a conventional square ring MMR. An E-shaped resonator coupled to the MSRMMR provides dual notch bands. The filter is designed for UWB wireless communication systems, offering a simple topology, compact size and excellent performance.■

ACKNOWLEDGMENT

This work was supported by the Shaanxi Provincial International Cooperation Project (2018KW-068), Shaanxi Provincial Department of Education Research Project (17JK0265) and Weinan City Science and Technology Project (2017 JCYJ-2-1).

References

1. L. Zhu, S. Sun and W. Menzel, "Ultra-Wideband (UWB) Bandpass Filters Using Multiple-Mode Resonator," *IEEE Microwave and Wireless Components Letters*, Vol. 15, No. 11, November 2005, pp. 796–798.
2. R. Gomez-Garcia and J. I. Alonso, "Systematic Method for the Exact Synthesis of Ultra-Wideband Filtering Responses Using High-Pass and Low-Pass Sections," *IEEE Transactions on Microwave Theory and Techniques*, Vol. 54, No. 10, October 2006, pp. 3751–3764.
3. B. W. Liu, Y. Z. Yin, Y. Yang, S. H. Jing and A. F. Sun, "Compact UWB Bandpass Filter with Two Notched Bands Based on Electromagnetic Bandgap Structures," *Electronics Letters*, Vol. 47, No. 13, June 2011, pp. 757–758.
4. H. Shaman and J. S. Hong, "Asymmetric Parallel-Coupled Lines for Notch Implementation in UWB Filter," *IEEE Microwave and Wireless Components Letters*, Vol. 17, No. 7, July 2007, pp. 516–518.
5. K. Song and Q. Xue, "Compact Ultra-Wideband (UWB) Bandpass Filters with Multiple Notched Bands," *IEEE Microwave and Wireless Components Letters*, Vol. 201, No. 8, August 2010, pp. 447–449.
6. F. Wei, Q. Y. Wu, X. W. Shi and L. Chen, "Compact UWB BPF with Triple-Notched Bands Based on Stub Loaded Resonator," *Electronics Letters*, Vol. 49, No. 2, January 2013, pp. 124–126.
7. J. D. Zhao, J. P. Wang and J. L. Li, "Compact UWB Bandpass Filter with Triple Notched Bands Using Parallel U-Shaped Defected Microstrip Structure," *Electronics Letters*, Vol. 50, No. 2, January 2014, pp. 89–91.
8. J. D. Zhao, J.P. Wang, G. Zhang and J. L. Li, "Compact Microstrip UWB Bandpass Filter with Dual Notched Bands using E-Shaped Resonator," *IEEE Microwave and Wireless Components Letters*, Vol. 23, No. 12, December 2013, pp. 638–640.
9. V. Sekar and K. Entesari, "Miniaturized UWB Bandpass Filters with Notch Using Slow-Wave CPW Multiple-Mode Resonators," *IEEE Microwave and Wireless Components Letters*, Vol. 21, No. 2, February 2011, pp. 80–82.
10. L. Wang, Z. J. Zhu and S. Y. Li, "High-Selectivity UWB Filters with Adjustable Transmission Zeros," *Progress in Electromagnetics Research Letters*, Vol. 52, January 2015, pp. 51–56.

INVITED PAPER

Low Phase Noise Oscillators Enable High Speed Optical Modules

Parker Traweek
SiTime, Santa Clara, Calif.

Widespread deployment of 5G networks will enable tremendous advancements in connectivity and communications, by increasing bandwidth 10× and reducing latency 50×. Hyperscale datacenters are major beneficiaries of this improved performance, from the cloud computing and storage of massive amounts of data generated by 5G applications. Such improvements in speed and latency require significant improvements in the equipment and components used in datacenters; however, because datacenters have limited space and are expensive to expand, newer generation equipment and components must increase data rates while minimizing any increase in size. Another requirement is minimizing power consumption, as the power needed to

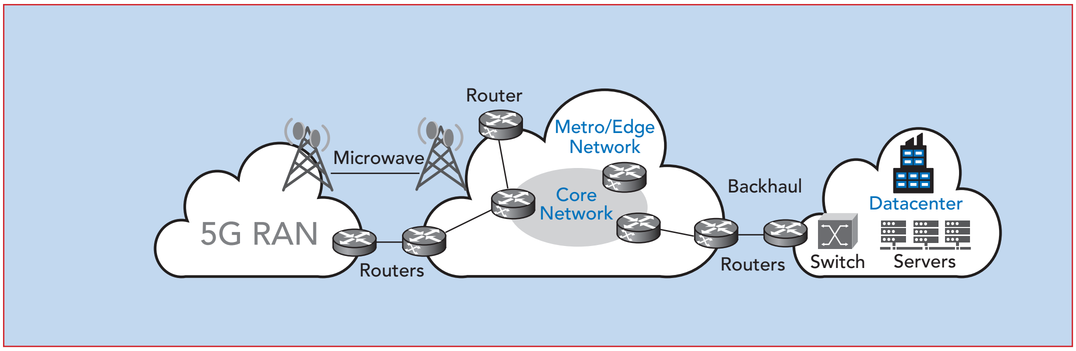

Fig. 1 **Optical modules are used from the 5G radio access network through the core network to the datacenter.**

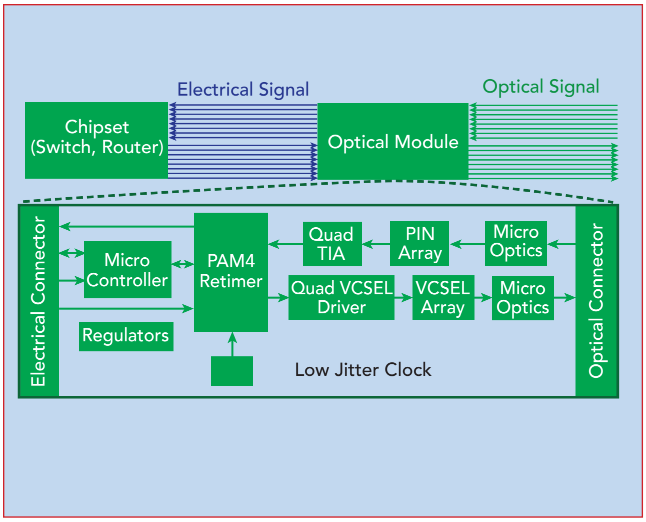

Fig. 2 **Optical module block diagram. The jitter of the clock limits the performance of the retimer.**

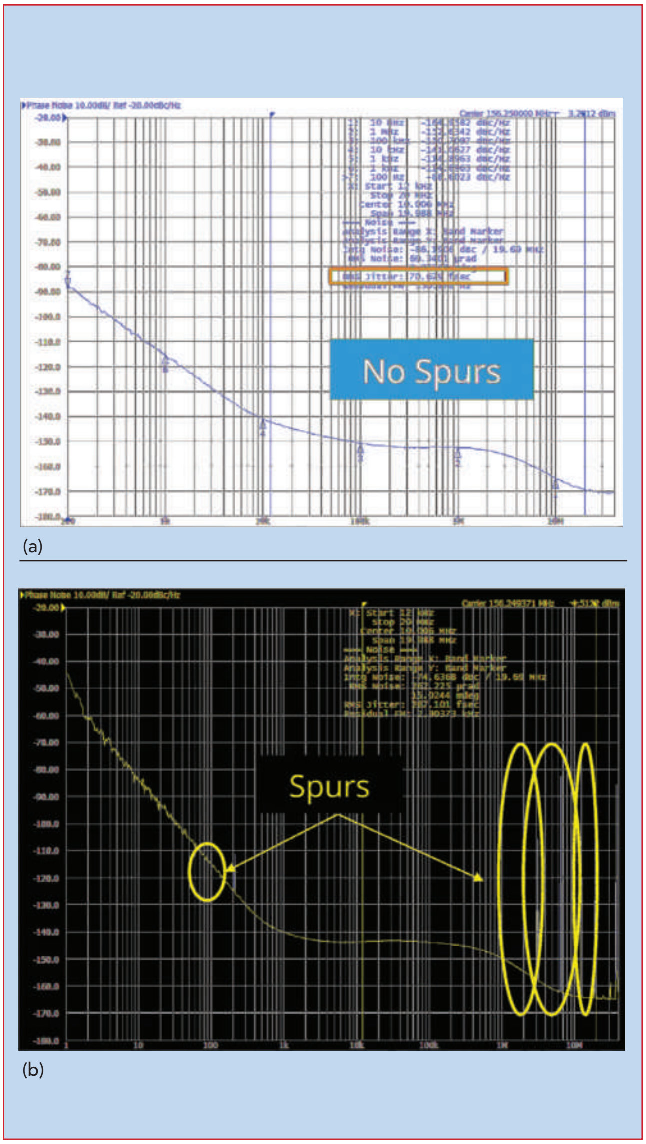

Fig. 3 **Phase noise and spur performance of MEMS-based (a) and phase-locked loop quartz (b) oscillators.**

operate datacenters is extraordinary—projected to consume as much as eight percent of global electricity usage by 2030, according to the sustainable information and communications technology expert Anders Andrae.

Optical transceivers, which connect and translate data carried over optical fibers into electrical signals within the datacenters, are one of the most important devices in the network connecting users to datacenters (see ***Figure 1***). To handle the increasing data traffic from 5G, optical module transmission rates are doubling—in some cases quadrupling. While 100 Gbps data rate modules were common in 2020, 400 Gbps modules are rapidly deploying, with 800 Gbps modules in development. Higher capacity 400 and 800 Gbps networks are extending demands on the optical modules for greater functionality, denser designs, lower power per bit and less jitter than their predecessors. This, in turn, requires significant improvements in oscillator technology, which sets the jitter performance of the clocks.

JITTER LIMITS DATA RATE

Optical modules convert optical signals into electrical signals and transform electrical signals into the optical format (see ***Figure 2***). To avoid introducing errors into the data, the conversion poses a complex challenge to synchronize two time domains: the optical network with the electronics chipset. Synchronization is critical, and the component responsible for synchronizing the timing—aptly named the retimer—requires a reference clock with low jitter. The phase jitter in the retimer adds to the jitter in the serial data stream passing through the module, resulting in data errors if the jitter is too large. This becomes increasingly important as the data rates increase from 100 to 400 to 800 Gbps. As the throughput doubles from 400 to 800 Gbps, the jitter should reduce by 2× to maintain the same timing margin.

The RMS phase jitter of the oscillator quantifies the variation of a clock edge, and it is typically computed by integrating the phase noise across a 12 kHz to 20 MHz offset frequency range. For example, a differential oscillator based on MEMS technology from SiTime has a phase noise of -89 dBc/Hz close in, dropping to a noise floor of -170 dBc/Hz. Integrated across a 12 kHz to 20 MHz offset from a 156.25 MHz clock yields an RMS phase jitter of 70 fs.

Another important factor determining oscillator performance is the presence of spurious signals, which will increase the jitter. ***Figure 3*** compares the phase noise responses of MEMS and phase-locked quartz oscillators. While the phase noise of the two appear comparable, the phase-locked quartz oscillator (Figure 3b) has several spurs, which increase the phase jitter to 267 fs, compared to 70 fs for the MEMS oscillator. Without the spurs, the RMS phase jitter of the quartz oscillator would be 90 fs, meaning the spurs contribute 66 percent of the total jitter. The MEMS oscillator uses an integer-N PLL architecture to avoid spurs and minimize the phase noise.

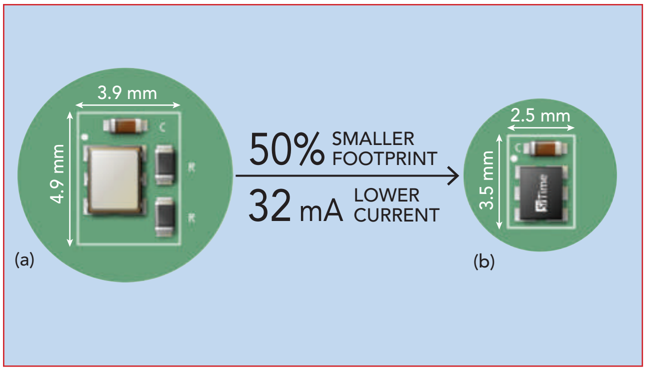

Fig. 4 Size and current consumption of AC-coupled LVPECL oscillator (a) and MEMS-based oscillator with integrated LVPECL source-bias resistors (b).

MINIMIZING SIZE

While the optical modules are increasing their data rates by 2× to 4×, the components used in the modules must support these higher data rates without significantly increasing circuit board footprint or power consumption. Reducing the footprint of the retimer is important because more than half of the optical module is used by the laser subassembly and its electronics, which leaves little room for the signal processing circuitry.

Comparing the MEMS and quartz oscillators, the MEMS oscillator has a 2.0 × 1.6 mm footprint compared to 2.5 × 2.0 mm for this quartz oscillator (see ***Figure 4***). The MEMS oscillator includes on-chip voltage regulators to filter power supply noise, which saves board area and improves the power integrity in the module. By integrating two source-bias resisters and using an AC-coupled output, the MEMS design reduced its footprint by 50 percent and current consumption by 32 mA. The MEMS oscillator design enables custom programming of the differential voltage swing at the factory so it can comply with the differential input swing of any chipset, including low voltage chipsets with nonstandard voltage swings. By matching the needs of the chipset, the typical termination can be eliminated, which reduces current to 16 mA with a DC-coupled LVPECL output.

SUMMARY

The evolution of the optical network to 400 and 800 Gbps data rates demands improved optical module performance without increasing size and current consumption, requiring the oscillator in the module to provide low jitter while minimizing power consumption and footprint. With innovations such as integrated bias resistors and programmable voltage swing, MEMS-based differential oscillators reduce the footprint and current consumption while achieving 70 fs RMS phase jitter. MEMS oscillators provide a timing solution that meets the needs of optical modules for 5G networks.■

Dalicap
DALICAP TECH. CORPORATION

Microwave / RF Ceramic Capacitor

DLC70 Series High Q,NPO, RF/Microwave MLCC

Product Features

- High Q
- Zero TCC
- Low ESR/ESL
- Low Noise
- Ultra-Stable Performance
- Extended WVDC available

SIZE:0402,0603,0505,0805, 0710,1111,2225,3838 for RF/Microwave; 6040,7575,130130 for High RF Power

Single LayerChip Ceramic Capacitor (SLC)

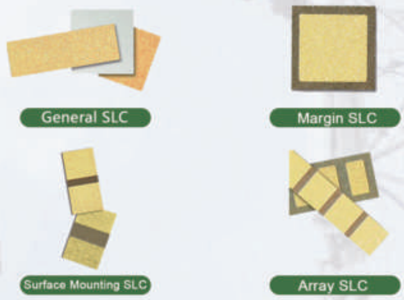

Product Features

- Broadband application for microwave and mmWave up to 100GHz
- Capacitance: 0.05pF to Max. 10,000pF
- Voltage Rating: up to 100 WVDC
- Used for DC Blocking, Low Noise Amplifiers, Power Amplifiers, tuning and Filters.

SIZE: 0.25 X 0.25 to 1.25 X1.25
Custom size is available

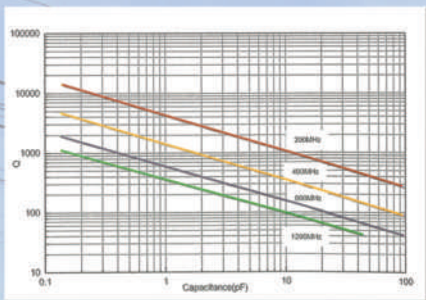

DLC70A(0505) Q Value and Capacitance Curve

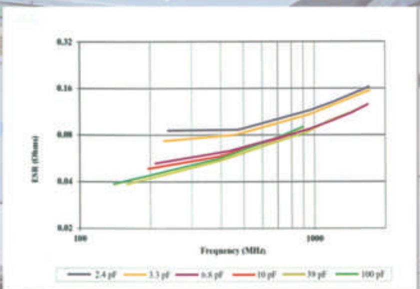

DLC75P(0603) Equivalent Series Resistances（ESRs）

Dalicap

Dalicap Tech. is a professional enterprise specializing in R&D, manufacturing and sales of multi-layer ceramic capacitors (MLCC). Dalicap is also a leading supplier of Hi-Q, ultra-low ESR RF/Microwave MLCC, applied especially on the fields of MRI, semiconductor device, industrial laser equipment, testing and analyzing instruments, balise and 4G/5G PA etc.

Dalicap is committed to providing high-performance, high-reliability products to customers. The R&D and engineering teams have extensive experience to quickly support and response to customized request.The company has an unique RF lab, by RF simulation and individual RF testing method to guarantee product realization.

www.dalicap.com dalicap@dalicap.com.cn +86-411-87632359

Updating the Historical Record: Gustav Engisch, Not Marconi, Believed to Have Conducted Early Wireless Experiments in Switzerland

Giuseppe Pelosi
Department of Information Engineering, University of Florence

Editor's Note: *In February 2006,* Microwave Journal *published an article about the IEEE dedication of a "Historical Milestone," acknowledging some of the first wireless experiments conducted in 1895 by Guglielmo Marconi in Salvan, Switzerland. The Historical Milestone was based on the memories of Maurice Gay-Balmaz, 70 years later, who recalled assisting a wireless researcher when Gay-Balmaz was about 10 years old. Further investigation concludes the researcher was not Guglielmo Marconi, nor the date 1895. It is now thought it was Gustav Engisch, a young electrical engineer from Vevey, Switzerland—a short distance from Salvan—who began to experiment with wireless technology in 1897.*

A 2006 *Microwave Journal* article titled *Salvan: Cradle of Wireless*, subtitled *How Marconi Conducted Early Wireless Experiments in the Swiss Alps*,[1] states:

"On September 26, 2003, the IEEE dedicated a 'Historical Milestone,' acknowledging some of the first wireless experiments conducted in 1895 by Guglielmo Marconi in Salvan, Switzerland, a picturesque resort in the Swiss Alps. This historical development had been described in detail by an elderly citizen who had assisted Marconi during his short stay in Salvan, Switzerland."

There are no written documents proving that Guglielmo Marconi was in Salvan—a small village close to Martigny and not far from Lausanne and Geneva—in 1895, as claimed. Further research has found:[2]

- Written permission by the Italian military authorities allowing Guglielmo Marconi to travel to London in 1896. Marconi was a young man, waiting to serve in the army, as it was compulsory at that time. He needed permission to exit Italy, and the only permission recorded is to London. It would have been an offense to exit Italy without permission.
- Guglielmo's brother was also claimed to be in Salvan, "Part of the equipment had been brought from Bologna by Marconi and his elder brother Alfonso."[1] However, the expense lists of Alfonso Marconi, which are very detailed, show many travel expenses during those years, yet none to Salvan or any other place abroad.

Shepherdess Stone.

The IEEE subsequently modified the attribution of the milestone, shifting the date from 1895 to 1897 and removing the name of Guglielmo Marconi.[3] The new Historical Milestone states:

"Early Swiss Wireless Experiments, 1897"

At this location in 1897, with local assistance, a researcher carried out some of the first wireless experiments. He transmitted a signal from this 'Shepherdess Stone' over a few meters and later, following six weeks of careful adjustments, over a distance of up to one and a half kilometers.

Salvan, Switzerland—26 September 2003 —IEEE Switzerland Section

References

1. F. Gardiol and Y. Fournier, "Salvan: Cradle of Wireless," *Microwave Journal*, February 2006, pp. 124-135.
2. G. Pelosi and S. Selleri, "Recent Outcomes of the Investigations on Guglielmo Marconi Supposed Experiments in Switzerland," *IEEE History of Electrotechnology Conference Proceedings*, September 2019, pp. 11-13.
3. "Early Swiss Wireless Experiments, 1897," *Engineering and Technology History WIKI*, https://ethw.org/Milestones:Early_Swiss_Wireless_Experiments,_1897.

30 kW, 900 to 930 MHz, Solid-State Microwave Generator

RFHIC Corp.
Anyang, South Korea

RFHIC Corporation has developed a 30 kW solid-state microwave generator for industrial and medical applications such as sterilizing, heating, drying, welding and scanning. An all solid-state design using GaN transistors, the RIK0930K-40T provides 30 kW CW output power at the RF cavity with a system efficiency of 56 percent across a 30 MHz bandwidth, tunable between 900 and 930 MHz.

RFHIC's GaN microwave generators offer many benefits compared to magnetron sources on the market, setting a new standard for microwave energy in the digital age. The RIK0930K-40T provides differentiated value from both the product and RFHIC's service.

MODULAR

The generator consists of eight rack-mountable shelves, each containing two, 2 kW GaN power amplifiers (PAs) which are water cooled. The shelf architecture makes the PAs easily accessible by users for quick PA replacement and output power scaling with minimum downtime and maintenance cost.

The generator has a three-phase, 50/60 Hz, air-cooled power supply unit, capable of 380 to 400 VAC operation, and a WR-975 waveguide converter. 220 to 240 and 480 VAC power supply voltages are available as custom options. Without the AC terminal box and external power combiner, the size of the generator system is 2048 cm high × 1018 cm deep × 810 cm wide and it weighs 520 kg. The generator height is being reduced by approximately 178 cm, i.e., 4U.

DIGITAL MONITORING AND CONTROL

RFHIC's solid-state microwave generator has many advantages over a magnetron. The output frequency of a magnetron is determined by the cavity's physical dimensions and, unlike GaN PAs, the magnetron cannot amplify the power of an applied microwave signal. It only serves as an oscillator, with limited control of frequency, power, phase and the signal source. The magnetron is controlled by an analog voltage, constraining users from controlling and monitoring the system remotely.

In comparison, the RIK0930K-40T uses a phase-locked loop synthesizer to digitally generate the desired frequency, producing more precise and stable frequencies with a low noise floor (see ***Figure 1***). The solid-state microwave generator system includes RFHIC's software suite, which includes accurate and nearly instantaneous power controls. Various frequency control modes are provided, including frequency sweeping. The software's built-in analytic feature performs real-time monitoring with automatic frequency adjustment, enabling users to create an optimal "recipe" for an application. The system constantly monitors and adjusts the key operating parameters to provide the optimal amount of microwave energy to the target, tuning the frequency and controlling phase over 360 degrees.

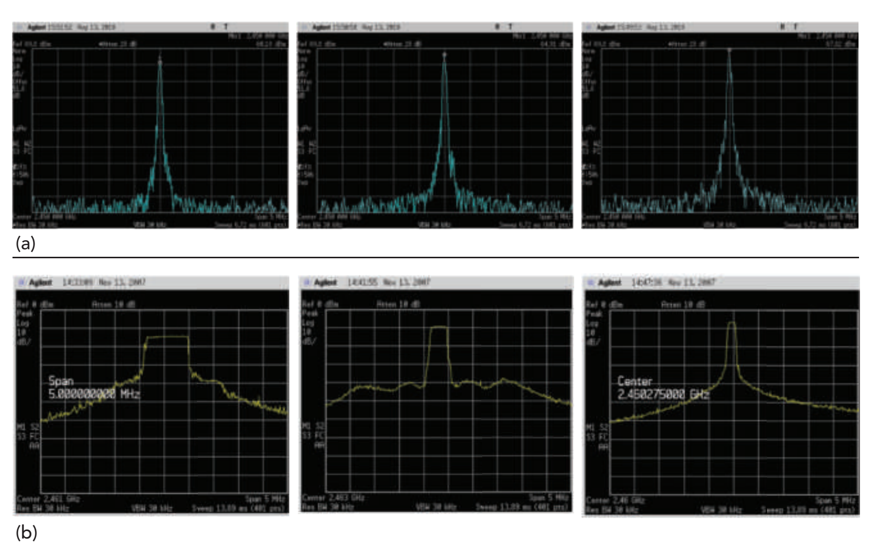

Fig. 1 A solid-state microwave generator (a) provides better frequency control and spectral purity than a typical magnetron generator (b). Output power for each at 1 (left), 3 (middle) and 6 (right) kW.

Fig. 2 60 kW solid-state microwave generator prototype, combining two 30 kW generators.

Another feature of the RIK0930K-40T is the high speed, pulse mode operation, with a pulse duty cycle of 1 to 99 percent and switching from CW to pulse within 100 ms. The pulse mode is beneficial for plasma generating, welding and sterilizing applications.

DURABLE AND RELIABLE

Magnetron systems are equipped with a single microwave source and operate at high voltage—up to 38 kV. Magnetron heads have an average lifetime from 2,000 to 5,000 hours, and they typically lose 30 to 40 percent of rated power over their lifetime. The short lifetime and high voltage operation have made magnetrons unsuitable for automated and industrial operations, where safety and minimum downtime are crucial.

To address this, RFHIC designed the PAs with GaN devices, so the microwave generators are durable and cost efficient, particularly for agile manufacturing. The RIK0930K-40T is equipped with reliable components and various protective features and has an average lifetime of 50,000 to 100,000 hours, depending on the operational settings and usage.

As noted, the RIK0930K-40T includes a three-phase, 400 VAC, 50/60 Hz power supply which provides 50 VDC bias for the generator. The generator provides a stable source of microwave energy without fluctuations and a safe environment for industrial manufacturing environments. The solid-state power supplies have a switch-mode design, which helps filter AC ripple, making the solid-state generator less sensitive than magnetrons to the quality of the AC power.

For added protection, the RIK0930K-40T is equipped with sensors that monitor the system's temperature, forward/reverse power and current. The PAs within the system have a maximum operating temperature of 80°C, and the maximum current is 60 A. If the system's sensors detect high reverse power, temperature or current, the system automatically shuts down to prevent damage. Each of the 16 PAs in the system is equipped with high power isolators to absorb any reflected power, preventing it from damaging the PAs. With a VSWR of 3:1 at maximum output, the system will withstand up to 25 percent of the reflected energy at maximum output power without any damage.

SCALABLE

RFHIC's GaN microwave generators are designed with a scalable architecture so users can easily add multiple power blocks to meet changing requirements. To increase the available power range, RFHIC is developing a 60 kW, 900 to 930 MHz, solid-state microwave generator (see ***Figure 2***). A sample is planned to be completed during July of this year.

VALUE

The microwave industry is generally aware of the low acquisition cost for magnetron systems. The magnetron head is sold at a low price, benefiting from its larger manufacturing volume but the power supply is sold for a premium. In comparison, RFHIC's systems use 50 VDC, cost-efficient power supplies, which increase system efficiency and reliability. Although the initial cost of the GaN PAs may be higher than a magnetron head, the differentiating features of RFHIC's microwave generators provide significant added-value in control, quality and reliability. Comparing the total cost of ownership, the GaN PA design is equivalent to a magnetron within two to three years.

RFHIC is semi-vertically integrated, the only company with a portfolio from GaN transistors and PAs to full systems, from commercial off-the-shelf products to custom modules and sub-systems delivering output power to multi-megawatts. RFHIC's GaN PA capabilities provide the highest quality and cost efficient solid-state microwave generators in the industry, supported with fast lead times—from three to six months—and excellent service.

RFHIC Corp.
Anyang, South Korea
www.rfhic.com

System Increases Dynamic Range of Digital Receivers

Precision Receivers Inc.
Marshall, Va.

Direct RF sampling is becoming the architecture of choice for applications ranging from electronic warfare and signals intelligence to radar and communications. However, an analog-to-digital converter (ADC) creates quantization, offset, gain, linearity and timing errors, resulting in spurious signals at its output. These "spurs" make it difficult—sometimes impossible—to separate the signal of interest from the noise, reducing the signal-to-noise ratio and spurious-free dynamic range (SFDR). Spurs can also interfere with the signals of interest, compromising the data and causing high bit-error rates and distortion, to the point where the signals of interest are compromised—even hidden by the spurs and undetected. Unlike the desired signal, spurs are not affected by analog filters prior to the ADC; they can appear at any frequency in the ADC's sampling frequency range, even well beyond the sampling frequency and aliased down to frequencies below the sampling frequency.

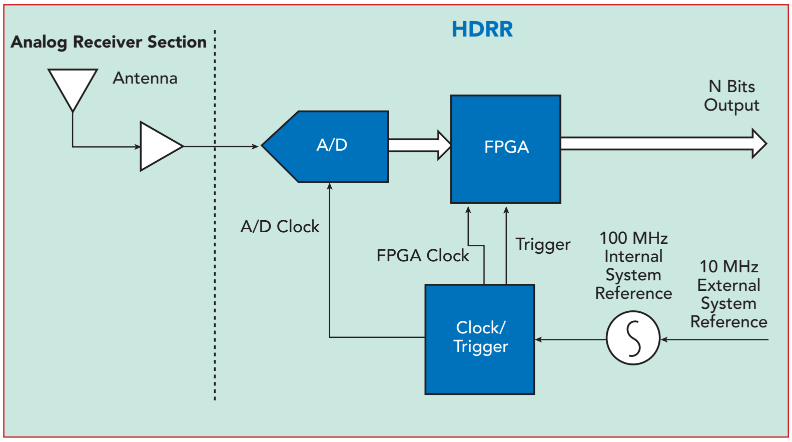

Fig. 1 **Direct sampled receiver using HDRR without an anti-aliasing filter and with digital tuning of the Nyquist zones.**

Various techniques are used to mitigate these problems, such as adding a dither signal that adds noise greater than the nominal quantization step size; however, this reduces the ADC's dynamic range and adds phase noise. ADC calibration can help, but it is temperature sensitive, a major problem for aircraft, which experience extremely wide temperature swings. To be effective in such situations, calibration requires updates in real-time. All these techniques for mitigating spurs become increasingly ineffective as system bandwidth extends to higher frequencies. Overall, they are complicated, unreliable, require considerable processing or are not particularly effective.

Precision Receiver's high dynamic range receiver (HDRR) technology does not suffer from these problems because it does not use the same approaches. It can be integrated within existing receivers (see ***Figure***

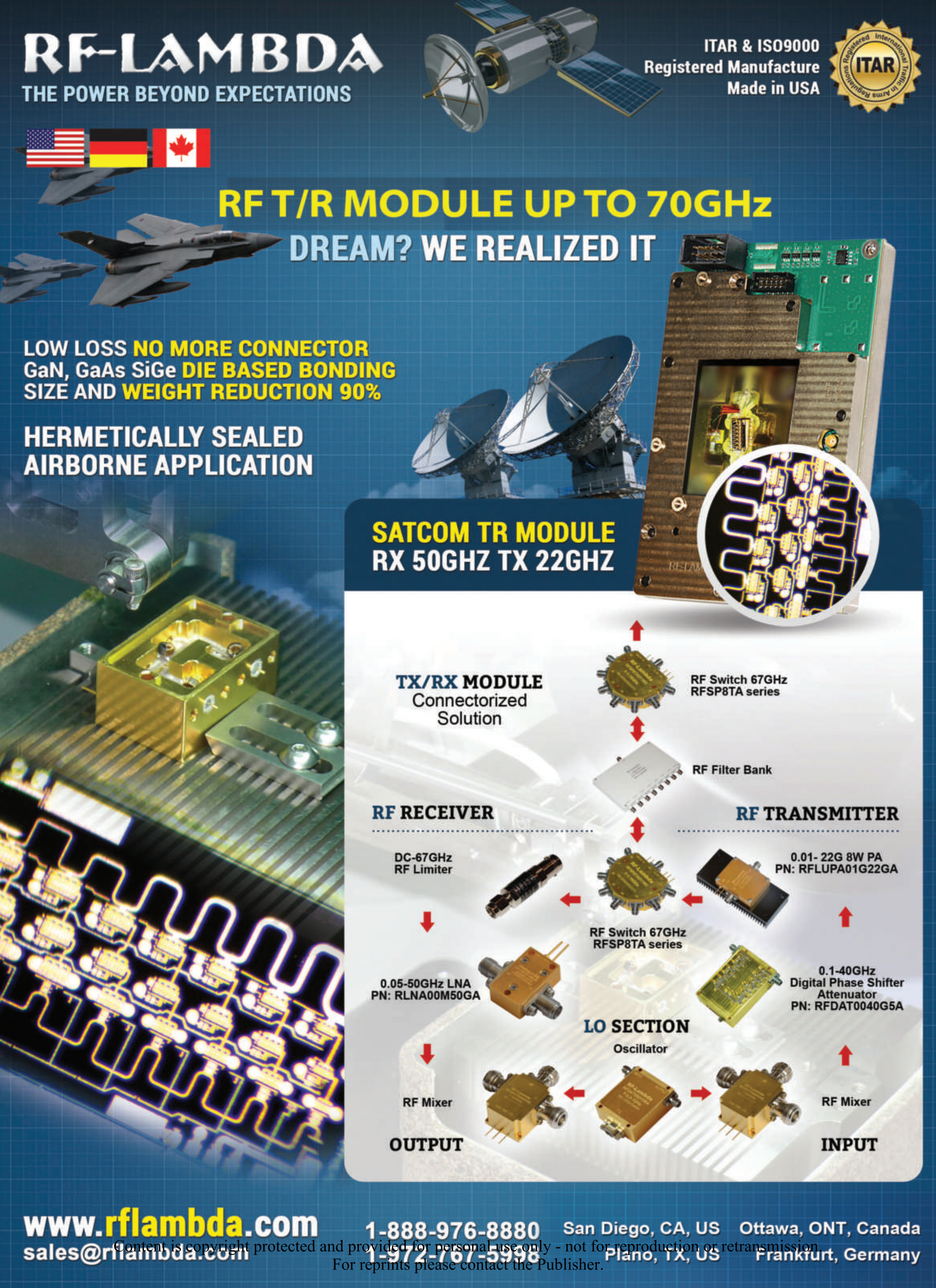
RF-LAMBDA
THE POWER BEYOND EXPECTATIONS
ITAR & ISO9000
Registered Manufacture
Made in USA
ITAR
Registered International Traffic in Arms Regulations
RF T/R MODULE UP TO 70GHz
DREAM? WE REALIZED IT
LOW LOSS NO MORE CONNECTOR
GaN, GaAs SiGe DIE BASED BONDING
SIZE AND WEIGHT REDUCTION 90%
HERMETICALLY SEALED
AIRBORNE APPLICATION
SATCOM TR MODULE
RX 50GHZ TX 22GHZ
TX/RX MODULE
Connectorized
Solution
RF Switch 67GHz
RFSP8TA series
RF Filter Bank
RF RECEIVER
RF TRANSMITTER
DC-67GHz
RF Limiter
0.01- 22G 8W PA
PN: RFLUPA01G22GA
RF Switch 67GHz
RFSP8TA series
0.05-50GHz LNA
PN: RLNA00M50GA
0.1-40GHz
Digital Phase Shifter
Attenuator
PN: RFDAT0040G5A
LO SECTION
Oscillator
RF Mixer
RF Mixer
OUTPUT
INPUT
www.rflambda.com
sales@rflambda.com
1-888-976-8880
1-972-767-5998
San Diego, CA, US
Plano, TX, US
Ottawa, ONT, Canada
Frankfurt, Germany

1) and does not require a significant investment in hardware or software. The SFDR improvements, especially in the higher Nyquist zones, is substantial: typically 9 to > 12 dBc. A 9 dB increase in SFDR will improve a system's effective reception range by 75 percent, and a 12 dB improvement expands that by 2×. HDRR technology enables ADCs to attain the highest effective number of bits (ENOB), typically increased by around 1.5 bits.

Figure 2 shows an example of the improvement provided by HDRR when used with a 2.5 GSPS ADC sampling a 1.52 GHz CW signal. Without HDRR, the SFDR at the output of the ADC is 61.3 dB, and the ENOB is 9.9 Bits (see Figure 2a). Applying HDRR (see Figure 2b) improves the SFDR 16.5 dB to 77.8 dB, and the ENOB by 1.7 bits to 11.6. The signal-to-noise and distortion ratio improves from 61.1 to 71.7 dB.

HDRR technology employs non-uniform sampling and advanced clocking and sampling to mitigate spurs and the resulting intermodulation distortion, while preserving the original phase and amplitude of the signal as measured at the antenna. Non-uniform sampling enables a receiving system to determine the signal's Nyquist zone location and extract additional information from it. As HDRR does not introduce dithering, there is no added phase distortion. A time series or frequency domain series is easily delivered at user-specified, low latency update intervals.

HDRR can also tune any Nyquist zones presented to the input or simultaneously tune all Nyquist zones. This enables systems to monitor broad bandwidths while reducing the complexity of anti-aliasing filters, possibly eliminating them. HDRR uses information available from the analog-to-digital conversion process, which is encoded in the HDRR clocking method. After the process is completed, the clocking information is used to separate the Nyquist information from the different zones, which keeps the desired frequencies in-band and rejects the out-of-band frequencies. Finally, HDRR helps mitigate overload, caused by jamming that can saturate the ADC and other elements of the system, by "softening" the compression of the ADC so its full range is used and preserving bits that would be lost.

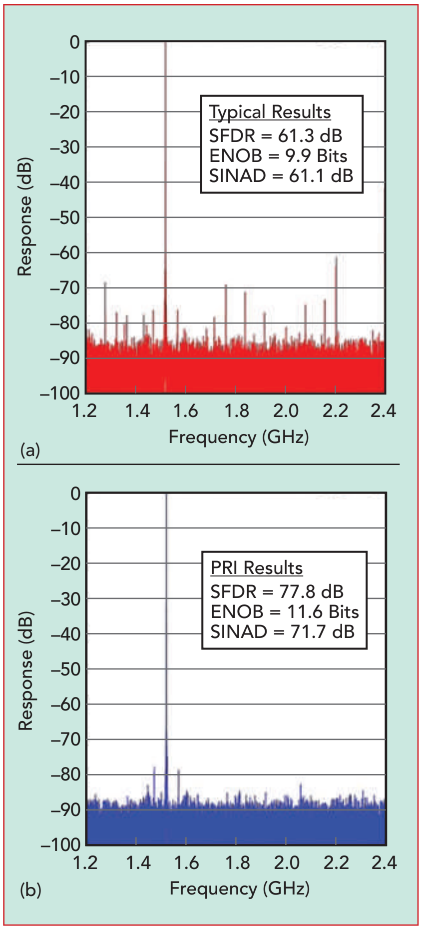

▲ Fig. 2 **Output of an ADC sampling a 1.52 GHz CW signal at 2.5 GSPS (a) and with HDRR processing (b).**

As HDRR is tailored to the needs of each system, Precision Receivers works with each customer, beginning with a demonstration system for evaluation. The demonstration system is a two-channel configuration with state-of-the-art 2.5 GHz ADCs and processing to perform a PRI-specific spur reduction algorithm that delivers a spur-free time series from the two channels. Direct conversion covers DC to 8 GHz. Alternatively, a block down-converter can be supplied to increase the input range to much higher frequencies.

Precision Receivers Inc.
Marshall, Va.
www.precisionreceivers.com

TechBrief

27 to 29 GHz, 10 to 40 W Solid-State Power Amplifiers with Optional Synthesizer

The Exodus AMP6034 series of power amplifiers cover 27 to 29 GHz at saturated power levels of 10, 20, 35 or 40 W. The class A/AB linear design provides excellent gain flatness, low noise figure and low harmonics, supporting all industry standards and modulations and 5G, satellite communications, EW and EMI applications.

A unique feature of the AMP6034 series is the option to add an integrated synthesizer. The frequency is set either from a front panel 7 in. color display or externally via Ethernet, USB or RS422 interface. The internal synthesizer provides both CW and pulsed signals with the capability to use a modulation signal from an external source, which is selected from the display or remote.

The AMP6034 series also offers the option of calibrated power monitoring in watts or dBm, accurate to within ±0.2 dB with an offset correction factor entered by the user. The power can be displayed on the color display or monitored remotely. If the optional calibrated power monitoring is not required, the AMP6034 series includes Exodus' standard monitoring of forward and reflected power, in watts and dBm.

The 10 and 20 W output power models use standard 2.92 mm (K) female connectors for the RF input and output. For the higher power 35 and 40 W models, the output RF interface is WR-28 waveguide. The AMP6034 series are compact: 2U or 3U high, depending on the output power and other options. The color touchscreen is available for both the 2U and 3U models (Exodus Option DMC). In addition to forward and reflected power, color touchscreen shows system voltages, currents and the operating temperatures of the heat sink and chassis.

VENDORVIEW

Exodus Advanced Communications
Las Vegas, Nev.
www.exoduscomm.com

REGISTER TODAY

IMS

Connecting Minds. Exchanging Ideas.

In-Person Event:	7-10 June 2021
Exhibition:	8-9 June 2021
Virtual Event:	20-25 June 2021

Atlanta • Georgia

Georgia World Congress Center (GWCC)

Come explore the latest and greatest communications, aerospace, automotive, IoT, THz and other emerging technologies.

IMS2021 and Microwave Week will be comprised of in-person and virtual participation options.

Pick up your badge onsite
Get equal access online

The best of both worlds

CONNECTING FOR A SMARTER, SAFER WORLD

Atlanta 2021

IEEE

MTT-S IEEE MICROWAVE THEORY & TECHNIQUES SOCIETY

RFIC

ARFTG

PROGRAM PREVIEW

Register by 4 June 2021 to receive the best rates!

www.ims-ieee.org

Exhibition, Mobile App & Social Media

Exhibition Overview:

The Exhibition consists of over 300 exhibiting companies who represent the state of the art materials, devices, components, and subsystems, as well as design and simulation software and test/measurement equipment. Whatever you are looking to acquire, you will find the industry leaders ready and willing to answer your purchasing and technical questions.

Exhibition Dates and Hours:

Tuesday, 8 June 2021	09:30 to 17:00
Wednesday, 9 June 2021	09:30 to 18:00

IMS Microwave Week Mobile App:

The IMS Microwave Week app is now available in the Apple App store and Google Play store. Install the app on your Android or iOS device to view the full schedule of Workshops, Technical Lectures, IMS and RFIC Technical Sessions, ARFTG, Panel Sessions, Social Events and Exhibition information. On-site during Microwave Week you will be able to download IMS and RFIC papers and presentations, locate exhibitors, upload photos and explore all that Atlanta, GA, has to offer! Download today!

Apple App Store   Google Play Store

MicroApps:

The Microwave Application seminars (MicroApps) offered Tuesday, 8 June and Wenesday, 9 June 2021, provide a unique forum for the exchange of ideas and practical knowledge related to the design, development, production, and test of products and services. MicroApps seminars are presented by technical experts from IMS2021 exhibitors with a focus on providing practical information, design, and test techniques that practicing engineers and technicians can apply to solve the current issues in their projects and products.

Industry Workshops:

The Industry Workshops are 2-hour industry-led presentations featuring hands-on, practical solutions often including live demonstrations and attendee participation. These Workshops are open to all registered Microwave Week attendees for a nominal fee.

Follow us on:

#IMS2021

For more information on MicroApps and Industry Workshops, please visit www.ims-ieee.org/exhibition.

Microwave Keynotes

Suresh Venkatarayalu
Chief Technology Officer
Honeywell

Dr. Ahmad Bahai, Chief Technology Officer and Senior Vice President, Texas Instruments

New Horizons for Millimeter-Wave Sensing

Prof. Bram Nauta, Distinguished Professor, University of Twente, The Netherlands

Transceiver Roadmap for 2035 and Beyond

IMS & RFIC Technical Sessions

IMS Technical Session Titles

- Advance in Phase Change Materials for Microwave Applications
- Heterogeneous and High-Density Flex RF Package Integration
- Additive Manufacturing Based RF Sensors and RFIDs for Rugged IoT and Digital Twins in Smart Cities
- Emerging Machine Learning Techniques for CAD of RF-Microwave Circuits
- Robert J. Trew
- Advances in Surrogate Modeling, Optimization, and Design Automation
- Advances in Numerical Methods for Electromagnetics and RF Circuits
- Innovations in Calibration and Measurement Techniques from MHz to THz
- Advanced Microwave and mm-wave Device Modeling Techniques
- Nonlinear Analysis, Simulation, and Design Techniques
- Integrated Waveguides and Composite Structures
- Nonlinear and Nonreciprocal Transmission Lines
- Recent Advances in Passive Components
- Advances in Planar Filters and Multiplexers
- Advanced Technologies for Non-Planar Filters Manufacturing
- New Solutions for Non-Planar Filters Design
- Advanced Reconfigurable and Integrated Filtering Components
- Acoustic Filters for Advanced Communication Systems
- Advances in MEMS, Acoustic and Ferrite Technologies for RF and Microwave Systems
- Advanced Fabrication Techniques for Up to Terahertz Packaging
- Advances in LNA Design for 5G Applications and Beyond
- Low Noise Devices and ICs
- Advanced Frequency Conversion Circuits and Oscillators
- Analog and Mixed Signal ICs for Wireline and Optical Communication
- High Power and Load Invariant PAs
- Compound Semiconductor PA Technologies for mmWave and 5G Applications
- Wideband, Efficiency-Enhancement Integrated Power Amplifiers in Silicon Technologies
- Linearization and Transmitter Techniques for Power Amplifiers
- Integrated Transmit-Receive Front-End Modules
- MMW and Sub-MMW Power Generation
- MMW and Sub-MMW Subsystems and Systems
- Microwave Photonics and Nanotechnology
- Array Beamformers and Calibration
- Recent Advances in Radar Systems and Technologies
- Phased Arrays and 5G-SATCOM Wireless Systems
- Characterization and Integration Techniques for 5G Wireless Systems
- Wireless Sensor Systems and Components
- Chipless RFID and Resonator-Based Sensors
- WPT Technologies for IoT and Bio-Medical Applications
- Instrumentation for Biomedical Measurements
- Sensor and Characterization Methods for Biological and Electronic Materials
- Enabling Advanced Technologies and Components for Transceiver and Communication Systems
- Innovative Technologies for Machine To Machine and Human To Machine Interactions
- Leveraging Electro-Magnetic Fields for Physical Security
- AI-ML Methods and Applications for Microwaves
- LATE NEWS - Broadband and High-Speed Circuits
- LATE NEWS - Technologies for 5G Wireless
- LATE NEWS - Millimeter-Wave Power Amplifiers
- LATE NEWS - Radar and Sensor Technologies
- LATE NEWS - Millimeter-Wave Arrays for Next Generation Wireless

RFIC Technical Session Titles

- Advanced Techniques for Power Amplifier Modules, Sub-THz and BIST
- mmWave Circuits for 5G Systems
- New Design Techniques for Frequency Generation
- Efficient Radios for IoT, GPS, WiFi, and Cellular
- Circuits and Systems for Microwave and mmWave Sensing, Radar and Communications
- CMOS Transmitters and Amplifiers from RF to mmWave
- Advanced N-Path Techniques and Associated Interference Mitigation
- mmWave and Sub-THz Power Amplifiers
- RF and mmWave VCOs
- Circuit Techniques for High-Speed Transceiver Front-Ends
- High-Performance Fractional-N PLLs and Building Blocks
- mmWave Circuits for Emerging Applications
- High Performance mmWave Front-End Circuits
- RF Systems for Emerging Wireless Applications

Technical Track Key:

Field, Device and Circuit Tech.	Passive Components & Packaging	Active Devices	Systems & Applications
Emerging Technologies	Focus or Special Sessions	RFIC Sessions	Late News

This information is accurate as of 3/10.

For the latest on IMS and Microwave Week visit www.ims-ieee.org

Panel Sessions, Technical Lectures & Workshops

Panel Sessions:

- Automotive Radars and AI: Is My Car Really Safe?
- Challenges of High Performing Energy Efficient and Reliable Radio Interface for 5G Infrastructure in Open Era
- Will Far-Field WPT Become a Reality?
- RF-Microwave Startups: A Dead Horse in the Era of Software Unicorns and Pandemics?

Technical Lectures:

- A Quick Tour Through the World of Si IC Power Amplifiers
- mm-Wave “Wireless Fiber” to Meet the Capacity Demands of Future Networks
- Micro-Motion Sensing Radar – Theory, System Architectures and Circuit Implementations
- Fully Integrated Terahertz Imaging and Spectroscopy: From Device to System

Workshops:

- mm-Wave Phased-Array Transceiver Design: From Basics to Advancements
- Fully Integrated Silicon vs. Hybrid RFFE Systems for mm-Wave 5G Highly Efficient PA Design Trade-offs
- Recent Advances in the Efficient Small- and Large-Signal Stability Analysis of Microwave Circuits
- Platforms, Testbeds and Trials – The Next Step for 5G and Future Wireless Networks
- Cryogenic RF and mmW Technology and Circuit Platforms: A Path Toward Quantum-Computing
- Advanced Micro-Scale Fabrication and Integration Techniques for Emerging Millimeter and Submillimeter-Wave Applications
- Recent Advances in Frequency Generation Techniques for sub-6GHz, mmWave and Beyond
- Spatiotemporal Metastructures for Microwave Applications
- Sub-6GHz Advanced Transmitter Architectures and PA Linearization Techniques
- Microwave Magnetic Materials and Devices for Novel Microwave Functionality
- Recent Advances in mmWave Radar Circuits and Systems for Emerging Sensing Applications
- Materials by Design for Microwave and mmWave Communications
- 100-300 GHz mmWave Wireless for 0.1-1 Tb-s Networks
- Beamforming in Massive MIMO for Millimeter-Wave New Radio
- Wireless Power Transmission – Myths and Reality
- CMOS mmWave Imaging Radars: State-of-the-Art and a Peek Into the Future!
- Microwave Acoustics and RF MEMS Enabling 5G
- Machine Learning and AI Techniques with Intelligent Systems for Wireless Communication, Sensing, and Computation
- Cryogenic Electronics for Quantum Computing and Beyond: Applications, Devices and Circuits
- State of the Art Characterization and Test Techniques from Design to Production of Antenna in Package-Module and on Chip
- Highly Linear and Linearized Power Amplifiers for mmWave Communications
- Non-Contact Vital Sign Detection and Human Motion Tracking using WiFi and Radar Techniques
- Advanced Multichip Modules and Packaging for 5G and Beyond
- Low Power Radios and Wireless Technologies for Indoor Positioning and Localization
- Satellite Systems: A Top-Down Review of Satellites, Space Communication and Hardware
- Coherent Optical Communications for Cloud Data Centers, Metro and Submarine Networks
- Calibrated Testbeds for the Characterization, Optimization and Linearization of Multi-Input Power Amplifiers
- Cutting-Edge THz Solid-State Technologies, From Devices to Earth-Space Applications: Surfing on Noise, Signal and Power Generation
- Millimeter-Wave and Terahertz Technologies for Multi-Gbps Wireline Interconnects
- Enabling Technologies for Efficient Ultra-High Speed Wireless Communication Systems Towards 100 Gb-s
- MIMO and Digital Beamforming Systems for 5G and Beyond
- Past and Future of Microwave Passive Components (in Memory of Professor Arthur A. Oliner)

This information is accurate as of 3/10.

Exhibitor List

3D Glass Solutions Inc.
3G Shielding Specialties
3RWAVE
A.J. Tuck Co.
A.L.M.T. Corp.
A-Alpha Waveguide Inc.
ACE-Accurate Circuit Engineering
ACEWAVETECH
ADMOTECH Co. Ltd.
AdTech Ceramics
Advanced Assembly
Advanced Circuitry International
AGC Nelco America Inc.
Agile Microwave Technology Inc.
AI Technology Inc.
Akoustis Inc.
Altum RF International
AMCOM Communications Inc.
American Microwave Corp.
American Standard Circuits Inc.
Amphenol SV Microwave
AmpliTech Inc.
Analog Devices Inc.
AnaPico Ltd.
Anoison Electronics LLC
Anokiwave
Anritsu Co.
AO Technologies
APITech
Applied Specialties/RF Depot
Applied Thin-Film Products
AR RF/Microwave Instrumentation
Arralis
Artech House
Association of Old Crows/Naylor
Astronics Test Systems
Atlanta Micro Inc.
Avalon Test Equipment
AVX Corporation
B&Z Technologies
Barry Industries Inc.
Benchmark Electronics
Berkeley Nucleonics Corp.
BSC
Cadence Design Systems Inc.
CAES
Cernex Inc./Cernexwave
Charter Engineering Inc.
Ciao Wireless Inc.
Cicor Group
Cinch Connectivity Solutions
CML Microcircuits
Coilcraft Inc.
Colorado Engineering Inc.
Colorado Microcircuits Inc.
Communications & Power Industries
Component Distributors Inc.
Conduct RF
Connectronics Inc.
Continental Resources
Copper Mountain Technologies
Corning Inc.
Criteria Labs Inc
Crystek Corp.
CTT Inc.
Cubic Nuvotronics
Custom Cable Assemblies Inc.
CX Thin Films
dB Control
Delta Electronics Mfg. Corp.
DeWeyl Tool Company
Diamond Antenna & Microwave Corp.
Diramics
DiTom Microwave Inc.
Doosan Corp/Electro-Materials
dSpace Inc.
Dow-Key Microwave
Ducommun Inc.
Dylan-Tek
Electro Rent Corp.
Element Six (UK) Ltd.
Elite RF
EM Labs Inc.
Empower RF Systems Inc.
EMSS Antennas
Eravant (formerly SAGE Millimeter Inc.)
Erzia Technologies
ETL Systems Ltd.
ETS-Lindgren
European Microwave Week
Everything RF
evissaP Inc.
Exodus Advanced Communications
F&K Delvotec Inc.
Filtronetics Inc.
Filtronic Broadband Limited
Fine-Line Circuits Limited
Flexco Microwave Inc.
Focus Microwaves Inc.
FormFactor
Frontlynk Technologies Inc.
Gamma Electronics Inc.
Geib Refining Corp.
Gel-Pak
General Microwave Corporation
GGB Industries Inc.
Global Communication Semiconductors
GLOBALFOUNDRIES
Gowanda Components Group (GCG)
Guerrilla RF
HASCO INC
Hermetic Solutions Group
Herotek Inc.
Hesse Mechatronics
High Frequency Electronics
Hirose Electric USA
HRL Laboratories LLC
Huang Liang Technologies Co. Ltd.
HYPERLABS
IHP GmbH
IMS2022
InCompliance Magazine
Indium Corp.
Innertron Inc.
Innovative Power Products Inc.
In-Phase Technologies Inc.
Intelliconnect LLC
International Manufacturing Services Inc.
inTEST Thermal Solutions
Ironwood Electronics
Isola
ITF Co. Ltd.
IW Microwave Products
JFW Industries Inc.
JQL Technologies Corporation
Junkosha Inc.
K&L Microwave Inc.
Keysight Technologies
Knowles Precision Devices
KOSTECSYS Co. Ltd.
KRYTAR Inc.
KVG Quartz Crystal Technology GmbH
Kyocera International Inc.
L3Harris Technologies
LadyBug Technologies LLC
Lake Shore Cryotronics Inc.
Laser Processing Technology Inc.
Leader Tech. Inc.
Linearizer Technology Inc.
Lintek Pty Ltd.
Logus Microwave
Lorentz Solution Inc.
LPKF Laser & Electronics
M2 Global Technology Ltd.
MACOM
Marki Microwave Inc.
Maury Microwave
MaXentric Technologies LLC
MegaPhase
Menlo Microsystems Inc.
Metamagnetics Inc.
Mician GmbH
Micro Harmonics Corporation
Micro Lambda Wireless Inc.
Micro Systems Technologies Inc.
Microchip Technology Inc.
MicroFab Inc.
Micro-Mode Products Inc.

This information is accurate as of 3/10.

For the latest on IMS and Microwave Week visit www.ims-ieee.org

Exhibitor List

Microsanj LLC
Microwave Applications Group
Microwave Development Labs
Microwave Journal
Microwave Products Group
Microwave Techniques LLC
Microwaves & RF
Millimeter Wave Products Inc.
Milliwave Silicon Solutions Inc.
Mini-Circuits
Mini-Systems Inc.
Mitsubishi Electric US Inc.
Modelithics Inc.
Modular Components National
Morion US LLC
Mouser Electronics Inc.
MPI Corp.
MRSI Systems LLC
MtronPTI
NEL Frequency Controls Inc.
Networks International Corp.
New Japan Radio
Norden Millimeter Inc.
Northrop Grumman
NSI-MI Technologies
Nxbeam Inc.
Oak-Mitsui Technologies LLC
OEwaves Inc.
Ohmega Technologies Inc.
Ophir RF Inc.
Optomec
Orbel Corp.
Orient Microwave Corp.
Pasquali Microwave Systems
Passive Plus Inc.
Pentek
Pickering Interfaces Inc.
Pico Technology
Piconics Inc.
Pivotone Communication Tech. Inc.
Planar Monolithics Industries Inc.
Pletronics - Taitien
Plexsa Manufacturing Hungary Kft
PM Industries Inc.
Pole/Zero Corporation
Polyfet RF Devices
PPG Cuming Microwave
Presidio Components Inc.
PRFI Ltd.
Printech Circuit Labs Ltd.
pSemi Corporation
Q Microwave Inc.
Qorvo
Quarterwave Corp.
Quik-Pak
QuinStar Technology Inc.
QWED Sp. z o.o
R&K Company Limited
Reactel Inc.
RelComm Technologies Inc.
Remcom Inc.
Renesas Electronics America Inc.
Res-Net Microwave Inc.
Response Microwave Inc.
RF Globalnet/VertMarkets Inc
RF Morecom Corea
RFHIC Corp.
RF-Lambda
RFM Integrated Device, Inc.
RFMW
Richardson Electronics Ltd.
RJR Technologies Inc.
RLC Electronics Inc.
Rogers Corp.
Rohde & Schwarz USA Inc.
Rosenberger North America
SAF North America LLC
Saint-Gobain
Sainty-Tech Communications Ltd.
Samtec Inc.
Sawnics Inc.
Scientific Microwave Corp.
Semi Dice Inc.
SemiGen
Sensorview Co. Ltd.
Shenzhen Superlink Technology Co. Ltd
Siglent Technologies NA
Signal Hound
Signal Microwave
SignalCore Inc.
Signatone
Skyworks Solutions Inc.
Smiths Interconnect
Solid Sealing Technology
SOMACIS
Sonnet Software Inc.
Southwest Microwave Inc.
Space Machine & Engineering Corp.
SRTechnology Corp.
SSI Cable Corporation
Statek Corp.
Stellar Industries Corp.
StratEdge Corp.
Sumitomo Electric Device Innovations
Sung Won Forming
Susumu International (USA) Inc.
Suzhou Hexagon Communication Technologies Co. Ltd.
Switzer
Synergy Microwave Corp.
Synmatrix Technologies Inc.
Tabor Electronics
Tagore Technology Inc.
Tai-Saw Technology Co. Ltd.
TDK-Lambda Americas
Tecdia Inc.
Tech Briefs Media Group
Teledyne Technologies
Telegartner Inc.
Telonic Berkeley Inc.
Ticer Technologies
TICRA
TMD Technologies Ltd.
TMY Technology Inc.
Tower Semiconductor
TPT Wire Bonder
Transcat Inc.
Transcom Inc.
Transline Technology Inc.
TTM Technologies
Ultra Herley
UTE Microwave Inc.
Varioprint AG
Vaunix Technology Corp.
Ventec Electronics (Suzhou) Co., Ltd.
VIAS3D
Virginia Diodes Inc.
Vishay Intertechnology Inc.
Vishay UltraSource
W. L. Gore & Associates Inc.
Waka Manufacturing Co. Ltd.
Wave Mechanics Pvt. Ltd.
WAVEPIA Co. Ltd.
Wavice
Weinschel Associates
Wenzel Associates Inc.
Werlatone Inc.
West Bond Inc.
WEVERCOMM Co. Ltd.
WIN Semiconductors Corp.
Winchester Interconnect
Winton Machine Company
Wireless Telecom Group
Wolfspeed, A Cree Company
X-COM Systems LLC
XMA Corporation
X-Microwave
Xpeedic Technology Inc.
Yokowo Co. Ltd.

This information is accurate as of 3/10.

For the latest on IMS and Microwave Week visit www.ims-ieee.org

30 GHz Traveling Wave Amplifier Designed for 32 Gbps NRZ and PAM4

HYPERLABS has developed a thermally compensated, ultra-linear amplifier/data driver for high speed digital networks and telecom systems. Model HL5867 is a single stage, GaAs MMIC traveling wave amplifier (TWA) providing 13 dB gain from 75 kHz to 30 GHz. For use as a data driver, the HL5867 was designed for 32 Gbps NRZ and PAM4 data signaling. It can also be used as a general-purpose gain stage in any application needing high pulse fidelity.

Using HYPERLABS' knowledge of broadband and time domain fidelity, the HL5867 was designed to have a flat step response, which produces a highly accurate representation of the input signal. Flat pulse response is crucial to keeping an eye diagram undisturbed with minimum added jitter. HYPERLABS has integrated a proprietary thermal compensation algorithm in the amplifier to automatically adjust the bias points to keep the crossing point and amplitude constant from 0°C to 60°C. The TWA's bias circuitry uses the technology in HYPERLABS' HL9447 67 GHz bias tees and HL9437 DC blocks, and the input and output RF ports are AC coupled. The amplifier is biased with dual supplies of +7 and -8 V and typically dissipates 1.5 W. The size of the standard housing for the HL5867 data driver is 1.45 in. x 1.10 in. x 0.40 in.

Founded in 1992 and privately owned, HYPERLABS offers an array of ultra-broadband components, including broadband baluns, bias tees, DC blocks, power dividers and matched pick-off tees with frequency coverage extending above 67 GHz. HYPERLABS' instrumentation line includes the first USB-powered and controlled time domain reflectometry instruments, controlled impedance analyzers, signal path analyzers and samplers, including harmonic mixers.

HYPERLABS INC.
Beaverton, Ore.
www.hyperlabs.com

COAXIAL AND WAVEGUIDE SWITCHES

RLC has the exact solution you're looking for.

RLC Electronics manufactures a complete range of RF switches including coaxial in the frequency range from DC to 65 GHz and rectangular or double ridge waveguide. The operating modes on all designs are failsafe, latching and manual.

Control options are DC voltages as low as 5V, TTL, BCD, RS232, and RS422. All switches have excellent repeatability and lifetimes in excess of one million operations. Many types are QPL listed per MIL-DTL-3928.

- SPDT to SP12T
- Transfer
- Low VSWR
- High Isolation
- Low Insertion Loss
- High Power
- Low Passive Intermodulation
- Surface Mount Options

For more detailed information on coaxial and waveguide switches, visit our web site.

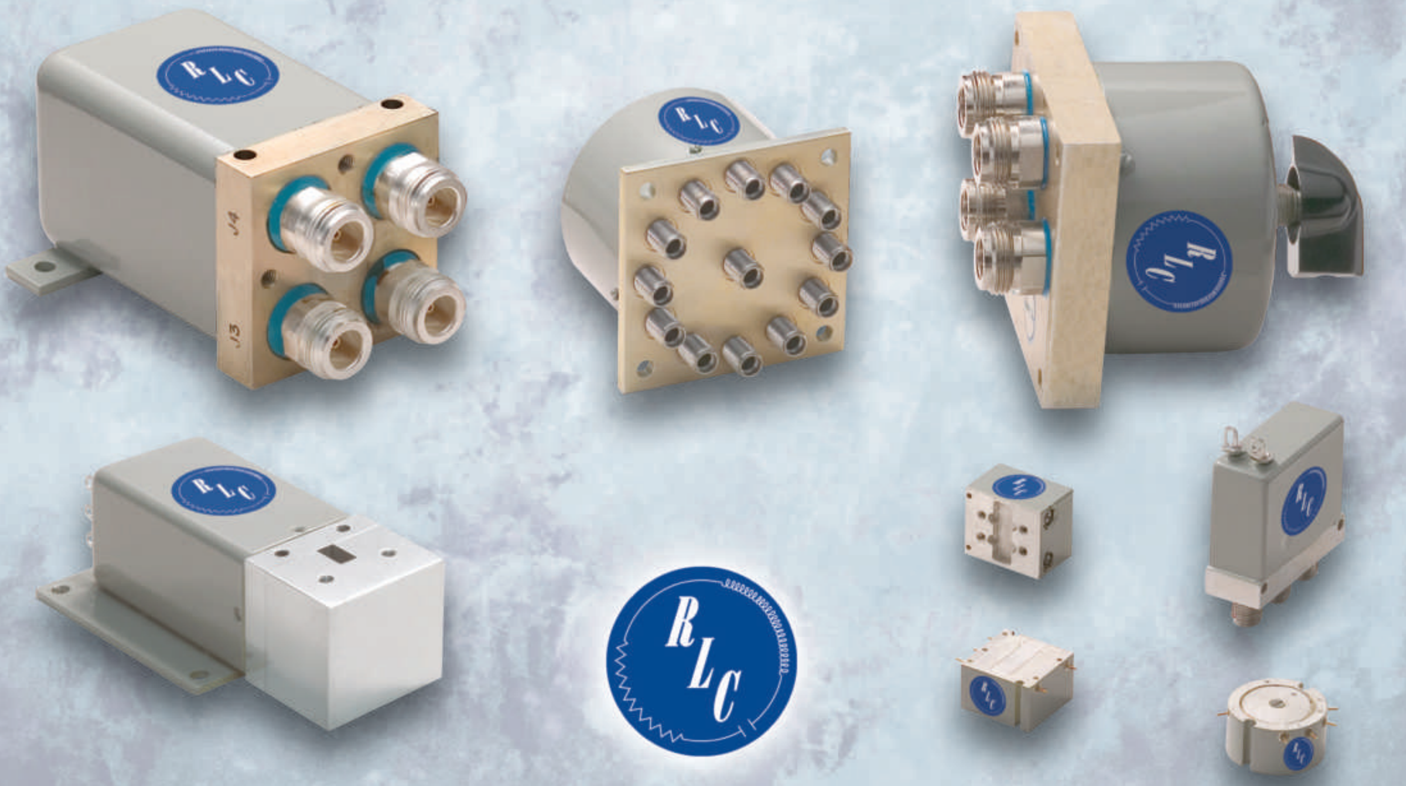

RLC ELECTRONICS, INC.

83 Radio Circle, Mount Kisco, New York 10549 • Tel: 914.241.1334 • Fax: 914.241.1753
E-mail: sales@rlcelectronics.com • www.rlcelectronics.com

ISO 9001:2000 CERTIFIED

VISA MasterCard

RLC is your complete microwave component source...
Switches, Filters, Power Dividers, Terminations, Attenuators, DC Blocks, Bias Tees & Detectors.

Quad-MxFE + Calibration Board User Guide

Analog Devices has a user guide for their new Quad-MxFE System Development Platform, which contains four MxFE® software defined, direct RF sampling transceivers, as well as associated RF front-ends, clocking and power circuitry.

Analog Devices
http://bit.ly/3uThQbF

Gain Equalizers by APITech

APITech has over 2,500 active gain equalizer designs, and more than 200 customer applications. Used in communications links, radar systems, military aircraft and EW applications.

APITech
https://youtu.be/x_ylvaIMzYQ

CMT Celebrates Ten Years

Copper Mountain Technologies (CMT) pioneered metrology-grade USB VNAs and celebrates ten years of engineer-focused solutions with excellent customer value. “Thanks for letting us share in your success.”

Copper Mountain Technologies
http://bit.ly/3aUGQHq

Satcom RF Calculator in App

Need an easy-to-reach Satcom RF calculator? Download the CPI mobile app for the calculator, quotes, datasheets and support at your fingertips. Search for “CPI Satcom” in the Play Store or the App Store.

CPI
www.cpii.com

New Radar Test Benches for OTA Testing

Senior Manager of Autonomous Driving Systems for dSPACE, Dirk Berneck, talks about using radar test benches for OTA testing in this episode of the dSPACE LearningBits podcast.

dSPACE
http://bit.ly/3sQYodY

Microsite for SUCOFLEX 570S

HUBER+SUHNER AG has added a microsite for their SUCOFLEX 570S. The microsite covers everything for the fully customized and readily available cable assembly with high precision and excellent insertion and return loss.

HUBER+SUHNER AG
www.hubersuhner.com/en/sucoflex-570x

Balancing Performance with Compact Quadrature Hybrid Couplers

Quadrature hybrid couplers' advantage allows the user to build a balanced circuit, essential for ultimately constructing balanced amplifiers, switches, phase shifters, mixers and other key microwave building blocks.

Knowles Precision Devices
http://bit.ly/3c2WqAp

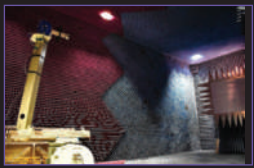

Advanced Radome & Antenna Testing Solutions

Meggitt Baltimore provides customized RCS, RF/LF and materials testing. Range rental bookings are also available. View their new test brochure for more information.

Meggitt Baltimore
www.meggittbaltimore.com/antenna-radome-testing

New Website Update

MIcable's new website offers complete solutions for cable assemblies, power dividers/combiners, couplers/dual couplers, adapters, terminations and butler matrices.

MIcable
www.micable.cn

Choosing the Right RF Coaxial Cable Assembly

Selecting the right RF/microwave cable assembly can be a confusing task considering the variety of products on the market. This blog post goes beyond the spec sheet to help you find the right cable for your needs more quickly and more knowledgeably.

Mini-Circuits
http://bit.ly/3sN31FS

30+ Years of In-house Semiconductor Measurement & Characterization Services

They're more than a distributor! Richardson RFPD services include validating your in-house measurements, solving supply chain challenges, simplifying product sourcing and improving efficiencies and cash flow. View their new brochure now.

Richardson RFPD
www.richardsonrfpd.com/docs/rfpd/RFPD_Services_Brochure.pdf

Spike™ Update Includes Noise Figure Analysis

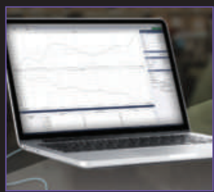

One of the most useful metrics for RF test engineers, characterizing the noise contributions of an electrical system, as well as the individual electrical components within the system.

Signal Hound
www.signalhound.com/spike

Here's How:

2021 IEEE MTT-S International Microwave Symposium
IMS
7-10 June • Atlanta, Georgia

Pick up your badge onsite
Get equal access online

The best of both worlds

IMS
LIVE EVENT IN ATLANTA, GA
7-10 JUNE 2021
Georgia World Congress Center

In-Person Event

- Technical Sessions featuring IMS and RFIC authors
- Joint IMS/RFIC Plenary Session, featuring speakers from Honeywell and Texas Instruments
- 97th ARFTG Microwave Measurement Conference
- Two-day exhibition
- IMS and RFIC Workshops and Technical Lectures
- Special focused highlights, including a Startup Pavilion and 5G Pavilion
- Industry workshops and MicroApps
- Networking events, including welcome reception and industry hosted reception

IMS
VIRTUAL EVENT
20-25 JUNE 2021
Anywhere you are!

Virtual Event

- Technical Sessions featuring IMS and RFIC authors
- Joint IMS/RFIC Plenary Session
- 97th ARFTG Microwave Measurement Conference
- Three-day exhibition
- IMS and RFIC Workshops and Technical Lectures
- Panel Sessions, including RFIC and IMS Panels
- Special focused highlights, including WIM Panel Session; Mobility Closing Panel with Competition results and 3MT Competition
- Industry workshops and MicroApps
- Expo auditorium with Industry Track
- Connected Future Summit (formerly 5G Summit)
- Networking events

IEEE MTT-S™ IEEE MICROWAVE THEORY & TECHNIQUES SOCIETY RFIC ARFTG

NEW PRODUCTS

FOR MORE NEW PRODUCTS, VISIT WWW.MWJOURNAL.COM/BUYERSGUIDE
FEATURING VENDORVIEW STOREFRONTS

COMPONENTS

Linear Regulators

VENDORVIEW

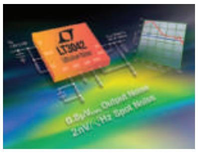

Ultra-low noise, ultra-high PSRR low dropout (LDO) linear regulators are key to power precision sensors, high speed data converters, frequency synthesizers and other noise-sensitive RF and microwave devices. Power by linear offers an outstanding family of robust positive and negative LDOs that produce ultra-low output noise and ultra-high power supply ripple rejection that cover a wide input voltage range, from 1.8 to 20 V, –20 to –1.8 V and a wide output current range, from 200 to 500 mA.

Analog Devices
www.analog.com

Integrated Receiver Module

VENDORVIEW

SSR-3331834012-28-S1 is an integrated receiver module. The receiver has a typical conversion gain of 12 dB with a typical noise figure of 4 dB in the frequency range of 24 to 42 GHz. The required LO power is 0 dBm between frequencies of 12 and 21 GHz. The RF receive port is WR-28 Uni-Guide™ waveguide with UG-599/U flange while the LO port is female 2.92 mm (K) connectors. Other port configurations are also available under different model numbers such as SSR-3331834012-KF-S1.

Eravant
www.eravant.com

Suspended Substrate Stripline

VENDORVIEW

Mini-Circuits' model ZHSS-K21G+ is a suspended substrate stripline highpass filter with wide passband of 21 to 40 GHz. The typical insertion loss is only 1.0 dB across the passband, with typical passband VSWR of 2.0:1. The typical stopband rejection is 80 dB from DC to 13 GHz and 40 dB from 13 to 16 GHz. Ideal for rejecting unwanted lower frequency signals from mmWave communications systems and test and measurement applications, the 50 Ω highpass filter handles input power levels as high as 2 W at room temperature (+25°C).

Mini-Circuits
www.minicircuits.com

Capacitors

PPI now offers traditional NPO, high-quality 0505 (0.055" × 0.055") capacitors for wireless broadcasting equipment, mobile base stations, GPS, MRI and radar applications; are available in magnetic or non-magnetic 100 percent RoHS tin or tin/lead terminations (90 percent Sn 10 percent Pb solder, SnPb 90/10) terminations; and are designed and manufactured to meet the requirements for MIL-PRF-55681 and MIL-PRF-123. Engineering design kits for the 0505C/P case size are available in magnetic and non-magnetic terminations. PPI provides technical information and support allowing engineers to determine the correct PPI capacitor for their requirements.

Passive Plus Inc.
www.passiveplus.com

Electromechanical Relay Switches

VENDORVIEW

Pasternack has released a new line of micro-sized, surface mount, single-pole, double-throw electromechanical relay switches that offer broadband performance and are ideal for a variety of applications that may involve high-power, switch matrices and test and measurement systems. Pasternack's six new SPDT electromechanical relay switches feature popular latching actuators in micro-size surface mount packages and offer impressive performance with very low insertion loss, high isolation and excellent repeatability. These rugged circuits are designed for high reliability with 5M typical lifecycle ratings.

Pasternack
www.pasternack.com

Waveguide Broadwall Coupler

RLC Electronics offers a standard range of multi-hole broadwall directional couplers covering the frequencies from 40 to 2.6 GHz in standard waveguide sizes. The electrical characteristics of high directivity and coupling flatness are achieved by using a precise machined coupling hole pattern and a precision load in the secondary arm. Non-standard configurations or selected electrical parameters are available on request.

RLC Electronics
www.rlcelectronics.com

SAW-Oscillators

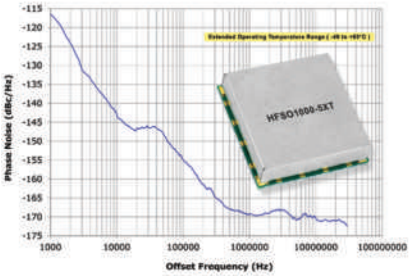

SMD-packaged SAW-oscillators are extensively used in modern communication applications, since the technology features low phase noise, low microphonic (tolerance to vibration) and low jitter. SAW-oscillators exhibit limited tuning and limited operating temperature range (-20 to 70°C), which limits the amount of correction needed to compensate frequency-drifts and tolerances of other components in the oscillator circuitry. The alternative is ovenized SAW-oscillators for extending the operating temperature but at the cost of high current and increase in size.

Synergy Microwave Corp.
www.synergymwave.com

CABLES & CONNECTORS

Microwave Cable Assembly Series

Carlisle Interconnect Technologies announced its new UTiPHASE™ microwave cable assembly series, an innovative solution that delivers outstanding electrical phase stability versus temperature without compromising microwave performance. UTiPHASE is ideal for demanding defense, space and testing applications. These cable assemblies are designed for applications including commercial and military phased array radars, as well as aerospace SATCOM and traffic collision avoidance systems, synthetic aperture radars, thermal test sets and any RF/microwave system operating at or near room temperature.

Carlisle Interconnect Technologies
www.carlisleit.com

Waveguide-to-Coax Adapters

VENDORVIEW

Fairview Microwave Inc. has launched a new line of euro-style flange, waveguide-to-coax adapters that are ideal for radar, SATCOM, wireless communications and test instrumentation applications. The adapters cover a wide range of waveguide sizes that

include European IEC standard flanges (including UBR square cover, UDR and PDR types), WR-22 to WR-430, right-angle and end-launch coaxial connector options and N-type, SMA, 2.92 mm and 2.4 mm connector choices. These new waveguide-to-coax adapters transform waveguide transmission lines into 50 Ω coaxial lines.
Fairview Microwave Inc.
www.fairviewmicrowave.com

Adapters

VENDORVIEW

MECA carries a full range of the most common between series adapters (bullets) to help simplify the connectivity of your projects. These rugged and reliable adapters are available off-the-shelf and complement the large variety of products the company sells every day. When connectivity issues arise in your projects, you now have the convenience of ordering between series adapters from MECA.
MECA Electronics Inc.
www.e-meca.com

RF mmWave Cable Assemblies

Samtec's precision RF mmWave cable assembly (RF047-A Series) on 0.047" flexible cable is now available with new SMPM connector options: direct solder, right-angle and bulkhead jacks. SMPM operating frequency is up to 65 GHz, with low insertion loss. Right-angle jacks offer a maximum VSWR of 1.45; all other connector options are 1.40 or better. Additional RF047-A Series cable assembly connector options include SMPM straight jack and full detent plug, 2.92 mm, 2.40 mm and 1.85 mm.
Samtec
www.samtec.com

AMPLIFIERS

Solid-State Power Amplifier Module

COMTECH PST introduced its latest development for the TWT replacement market covering the full 2,000 to 6,000 MHz band providing 75 W linear power in a small, compact, lightweight, ruggedized form factor, ideally suited for UAV, fixed wing, rotary wing applications. This solid-state power amplifier (SSPA) features built-in protection and monitoring circuits, low voltage prime power input, high efficiency and reliable solid-state technology. Unit will self-protect under fault conditions and automatically return to normal operation when fault conditions are removed.
COMTECH PST
www.comtechpst.com

LNA

Kuhne's latest development is the "KU LNA 750850 A-WG." Its WR112 RF-input enables a low-loss connection to waveguides resulting in a noise figure of typ. 0.7 dB (upper half band) and typ. 0.8 dB (lower half band). In its frequency range from 7.5 to 8.5 GHz, the LNA offers a high gain of 65 dB. Together with a high linearity (P1dB = 13 dBm, IP3 = 23 dBm), the LNA hence shows a very high dynamic range. Available now.
Kuhne electronic GmbH
www.kuhne-electronic.de

Dual Gain Amplifier

VENDORVIEW

PMI Model No. PEC-40-25-0R518-20-12-SFF-TTLVG is a dual gain amplifier operating over the frequency range of 0.5 to 18 GHz. Has

a maximum VSWR of 2.0:1 and an input power of +20 dBm CW. This unit is outfitted with SMA female connectors in a housing that measures 2.54" × 1.00" × 0.383".

Planar Monolithics Industries Inc.
www.pmi-rf.com

High Efficiency Power Amplifier

The SKY66320-11 is a highly efficient, wide instantaneous bandwidth, fully input/output matched power amplifier (PA) with high gain and linearity. The compact 5 × 5 mm PA is designed for 5G NR and 4G LTE systems operating from 3,600 to 3,800 MHz. Active biasing circuitry is integrated to compensate for temperature, voltage and process variation. The SKY66320-11 is part of a high efficiency, pin-to-pin compatible PA family supporting major 3GPP bands.

Skyworks Solutions Inc.
www.skyworksinc.com

SOFTWARE

Spike™ Update

Signal Hound's Spike™ software now includes noise figure analysis. Noise figure analysis is one of the most useful metrics for RF test engineers, characterizing the noise contributions of an electrical system, as well as the individual electrical components within the system. Spike's new analysis mode performs noise figure measurements quickly and accurately. Signal Hound is proud to offer this as part of its free software package that comes with all Signal Hound spectrum analyzers.

Signal Hound
www.signalhound.com

PACKAGING

Multi-layer Circuit Board Prepreg Material

Panasonic Corp. launched R-5410, halogen-free ultra-low transmission loss multi-layer circuit board prepreg material. This leading-edge product is especially well suited for automotive mmWave radar and 5G wireless communication base station applications. R-5410 enables multi-layer antenna constructions using industry-standard circuit board lamination processes and equipment which increases the flexibility of high frequency circuit board designs, improves the efficiency of antenna performance and reduces material and processing costs.

Panasonic Corp.
www.industrial.panasonic.com

ANTENNAS

WLAN Antennas

Richardson RFPD Inc. announced the availability of Ethertronics WLAN antennas which use specific technology in a trace configuration to provide high performance. This antenna has unique features enabling limited range RF tuning. Ethertronics antennas requires a smaller design keep-out area, carry lower program development risk which yields a quicker time-to-market, without sacrificing RF performance.

Richardson RFPD
www.richardsonrfpd.com

TEST & MEASUREMENT

Digitizer & AWG Cards

VENDORVIEW

For all 65 different PCIe digitizer and signal generators, Spectrum Instrumentation released a driver for the Nvidia Jetson development kit that is based on an embedded ARM processor. The Nvidia Jetson consists of an ARM CPU and a CUDA-based GPU for high performance parallel processing, as well as one PCIe slot e.g. for a Spectrum M2p.5968 digitizer card as shown. This small but powerful combination is able to sample eight signals in parallel with 125 MS/s.

Spectrum Instrumentation
www.spectrum-instrumentation.com

MICRO-ADS

E LEARNING CENTER

Presented by: Microwave Journal

NOW

4/20 EW in Space

Sponsored by: ROHDE&SCHWARZ Make ideas real

4/21 Optimized Silicon Wafers: The Ultimate Solution for Improved RF Filter and Device Performance

Sponsored by: OKMETIC

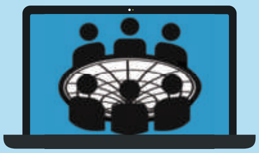

ONLINE PANEL SERIES

4/27 What is the Best 5G mmWave Beam Steering Architecture?

Sponsored by: Anokiwave, Pivotal Commware, Taoglas, Tektronix, Sivers Semiconductors

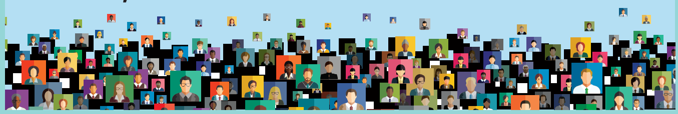

4/28 Topic: Defense and Radar

Sponsored by: RFMW It's who we are It's what we do

qorvo

Register to attend at mwjournal.com/webinars

FEATURED eBooks

mwjournal.com/ebooks

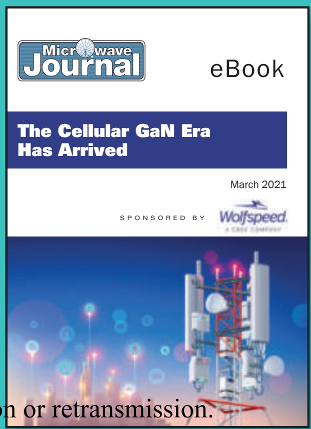

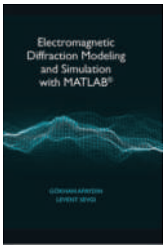

Electromagnetic Diffraction Modeling and Simulation with MATLAB

Gökhan Apaydin, Levent Sevgi

This exciting new resource presents a comprehensive introduction to the fundamentals of diffraction of two-dimensional canonical structures, including wedge, strip and triangular cylinder with different boundary conditions. Maxwell equations are discussed, along with wave equation and scattered, diffracted and fringe fields. Geometric optics, as well as the geometric theory of diffraction are explained. With MATLAB scripts included for several well-known electromagnetic diffraction problems, this book discusses diffraction fundamentals of two-dimensional structures with different boundary conditions and analytical numerical methods that are used to show diffraction.

The book introduces fundamental concepts of electromagnetic problems, identities and definitions for diffraction modeling. Basic coordinate systems, boundary conditions, wave equation and Green's function problem are given. The scattered fields, diffracted fields and fringe fields, radar cross section for diffraction modeling are presented. Behaviors of electromagnetic waves around the two-dimensional canonical wedge and canonical strip are also explored. Diffraction of trilateral cylinders and wedges with rounded edges is investigated as well as double tip diffraction using finite difference time domain (FDTD) and method of moments (MoM). A MATLAB-based virtual tool, developed with graphical user interface, for the visualization of both fringe currents and fringe waves is included, using numerical FDTD and MoM algorithm and high frequency asymptotics approaches.

To order this book, contact:

Artech House
www.artechhouse.com
Email: artech@artechhouse.com
US 800-225-9977
UK +44 (0)20 70596 8750

ISBN: 978-1-63081-779-4
364 pages
$149
£129

Use code APA25 to receive 25% discount on this title! (expires 04/30/2021)

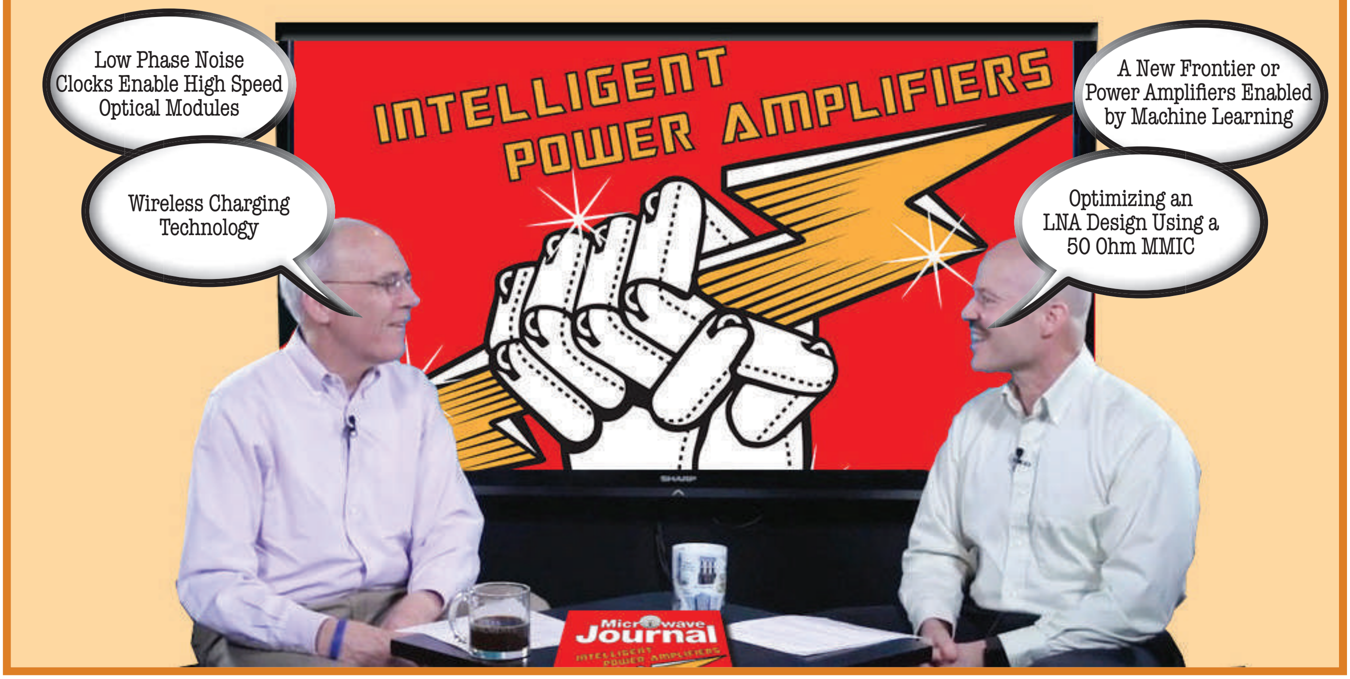

ONLINE PANEL SERIES

What is the Best 5G mmWave Beam Steering Architecture?

April 27

This panel will discuss the various RF architectures and antenna technologies being developed to produce low-cost phased arrays for 5G applications including fixed wireless access and cellular repeaters. Panelists will debate and discuss the best architectures, semiconductor platforms and antenna solutions including performance achieved by their products and partners to date in the market.

Sponsored by:

Anokiwave mmW Solutions. Enabling a new world — PIVOTAL COMMWARE® — TAOGLAS® Next Gen IoT — sivers SEMICONDUCTORS — Tektronix®

RF/Microwave Test and Component Solutions for New Space

May 18

This panel will discuss the best device and component solutions for New Space applications that maximize performance and minimize cost/power consumption available from semiconductor companies along with the best test & measurement solutions to verify their performance. They will address the main challenges in these areas along with solutions being introduced to meet industry demands.

Sponsored by:

apitech™ — TERADYNE — ANALOG DEVICES AHEAD OF WHAT'S POSSIBLE™ — SKYWORKS® — ROHDE&SCHWARZ Make ideas real

Organized by: Microwave Journal

Register Now at mwjournal.com/onlinepanels

Advertising**Index**

Sales Representatives

Microwave Journal

Eastern and Central Time Zones
Michael Hallman
Associate Publisher
(NJ, Mid-Atlantic, Southeast, Midwest, TX)
Tel: (301) 371-8830
Cell: (781) 363-0338
mhallman@mwjournal.com

Shannon Alo-Mendosa
Northeastern Reg. Sales Mgr.
(New England, New York, Eastern Canada)
Tel: (781) 619-1942
salomendosa@horizonhouse.com

Ed Kiessling
Traffic Manager
(781) 619-1963
ekiessling@mwjournal.com

Pacific and Mountain Time Zones
Brian Landy
Western Reg. Sales Mgr.
(CA, AZ, OR, WA, ID, NV, UT, NM, CO, WY, MT, ND, SD, NE & Western Canada)
Tel: (831) 426-4143
blandy@mwjournal.com

International Sales
Richard Vaughan
International Sales Manager
Tel: +44 207 596 8742
rvaughan@horizonhouse.co.uk

Germany, Austria, and Switzerland (German-speaking)
WMS.Werbe- und Media Service
Brigitte Beranek
Tel: +49 7125 407 31 18
bberanek@horizonhouse.com

France
Gaston Traboulsi
Tel: +44 207 596 8742
gtraboulsi@horizonhouse.com

Israel
Dan Aronovic
Tel: +972 50 799 1121
aronovic@actcom.co.il

Korea
Young-Seoh Chinn
JES MEDIA, INC.
Tel: +82 2 481-3411
yschinn@horizonhouse.com

China
Shenzhen
Jenny Li
ACT International
jennyl@actintl.com.hk

Shanghai
Linda Li
ACT International
Tel: 86-021-62511200
lindal@actintl.com.hk

Wuhan
Sky Chen
ACT International
skyc@actintl.com.hk

Beijing
Cecily Bian
ACT International
Tel: +86 135 5262 1310
cecilyb@actintl.com.hk

Hong Kong, Taiwan, Singapore
Floyd Chun
ACT International
Tel: +86-13724298335
floydc@actintl.com.hk

Japan
Katsuhiro Ishii
Ace Media Service Inc.
Tel: +81 3 5691 3335
amskatsu@dream.com

Corporate Headquarters: 685 Canton Street, Norwood, MA 02062 • Tel: (781) 769-9750

FABS and LABS

X-Microwave: Accelerating the Development of Complex RF/Microwave Systems


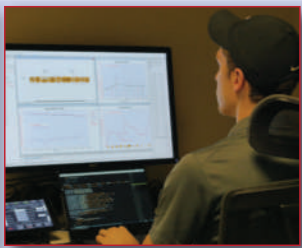

Fielding new technologies and systems has always been paced by the time required for development, particularly for complex military platforms. The process is arduous: beginning with the functionality of the system, defining the block diagram, flowing specs to the individual components, finding suppliers, procuring components, building and testing breadboards, identifying performance gaps, iterating the design and finally converting the breadboards to integrated microwave assemblies (IMA) meeting the size and weight constraints. The process can take years. Everyone complains about the long time—the Department of Defense, company CEOs, program managers, designers. John Richardson had an idea to accelerate the development of RF systems, which led him to cofound X-Microwave in October of 2013 and unveil an innovative modular building block concept at the 2015 International Microwave Symposium.

The concept is simple: an industry library of 50 Ω die and packaged components in standard-size building blocks—imagine RF/microwave Legos called X-MWblocks—quickly combined via solderless interconnects on a prototype plate and easily tested using low VSWR X-MWprobes or X-MWconnectors.

To define the design, X-Microwave provides an online, interactive design environment where designers can create a signal chain block diagram, select X-MWblocks and analyze the cascaded performance. Two additional online analysis tools provide 1) nonlinear simulation through an interactive interface with Keysight's Spectrasys RF system simulator and 2) a tool for analyzing and comparing S-parameter files, handling up to four-port blocks. In addition to these online tools, X-Microwave is collaborating with Keysight to bring its full portfolio of characterized drop-in X-MWblocks into Keysight's PathWave Advanced Design System Genesys and SystemVue simulation software.

Once a design is finalized, transferring the X-MWblocks from the prototype plate to a conventional machined housing is straightforward, eliminating the costly and time-consuming step of designing new PCB layouts to integrate the functional blocks. X-Microwave will convert the prototype to an IMA in a machined housing and build the production run, so the customer does not have to generate a drawing package for all the assemblies. Production is part of X-Microwave's business model.

Illustrating the power of this concept, a customer came to X-Microwave needing to develop four custom IMAs to meet a critical milestone. X-Microwave had the necessary blocks in the library, prototyped and validated the performance, then integrated the blocks into four machined housings and delivered production IMAs—all within three months, enabling the customer to meet the program deadline.

More proof that the modular building block approach works: since launching X-Microwave, the library of components has grown to almost 6,000 part numbers from 15 companies, representing leading RF/microwave brands such as Analog Devices, MACOM, Marki Microwave, Mini-Circuits and Qorvo. New companies are calling to add their products.

John Richardson sees X-Microwave as an extension of his customers' design teams. Spending 25 years at Wenzel Associates before starting X-Microwave, he has extensive experience in RF/microwave design and manufacturing and is willing to share that expertise with customers to collaborate on their designs.

X-Microwave's revenue grew more than 100 percent annually in 2017, 2018 and 2019. In 2020, because of the pandemic, the company "only" grew 53 percent; however, by the fourth quarter of 2020, the rate of growth had returned. To support this, X-Microwave just moved into a new facility in north Austin, expanding floor space from 5,700 to almost 22,000 square feet.

With the industry clearly embracing the X-Microwave concept and almost 4x the floor space to grow into, Richardson says his biggest challenge now is recruiting staff with RF/microwave experience to fulfill his goal of having "all the components from all the manufacturers" in the X-Microwave library, to finally solve the development schedule challenge. If you'd like to join the X-Microwave team, please reach out.

www.xmicrowave.com

WERLATONE®

WE ARE HIGH POWER

HIGH POWER COMBINERS & ABSORPTIVE FILTERS

Multi-kW Power Levels ✦ Low Loss Circuits ✦ ***Mismatch Tolerant***® Designs

Combiners & Dividers

- Frequency Bands Covering DC through C-Band
- Power Levels to 60 kW CW & 200 kW Peak!
- Rack Mount, Drawer Mount, & Radial Type Available
- Low Loss Designs, Ideal for Coherent & Non-Coherent Combining

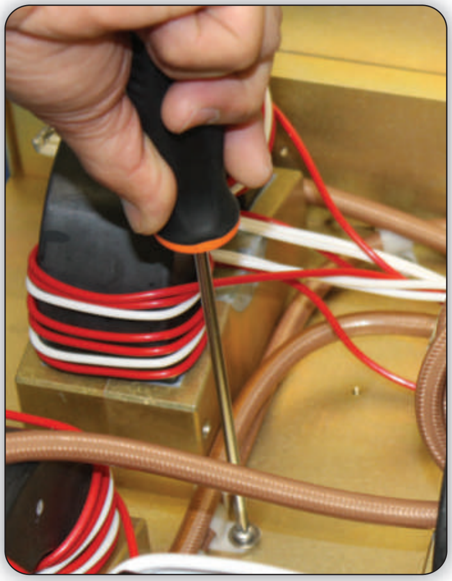

Absorptive Filters

- Low and High Pass Filters are Non-Reflective!
- Out-of-Band Signals are Internally Terminated
- Absorptive Filters are Less Susceptible to Temperature Change
- **HF, 1.5 kW Switch Filter Bank Available**

Our Designs Are:

- Supplied with Plotted Test Data by Serial Number
- Built to Withstand High Unbalanced Input Powers
- Designed for High Humidity, Temperature, Vibration & Shock

Send Us Your Specs for Custom Designs!

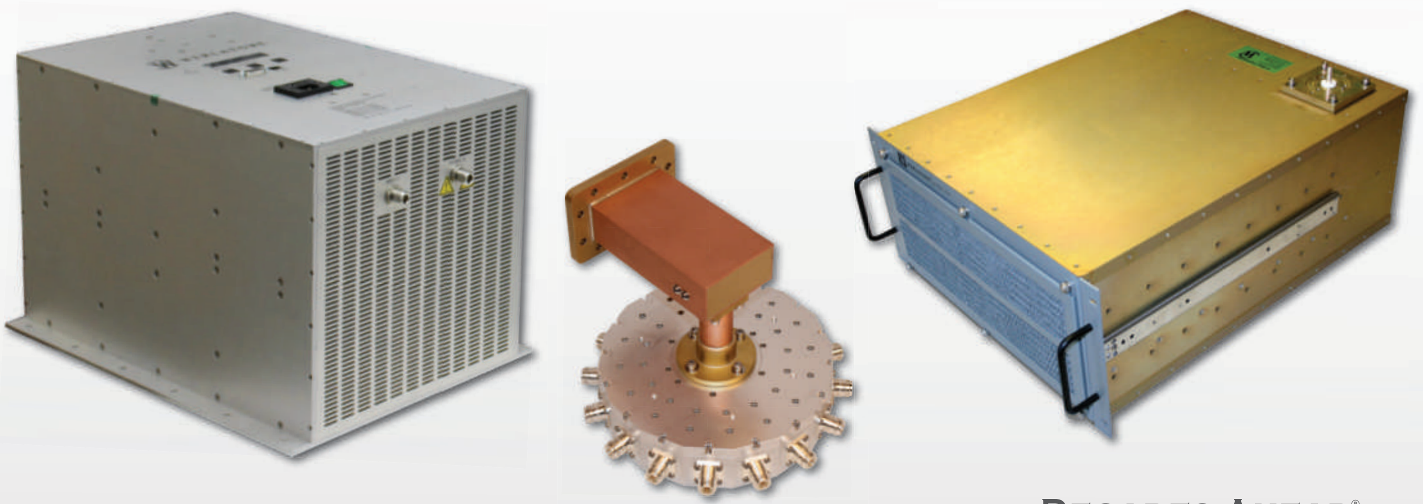

DECADES AHEAD®

Werlatone, Inc. 17 Jon Barrett Road Patterson, NY 12563 845-278-2220 sales@werlatone.com www.werlatone.com